January 27, 1977

To the Graduate Council:

I am submitting herewith a thesis written by John S. Arendt entitled "Development of Methods for In Situ Testing of Response Times of Resistance Temperature Detectors in Commerical Pressurized Water Reactors." I recommend that it be accepted in partial fulfillment of the requirements for the degree of Master of Engineering, with a major in Nuclear Engineering.

T. W. Kerlin, Major Professor

We have read this thesis
and recommend its acceptance:

Accepted for the Council:

Vice Chancellor
Graduate Studies and Research

Thesis
77
.A735
cop. 2

DEVELOPMENT OF METHODS FOR IN SITU TESTING OF RESPONSE TIMES OF RESISTANCE TEMPERATURE DETECTORS IN COMMERCIAL PRESSURIZED WATER REACTORS

A Thesis

Presented for the

Master of Engineering

Degree

The University of Tennessee, Knoxville

John S. Arendt

March 1977

1317597

ACKNOWLEDGEMENTS

The author wishes to express his sincere appreciation to his advisor Dr. T. W. Kerlin who offered invaluable guidance during the course of this research and without whose help and advice this thesis would not have been completed.

The author also wishes to thank Dr. P. F. Pasqua for making available the educational opportunity in the form of a research assistantship. Sincere thanks is also given Mr. H. M. Hashemian who aided in the realization of the project's goals.

Special appreciation is reserved for Mrs. Juanita Rye who prepared the final documentation of this thesis.

The work reported herein was performed under a contract between the Nuclear Engineering Department, The University of Tennessee, and the Electric Power Research Institute (EPRI).

ABSTRACT

Resistance temperature detectors (RTD's) are used in nuclear plant safety systems to measure process temperatures. The purpose of this research was to develop and evaluate suitable methods for in situ testing of the response time of RTD's.

Three testing procedures were used in laboratory experiments: (1) loop current step response (LCSR) test, (2) self-heating test, and (3) plunge test. The LCSR test involved a step change in the internal ohmic heating of a sensor. The self-heating test involved measurement of steady state temperature changes due to incremental changes in ohmic heating current. The plunge test was used to approximate a fluid temperature step response.

The LCSR results were compared to plunge test results through use of an analytical transformation. Because the physical makeup of the sensor used in the laboratory testing did not conform to the assumptions required in the heat transfer model used in the transformation, the transformation failed.

Empirical transformations were developed using the LCSR, self-heating, and plunge tests. The correlation curves that were developed were used to predict sensor plunge test time constants.

Finally, time response testing was conducted at Turkey Point Nuclear Plant and results obtained are discussed.

Results from the laboratory testing indicate that the LCSR and self-heating tests are valid procedures for predicting response times of resistance temperature detectors.

TABLE OF CONTENTS

CHAPTER		PAGE
1.	INTRODUCTION AND BACKGROUND CONSIDERATIONS	1
	Introduction	1
	Statement of the Problem	2
	Qualifying Criteria for Response Time Testing	3
	Previous Work in This Area	3
	Proposed Solution	6
	Importance of This Work	7
	Organization of the Text	7
2.	SYSTEM DESCRIPTION	9
	Resistance Thermometry Background	9
	Design Considerations for RTD's Used in PWR's	14
	RTD Description	14
	RTD Heat Transfer Characteristics	16
	Modes of RTD Failure or Time Response Degradation	18
	RTD Process Instrumentation Description	21
	Types of Bridges	21
	Results of Circuit Analysis for Two- and Three-Wire Bridges	34
	RTD Implementation in PWR's	39
3.	THE LOOP CURRENT STEP RESPONSE (LCSR) TEST	41
	Description of Testing Method	41
	Theory and Principle of Method	41
	Discussion of Analytical Transformation	48
	Restrictions Inherent to the Analytical Transformation	55
	Development of an Empirical Transformation Using the LCSR Test	56
4.	THE SELF-HEATING TEST	59
	Description of Testing Method	59
	Theory and Principle of Method	60
	Development of an Empirical Transformation Using the Self-Heating Test	62
5.	LABORATORY TIME RESPONSE TESTING OF AN RTD USED IN WESTINGHOUSE PWR's	63
	Introduction	63
	Experimental Equipment Description and Setup	63
	Laboratory Testing	71

CHAPTER PAGE

Plunge Test 71
Loop Current Step Response Test 76
Self-Heating Test 82
Results of Computer Aided Analysis and Transformation of Laboratory Test Data 84
Discussion of Empirical Relationships Obtained from Experimental Results 86

6. IN-PLANT TIME RESPONSE TESTING 104

Description of Testing Apparatus 104
Test Description and Problems Encountered 105
Discussion of Results 115

7. CONCLUSIONS AND RECOMMENDATIONS 129

Conclusions 129
Recommendations 130

LIST OF REFERENCES 132

APPENDIXES 135

A. TWO-WIRE BRIDGE CIRCUIT ANALYSIS 136

B. USE OF COMPUTER-AIDED TRANSFORMATION OF LCSR LABORATORY TEST DATA 140

C. STATISTICAL ANALYSIS AND INTERPRETATION OF LABORATORY TEST RESULTS 144

VITA 152

LIST OF TABLES

TABLE		PAGE
2.1	Characteristics of Platinum	13
5.1	Self-Heating Test Data for RTD with Augmented Surface Resistance	91
5.2	Laboratory Time Response Test Data	93
B.1	Transformed LCSR Test Data	141
C.1	Upper Bounds for 99% Confidence Interval	147

LIST OF FIGURES

FIGURE		PAGE
2.1.	Relative Resistance of Materials	11
2.2.	Resistance-Temperature Curves for Pure Metals	12
2.3.	Resistance Temperature Sensor	15
2.4.	RTD in Thermowell	17
2.5.	RTD Without Thermowell	19
2.6.	Wheatstone Bridge	23
2.7.	Two-Wire Bridge Circuit Diagram	24
2.8.	Three-Wire Bridge Circuit Diagram	26
2.9.	Four-Wire Bridge	28
2.10.	RTD Lead Wires for 4-Wire Bridge in Figure 2.9	29
2.11.	Alternative Four-Wire Bridge Configuration	30
2.12.	RTD Lead Wires for Alternative Four-Wire Bridge	32
2.13.	Multiple Bridge Circuit Diagram	33
2.14.	Lead Wire Resistance Effects on Two-Wire Bridge Output	36
2.15.	Two-Wire Bridge Error Versus R_L/R_{RTD}	37
3.1	LCSR Test Result with $R_d = R_{RTD}$ Initially	43
3.2	LCSR Test Result with $R_d > R_{RTD}$ Initially	45
3.3	LCSR Test Result with $R_d < R_{RTD}$ Initially	47
3.4	One-Dimensional Nodal Heat Transfer Model	50
4.1	Typical Self-Heating Curve	61
5.1	Stirred Bath	64

FIGURE PAGE

5.2 Laboratory Testing Bridge Circuit Schematic 66

5.3 Resistor Response to Step Change in Current 70

5.4 Rosemount Model 176-KF RTD 72

5.5 Plunge Test Response for Bare 176-KF Sensor 74

5.6 Laboratory Plunge Test Bridge Circuit 75

5.7 Plunge Test Battery Circuit 77

5.8 Determination of Plunge Test Time Constant for Bare 176-KF Sensor 78

5.9 LCSR Computer Data Acquisition Setup 80

5.10 LCSR Manual Data Acquisition Setup 81

5.11 LCSR Test on Bare 176-KF Sensor 83

5.12 Self-Heating Test Result for Bare 176-KF Sensor 85

5.13 Typical Simulated Heat Transfer Configuration 88

5.14 Plunge Test for Rosemount 176-KF RTD with Augmented Surface Resistance 89

5.15 LCSR Test for Rosemount 176-KF RTD with Augmented Surface Resistance 90

5.16 Self-Heating Test for Rosemount 176-KF RTD with Augmented Surface Resistance 92

5.17 τ_{LCSR} Versus τ_{PLUNGE} 95

5.18 τ_{LCSR} Versus τ_{PLUNGE}: Lower Region 96

5.19 Self-Heating Slope Versus τ_{PLUNGE} 97

5.20 Self-Heating Slope Versus τ_{PLUNGE}: Lower Region 98

5.21 τ_{LCSR} Versus τ_{PLUNGE} with a 99% Upper Confidence Bound 100

5.22 τ_{LCSR} Versus τ_{PLUNGE}: Lower Region with a 99% Upper Confidence Bound 101

5.23 Self-Heating Slope Versus τ_{PLUNGE} with a 99% Upper Confidence Bound 102

5.24 Self-Heating Slope Versus τ_{PLUNGE}: Lower Region with a 99% Upper Confidence Bound 103

FIGURE PAGE

6.1 Possible LCSR Test Switching Clatter 106

6.2 LCSR Data on Sensor in Bucket 107

6.3 LCSR Test PTP014 RTD Data 108

6.4 LCSR Test PTP017 RTD Data 109

6.5 LCSR Test PTP019 RTD Data 110

6.6 LCSR Test PTP020 RTD Data 111

6.7 LCSR Test PTP021 RTD Data 112

6.8 LCSR Test PTP023 RTD Data 113

6.9 Voltmeter Transient Effect on LCSR Test in Laboratory . . 114

6.10 LCSR Test PTP014 RTD Transformed Results 116

6.11 LCSR Test PTP017 RTD Transformed Results 117

6.12 LCSR Test PTP019 RTD Transformed Results 118

6.13 LCSR Test PTP020 RTD Transformed Results 119

6.14 LCSR Test PTP021 RTD Transformed Results 120

6.15 LCSR Test PTP023 RTD Transformed Results 121

6.16 LCSR Test PTP014 RTD Time Constant 123

6.17 LCSR Test PTP017 RTD Time Constant 124

6.18 LCSR Test PTP019 RTD Time Constant 125

6.19 LCSR Test PTP020 RTD Time Constant 126

6.20 LCSR Test PTP021 RTD Time Constant 127

6.21 LCSR Test PTP023 RTD Time Constant 128

B.1 Computer-Aided LCSR Transformed Result of the Bare 176-KF Sensor 142

C.1 τ_{LCSR} versus τ_{PLUNGE} Interpretive Example 149

C.2 Self-Heating Slope versus τ_{PLUNGE} Interpretive Example . . 150

CHAPTER 1

INTRODUCTION AND BACKGROUND CONSIDERATIONS

1.1. INTRODUCTION

In order to insure the safe operation of nuclear plants, many process variables must be monitored. Variables such as coolant inlet and outlet temperature and steam pressure are measured and control action is taken to maintain their values within limits set forth by the plant's technical specifications. It is important to know the operational status of the system for control and safety purposes. It is imperative that the process variable information received by the safety system be correct and be available with minimal delay.

Accurate temperature measurements are impossible when the sensor is out of calibration, and timely temperature measurements are impossible when its response time has degraded. It is necessary to be able to test a sensor, and recalibrate, modify or replace it if necessary. The temperature sensors in a nuclear plant are normally welded directly into coolant piping or are located in a thermowell. This makes it difficult, if not impossible, to remove a sensor-well system for testing purposes. The problem that this research is directed toward is developing a method to test, in situ, the response times of resistance temperature sensors in pressurized water reactors. All of the hardware between the sensing element and the process such as sheaths, wells, insulation, gas gaps, and filling compounds must be included in the analysis.

The response of a temperature sensor is usually given in terms of a time constant. The time constant is arbitrarily defined as the time required by the sensor to attain 63.2% of its final output following a step change in ambient temperature. The purpose of response time testing in nuclear reactors is to insure the capability of the sensor to respond quickly enough to fluid temperature variations to insure timely safety system actuation.

1.2. STATEMENT OF THE PROBLEM

Normally all plant protection systems are tested at specified intervals during the life of the plant to assure plant operators of their availability in case of an accident. The inputs to the reactor protection system in a pressurized water reactor include temperature readings in the reactor hot leg and cold leg using resistance temperature detectors (RTD's). If an excursion were to start, the RTD's must be able to provide the correct process information within an adequately short time. If the process information were incorrect or the response time of the sensor too slow for action to be taken, damage to the plant could occur.

The most common method for response time testing involves out-of-plant plunge testing. A plunge test allows one to obtain the approximate response of a sensor due to a step change in fluid temperature. It is performed by suddenly immersing (plunging) the sensor into a fluid at a different temperature. The response of the sensor is recorded and the time constant is determined.

The value of the time constant, τ, obtained in this test is a close approximation of the actual fluid temperature step response of the sensor. It is not exact because of variations in surface heat transfer conditions associated with plunging the sensor into the fluid. Moreover, this method is unsatisfactory for reactor applications for two reasons: (1) removal of the sensor may require shutdown of the plant which is both costly and impractical, and (2) the value of the plunge test time constant is limited since the test fails to measure the response in the same environment that exists during normal reactor operation.

1.2.1. Qualifying Criteria for Response Time Testing

A testing method is needed which satisfies the following criteria: (1) it must allow testing of the sensor as it is installed in the system (in situ); (2) the method should at least determine whether the sensor-system response time is less than a maximum value that guarantees satisfactory performance; (3) it must be possible to perform the test while the plant is operating or during shutdown; (4) it must be simple, suitable for existing sensors, and adaptable to all reactors; and (5) it should be inexpensive. The most important of the criteria is that the test must be conducted in situ.

1.2.2. Previous Work in This Area

Extensive research has been performed in the area of resistance thermometry, including standards development and error analysis. D. J. Curtis[1] conducted experiments to determine the effects of various operational characteristics and errors such as self-heating, thermal emf,

and heat conduction losses from the supports and ends in RTD's. Techniques for determining the magnitude of these errors and minimizing their effects are discussed from both the design and use aspects.

The effects of thermal cycling on resistance thermometers have been analyzed by D. A. Lucas.[3] Experiments determining the long term drift characteristics of platinum sensors were conducted. Miniature platinum resistance thermometers were tested over a period of twelve months and it was found that the ice point resistance remained constant within 10 ppm (parts per million). Time response measurements were performed in a laboratory environment.

K. R. Carr[2] of Oak Ridge National Laboratory performed tests between 0 and 650 °C to determine the performance of industrial platinum resistance thermometers, discover problem areas, and establish specification requirements for high reliability service. Time response testing was conducted in the laboratory using the sudden immersion technique. His conclusions included: (1) thermometers can survive more than 2500 thermal cycles (8 °C/sec) between 650 and 260 °C (however, R_0 changes as much as 0.07 ohms and temperature coefficient of resistance changes of as much as 0.44% may result after 1000 cycles) (2) industrial RTD's are available which will remain stable within 1 °C for several thousand hours of service at a fixed temperature of 650 °C; and (3) the time response of 0.63 cm-O.D. thermometers may be as great as 8 seconds.

An overview of resistance thermometry applications with considerations to thermometer bulb design requirements was given by E. F. Adams.[4] Different methods of resistance measurement are discussed and various types of resistance measuring circuits are offered.

Development of the loop current step response (LCSR) test for thermocouples to measure time constants was described by Shepard and Carroll.[5] Experimental verification of the LCSR test was performed, and effects of temperature on the response time of thermocouples were determined. The data shows that a longer time is required for response when the thermocouple operates a higher temperature. The physical explanation of this behavior is simple. As the sensor heats up, the element, insulating material, and sheath expand according to their temperature coefficient of expansion. Because of nonequal expansion the gap dimension may change. This resulted in a larger heat transfer resistance for the thermocouples used in these tests.

Various other effects on thermocouple response rates were considered: sheath swagging, sheath diameter, sheath closure thickness, and others. Among the conclusions of Shepard and Carroll was that the LCSR method provides a unique means of measuring the response of a thermocouple after it is installed in the system. They also found that the apparent response time of thermocouples is strongly affected by heat transfer at the sheath surface.

Warshawsky[6] described in detail multiple bridge circuits for measurement of small changes in resistance. First-order effects of random resistance variations occurring at the junctions of a Wheatstone bridge are eliminated by an extension of Kelvin's method, which involves adding an auxiliary resistor pair at each bridge corner at which the variations occur. The remaining second-order error, and effects of thermal emf's, are evaluated. Warshawsky[7] also performed response time

testing. He described methods for finding an "internal" time constant and an "external" time constant. The latter response was from a plunge test. The "internal" response was due to a step increase in internal heating.

1.2.3 Proposed Solution

The testing method needed must satisfy the requirements stated earlier. A simple method developed at Oak Ridge National Laboratory called the loop current step response (LCSR) test appears to be adequate for in situ testing of resistance temperature detectors (RTD's). This test involves temporary ohmic heating of the sensing element by passing a higher than normal current (20-60 mA rather than the normal 1-2 mA) through the sensor leads. The resistance changes are monitored as the RTD heats up. The current is then returned to its normal value and the signal is again monitored as the sensor cools. Detailed discussion of the LCSR theory and method is offered in Section 3.2.

The LCSR method provides the response to a step change in internal heating of the sensor. However, the response of interest is the response of the sensor when subjected to a step change in fluid temperature. Since both responses depend upon the same heat transfer resistances and heat capacities, the fluid step response can be synthesized from the LCSR result (as shown in Section 3.3).

Another testing method called the self heating test may be useable for in situ response time testing. In this test, the sensing current is increased incrementally and the steady state resistance of the sensor is measured for each current level. For platinum, this results in a linear relationship between resistance and the power generated

in the sensor and the slope of the curve can be determined. Empirical correlation curves can be developed relating the slope of the self heating curves ($\frac{\Delta R}{\Delta P} \frac{\Omega}{mw}$) and the plunge test time constant. Further discussion of the self heating test is given in Chapter 4.

1.3. IMPORTANCE OF THIS WORK

Recently, the Nuclear Regulatory Commission submitted for comment to the utilities proposed requirements for testing the response time of components in nuclear plant safety systems.[8] In the past, it was adequate to test only the hardware downstream of the process sensor. However, this excluded the sensor itself (possibly the most important component in determining response times). The new revision recommends that the sensor also be tested in order to verify correct operation and adequate response time.

The purpose of this research was to evaluate the validity of the loop current step response test and self heating test in commercial RTD's and to advance the understanding and technology in sensor time response testing. Finally, this work provides documented experimental experience on in-plant testing and on a sensor used in Westinghouse PWR's and preliminary formalization of testing procedures to be used in in situ temperature sensor time response testing in operating pressurized water reactors.

1.4. ORGANIZATION OF THE TEXT

Chapter 2 gives a background description of resistance thermometry. A description of a resistance temperature detector (RTD) is given and

possible modes of failure are discussed. Resistance measurement instrumentation is also discussed.

In Chapter 3, the loop current step response (LCSR) method is introduced. The theory behind it and an analytical transformation is presented.

Chapter 4 describes the self-heating test. This test determines a sensor's response to incremental changes in internal heating. A possible method for converting the self-heating results empirically to responses that would be expected from the sensor following a fluid temperature step perturbation is offered.

The laboratory testing of a specific RTD using LCSR, self-heating, and plunge tests is described in Chapter 5. The results are used to develop empirical correlations to be used when the analytical transformation fails. A statistical analysis on the data is performed that allows one to draw conservative conclusions from the tests.

Chapter 6 describes the implementation of the LCSR tests at Turkey Point Nuclear Plant Unit 3. Examples of data are given and results are discussed.

Some concluding remarks and recommendations for future research work are given in Chapter 7.

CHAPTER 2

SYSTEM DESCRIPTION

2.1. RESISTANCE THERMOMETRY BACKGROUND

The effect of temperature variation on the resistance of materials was discovered early in the history of the study of electricity.[9] Practical applications of the phenomenon for temperature measurement have been limited to the past 100 years, probably because of the problems in making the sensing elements. The sensing element employs the resistance temperature effect to convert the action of a physical quantity into a measurable signal. Generally, when the temperature of a substance increases, its electrical resistance increases (except for thermistors).

Materials usable as sensing elements are divided into three classes: (1) metals, (2) semiconductors, and (3) insulators. The first two groups are used extensively as sensing elements. Insulators have not been used in the past and have only recently been exploited for their resistance-temperature qualities at very high temperatures where other materials become physically unstable. The parameter used to describe the resistance in materials is resistivity, ρ, and is defined as

$$\rho = \frac{RA}{\ell} \tag{2.1}$$

where

A = cross sectional areas of the material

R = electrical resistance at temperature T

ℓ = length of material.

For quantitative purposes, the three classes of materials are divided according to these ranges of resistivity: (1) in metals, resistivities vary from 10^{-4} to 10^{-7} ohm-cm, (2) in semiconductors, they vary from 10^{-3} to 10^{9} ohm-cm, and (3) in insulators, they are above 10^{10} ohm-cm.[4] Figure 2.1 shows the relative resistivities of typical materials.

Another quantity of interest is the temperature coefficient of resistance. This is defined as the change in the electrical resistance of a material for a given change in material temperature and is expressed in units of ohms per degree per ohm. For most metals, this coefficient is positive. For very pure metals, the change is practically linear over a large portion of the resistance temperature curve. This relationship is expressed as[4]

$$R_T = R_0(1 + \alpha T) \tag{2.2}$$

$$\alpha = \frac{R_T - R_0}{R_0 T} \tag{2.3}$$

$$\alpha = \frac{1}{R}\frac{dR}{dT} \tag{2.4}$$

where

R_T = resistance at temperature T in ohms

R_D = resistance at 0 °C in ohms

α = temperature coefficient of resistance

R_0 = ice point resistance in ohms.

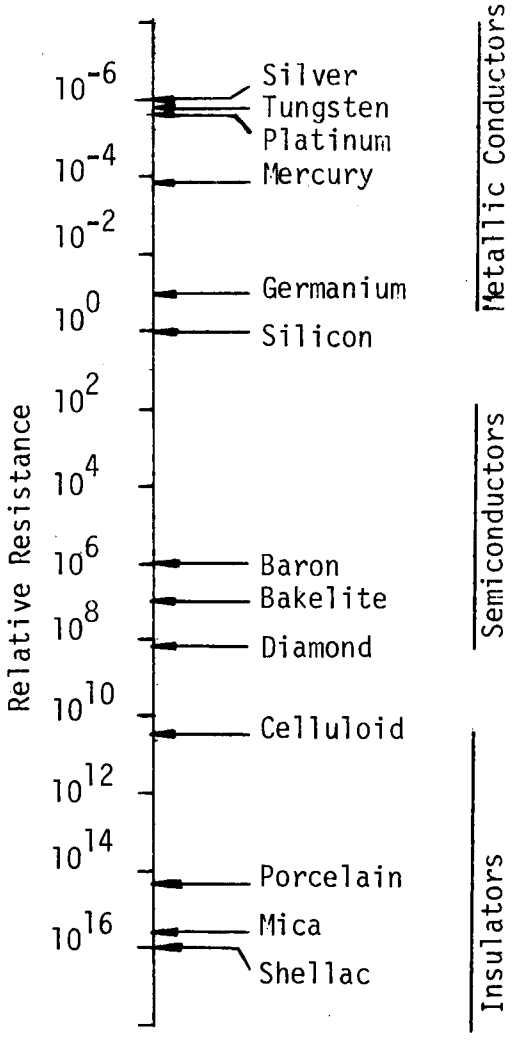


Figure 2.1 Relative Resistance of Materials.

If, however, the resistance temperature relationship is not linear, R_T can be written as an expansion of higher order terms to describe the behavior adequately. Figure 2.2 shows typical resistance temperature curves.[4]

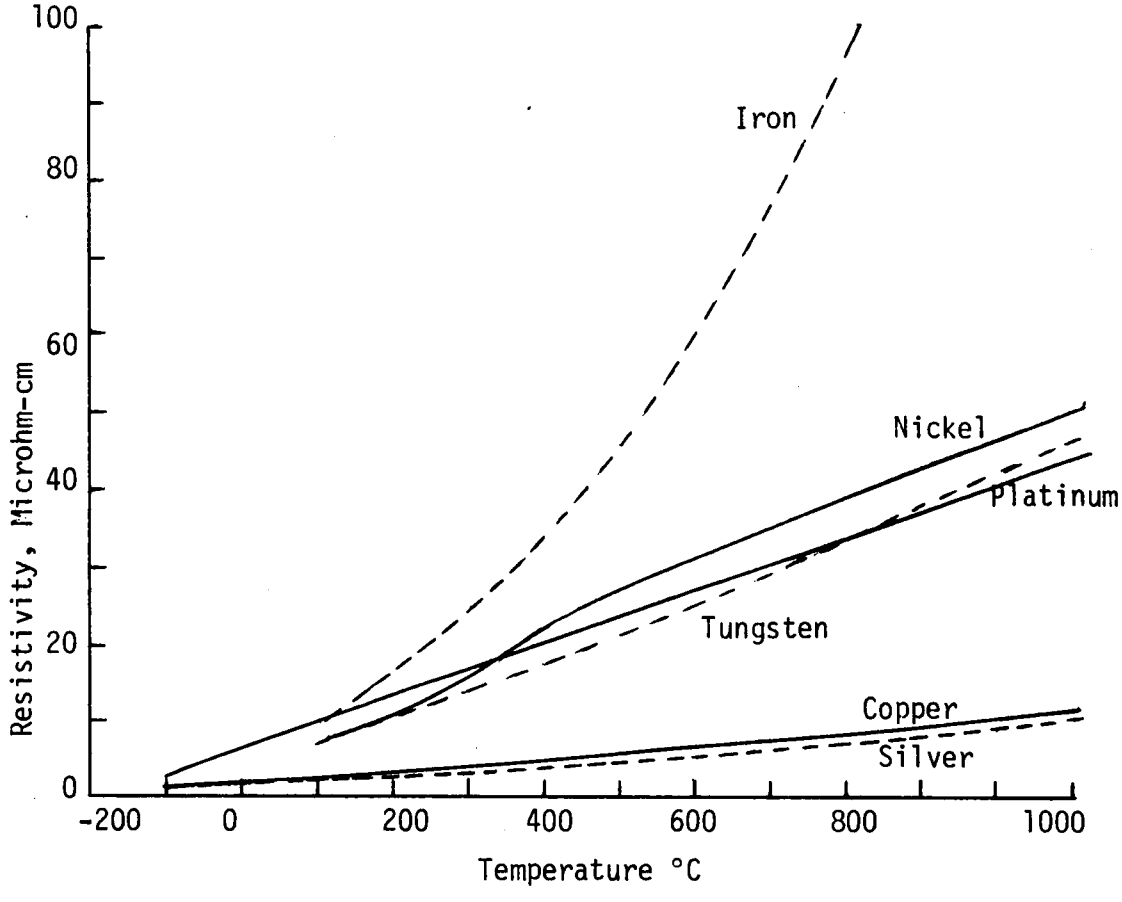


Figure 2.2 Resistance-Temperature Curves for Pure Metals.

There are five characteristics that a material should have in order to be considered for use as a sensing element. They are (1) high temperature coefficient of resistance, (2) linearity of the resistance temperature relationship, (3) high resistivity, (4) physical and chemical stability over a long period of time and wide temperature ranges, and (5) ductility and strength. The most suitable of all metals for resistance thermometry is platinum. Some of the more important properties of platinum for thermometry applications are listed in Table 2.1.[4]

TABLE 2.1

CHARACTERISTICS OF PLATINUM

Temperature Coefficient of Resistance	0.00392 Ω/Ω °C from 0 °C to 1000°C
Resistivity	60.0 Ω/cir mil* at 0 °C
Useful Temp Range	-258 °C to 900 °C
Minimum Practical Wire Diameter	.002 in.
Tensile Strength	18,000 psi annealed
Cost (1972 dollars)	$.04 to $0.07 per foot

*A circular mil is the area contained in a circle with diameter of 0.001 inch.

The resistance temperature relationship for platinum can be expressed with the Callendar Equation[4]

$$T = \left(\frac{R_T - R_0}{R_{100} - R_0}\right) 100 + \delta\left(\frac{T}{100} - 1\right) \frac{T}{100} \qquad (2.5)$$

where

T = temperature of material in °C

R_T = resistance at temperature T, ohms

R_D = resistance at °C ohms,

R_{100} = resistance at 100 °C ohms

δ = constant, characteristic of each winding, approximately 1.50 per degree centigrade.

2.2. DESIGN CONSIDERATIONS FOR RTD's USED IN PWR's

2.2.1. RTD Description

The resistance temperature detector (RTD) as shown in Figure 2.3 consists of a coiled platinum sensing element wound around a support core and enclosed in a stainless steel shell. The choice of structure depends on such factors as (1) compatibility of the resistance material with the environment, (2) requirements for the speed of the response, (3) extent of immersion permitted, and (4) expected mechanical and thermal stresses to be experienced. The ends of the platinum sensing element are connected to lead wires normally made of constantan inside the thermometer bulb. The insulated leads exit from the top and the shell is backfilled to a desired density with a material that electrically insulates the platinum element from the stainless steel shell while not appreciably hindering heat transfer from the shell to the element. Magnesium oxide, otherwise known as magnesia, is an adequate electrical insulator, is a sufficient heat transfer medium for RTD applications, and is normally used as a

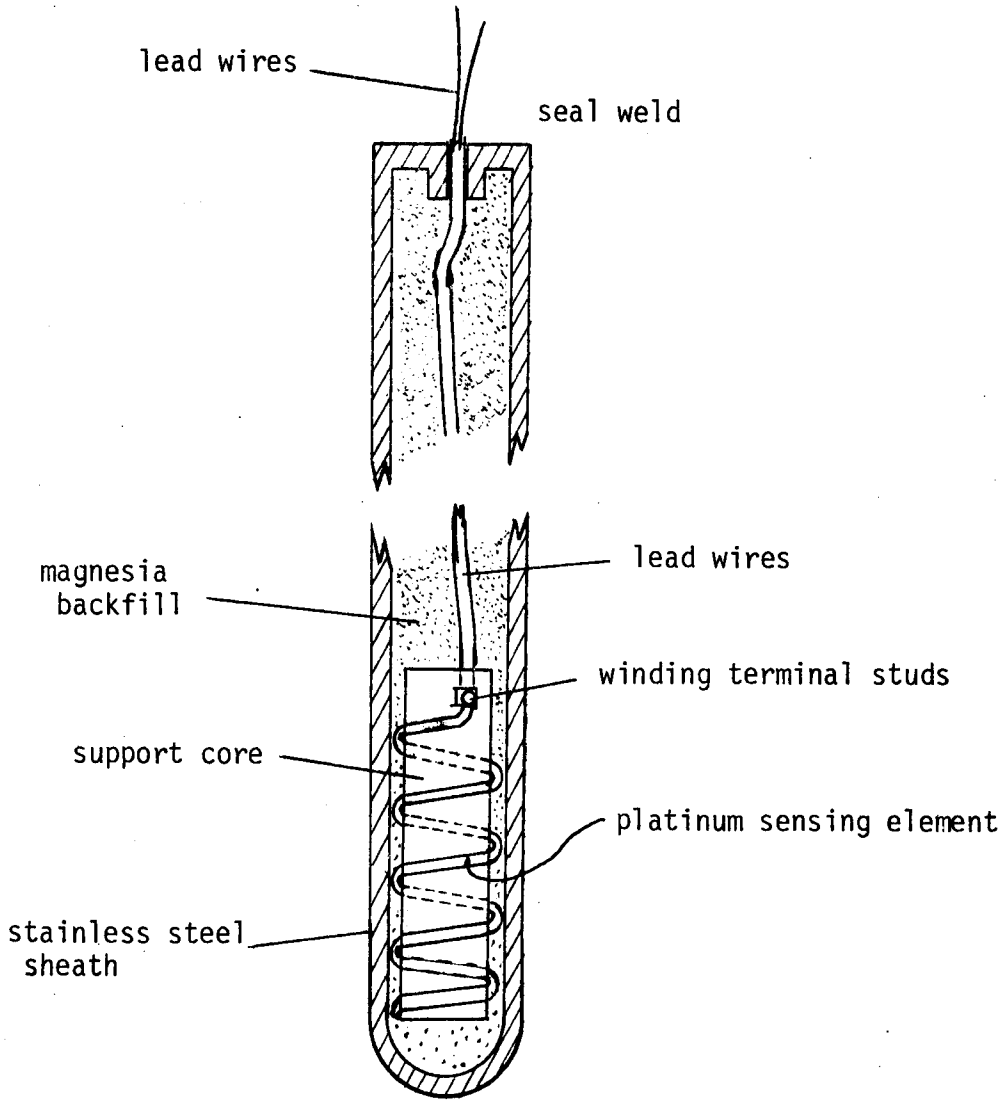


Figure 2.3. Resistance Temperature Sensor.

backfilling material. The top of the RTD is sealed with the leads protruding.

In the first step in a typical RTD fabrication process, the stainless steel tube sheath is plugged and seal welded at the bottom. The platinum wound around the support core is lowered inside with lead wires extending out of the tube. Magnesium oxide powder is poured into the tube and the RTD is centrifuged to obtain the desired compaction. The tube is cut at the proper length at the top and sealed with an epoxy resin. The diameter of the RTD ranges from one to four centimeters depending on the manufacturer.

2.2.2. RTD Heat Transfer Characteristics

Generally speaking, the response time of an RTD is proportional to the rate at which heat is transferred from the fluid, through the shell and insulating material, to the resistance coil. The response time is inversely proportional to the heat capacity of the sensor one tries to minimize both the heat transfer resistances between the fluid and the sensing element and the heat capacity of the construction material. Eventually, this becomes an optimization problem where the designer sacrifices some response speed for structural strength so the RTD is able to withstand the environmental conditions experienced in reactor coolant piping.

Two cases are of interest in reactor applications. One is when the temperature sensor is placed into a well or protective sheath that is welded into the coolant piping. The RTD in this case, as shown in Figure 2.4, has a thin shell since it will not directly feel the force

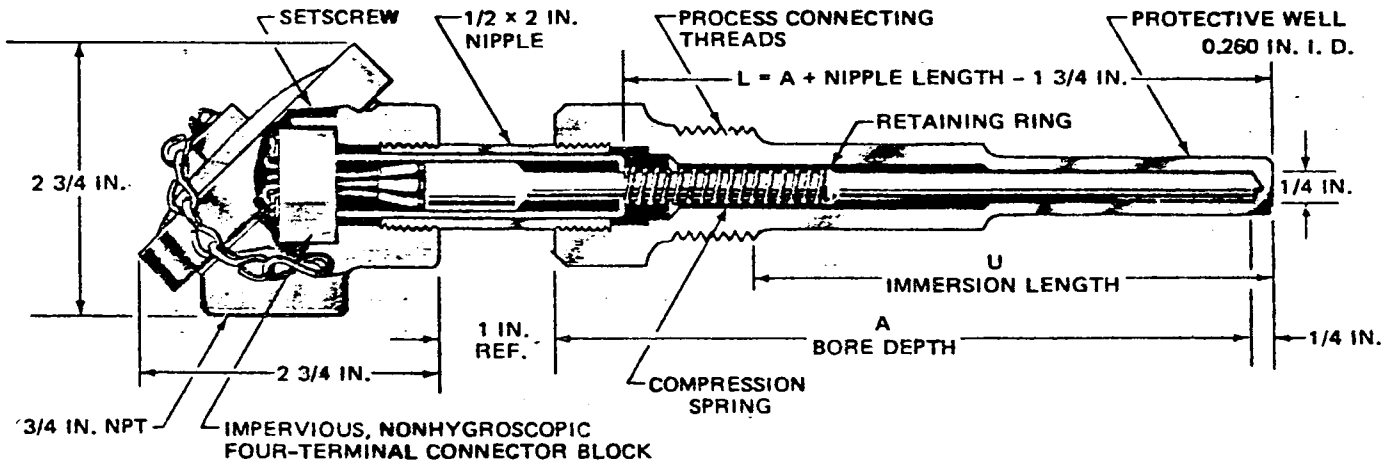


Figure 2.4 RTD in Thermowell.

of coolant flowing across it. This gives rise to a small annular region between the well wall and the sensor. A heat-conducting fluid is usually placed in the annular region to improve thermal contact between the well and the sensor sheath. In this application it is possible to remove the sensor from the well for inspection or replacement.

The other case is when the sensor is welded directly into the coolant channel and experiences the force of coolant flowing across it. In this case, the stainless steel containing the sensor is somewhat thicker in order to withstand the stress associated with the flow conditions present in the pipe. Figure 2.5 shows an immersion-type sensor.

2.3. MODES OF RTD FAILURE OR TIME RESPONSE DEGRADATION

The failure of a resistance temperature sensor to respond adequately to variations in fluid temperature could result from a failure internal to the sensor itself, or from a degradation of the response time of the sensor-well system. Failure modes of industrial platinum resistance thermometers were investigated by Carr[2] and discussed in Section 1.2.2.

In the course of this research, several additional potential modes of malfunction were identified. The response of an RTD is very sensitive to its heat transfer environment. The sensor is normally installed in a coolant pipe either alone or inside a thermowell. The sensor-well system protrudes into the channel up to a few inches. In this installation it is plausible to assume that reactor coolant "crud" comprised of corrosion products, coolant additives, or dirt could collect

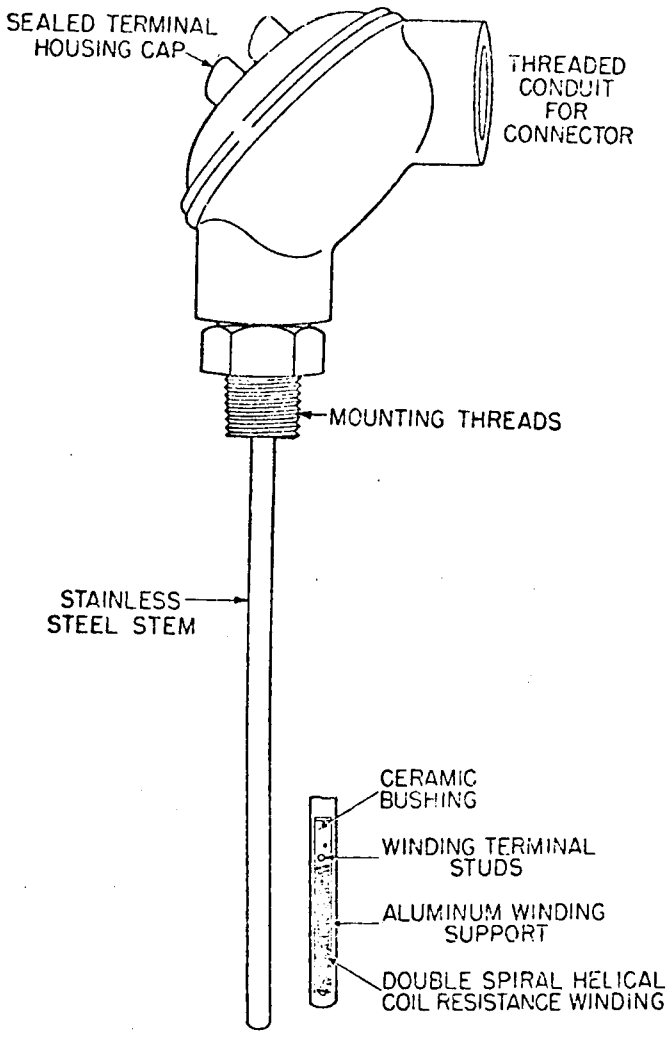


Figure 2.5 RTD Without Thermowell.

on the outside of the sensor-well system. This "fouling" would add resistance to heat transfer and would result in a lengthening of the time required for the sensor to respond to a fluid temperature change.

This fouling or scaling phenomenon has been observed in many reactors.[10] It would occur over a long period of time and would not be discovered in a simple calibration test. Response time testing would discover a significant change in sensor-well system response time and account for this mode of failure.

Another potential mode of failure is a change in the physical properties of the insulating material. The insulating material, usually magnesium oxide, is backfilled to a desired density as described in Section 2.2.2. A cross sectional view of an RTD would show that the space between the platinum element and the sheath is filled with the tightly packed magnesia powder interspersed with pores or gaps. Although the porosity of the filler is controlled, it may be possible for the filler to settle somewhat. This changes the density of the heterogeneous mixture and would result in a possible change in the effective thermal conductivity.

Coville and Dujolo[11] conducted experiments on the thermal conductivity of insulants used in sheathed cables. All of their results show that heat transfer by gas conduction in pores is a more important factor than conduction through the solid grains. The gas conduction also depended strongly on porosity, nature of the gas, and its pressure. The settling of the magnesia, and subsequent changes in thermal conductivity and heat transfer coefficient in the insulating medium would result in a

degradation of the response time of the sensor. This mode of failure might occur in a rather short period of time. The calibration of the sensor would not be affected, and normal testing would not discover the fault. In situ response time testing would discover the increase in the sensor response time.

Other potential modes of failure or time response degradation include improper installation of the sensor into a well, and failure to properly fill the sheath-well gap with an adequate portion of thermal contact fluid. Each of these potential failure modes would result in an increase in the response time of the sensor.

2.4. RTD PROCESS INSTRUMENTATION DESCRIPTION

A temperature change in a fluid is detected by a resistance thermometer as a change in resistance of the sensing element. Thus, the measurement of electrical resistance is required in resistance thermometry applications. For temperature measurements, a constant average current is supplied to the platinum resistance element. If the current passing through the element is small, the internal resistive "self-heating" is negligible. This "sensing" current, typically 1-2 mA is used to detect the change in resistance of the resistance temperature element.

2.4.1. Types of Bridges

The most widely used method of measuring resistance involves bridge circuits. The bridge technique is a measurement in which three known resistors are balanced against the fourth unknown varying resistance

(the RTD). For many applications, a simple Wheatstone bridge as shown in Figure 2.6 offers adequate accuracy and sensitivity for industrial resistance measurements. However, as more accuracy is required in the resistance measurements, multiple-wire or multiple-bridge circuits are employed. These more complex circuits are of great value for minimizing the effects of lead wire (which can be hundreds of feet long) and contact resistances, ambient temperature effects on lead wire resistances, and random resistance variation errors.

Four types of bridges are currently the most common ones employed in resistance thermometry. They are: (1) the Wheatstone, or two-wire, bridge, (2) three-wire bridge, (3) four-wire bridge, and (4) the multiple bridge. The difference between (1), (2), and (3) is the number of connections to the sensing element. The multiple bridge is a combination type bridge used for only the most accurate measurements.

2.4.1.1. Two-wire bridge. The circuit diagram for a typical Wheatstone bridge is shown in Figure 2.7. This configuration consists of two relatively low resistance leads x and y connecting the resistance coil with the measuring apparatus. The resistors a, b, and d are accurately known resistors with d being a variable resistance decade box. The resistor RTD is the unknown resistor, the resistance temperature element.

It is important to note here that the total resistance of the leg containing the resistance sensor is a series resistance comprised of the platinum element plus the resistance of the two lead wires x and y. Therefore, the leads x and y, unless of very low resistance, can add

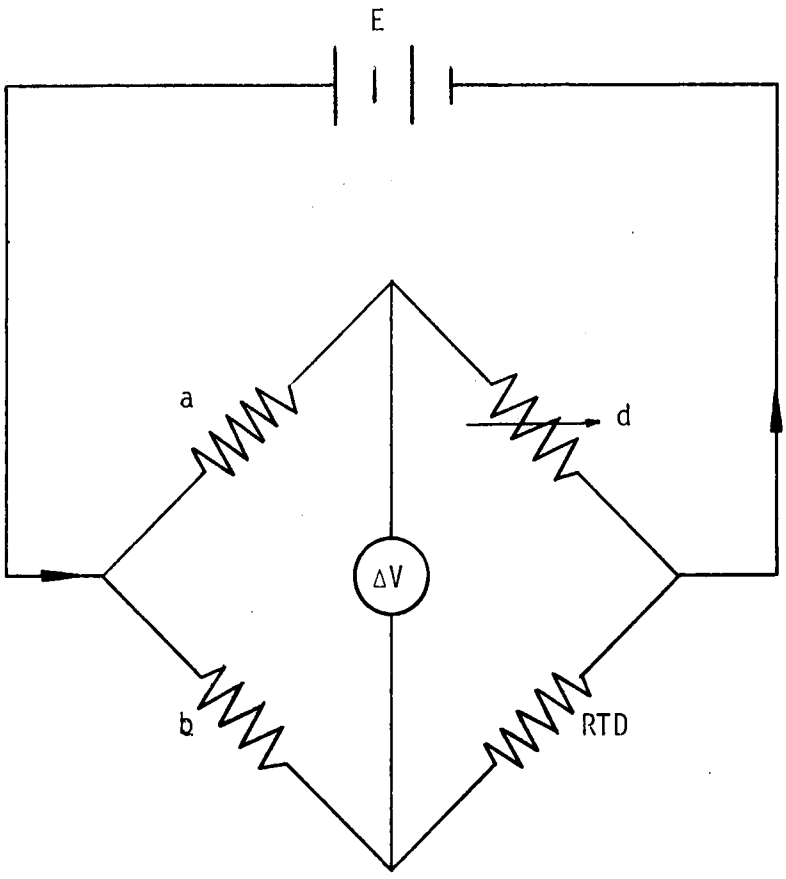


Figure 2.6 Wheatstone Bridge.

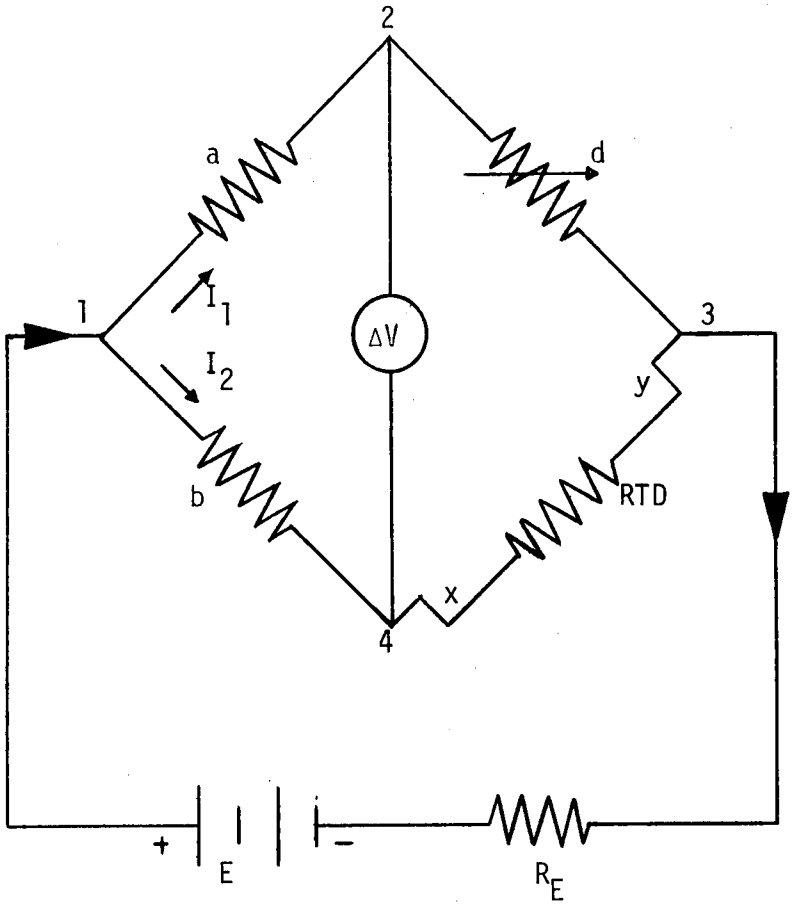


Figure 2.7 Two-Wire Bridge Circuit Diagram.

appreciably to the apparent resistance of the RTD, and could be a large source of error. Even though the resistance of the leads may be accurately known and allowed for in the calibration measurement of the sensor, the leads are subject to ambient temperature changes, and accompanying resistance changes. The effects of the lead wire resistances can be mitigated, however, in either of two ways. The apparent resistance of the RTD leg is comprised of the leads x and y in series with the temperature sensor. If the resistance of the RTD is chosen to be of the order of 100 ohms, the inherent error could be reduced to a few percent because typical lead wire resistances are less than 5 ohms. The other way to compensate for the lead wire effects concerns the use of the three- or four-wire connections which will be discussed in Sections 2.4.1.2 and 2.4.1.3.

A voltmeter or galvanometer is inserted across terminals 2 and 4 to indicate the balance of the bridge. A voltage source E and a resistor R_E are employed to control the current to the bridge. The placement of the power supply and the voltmeter can be interchanged. However, for a particular configuration of the resistors in a given application, it may be of value to interchange the voltmeter and the voltage source. Kotter[12] has developed the criterion for maximum sensitivity in balancing the bridge which indicates the best location for the voltmeter and the power supply. The circuit analysis of the two-wire bridge is given in Appendix A.

2.4.1.2. Three-wire bridge. The three-wire bridge design, as shown in Figure 2.8, is the most practical and widely used method in industrial resistance thermometry today.[13] In this configuration, two of the sensing leads, y and z are connected directly to one end of the platinum

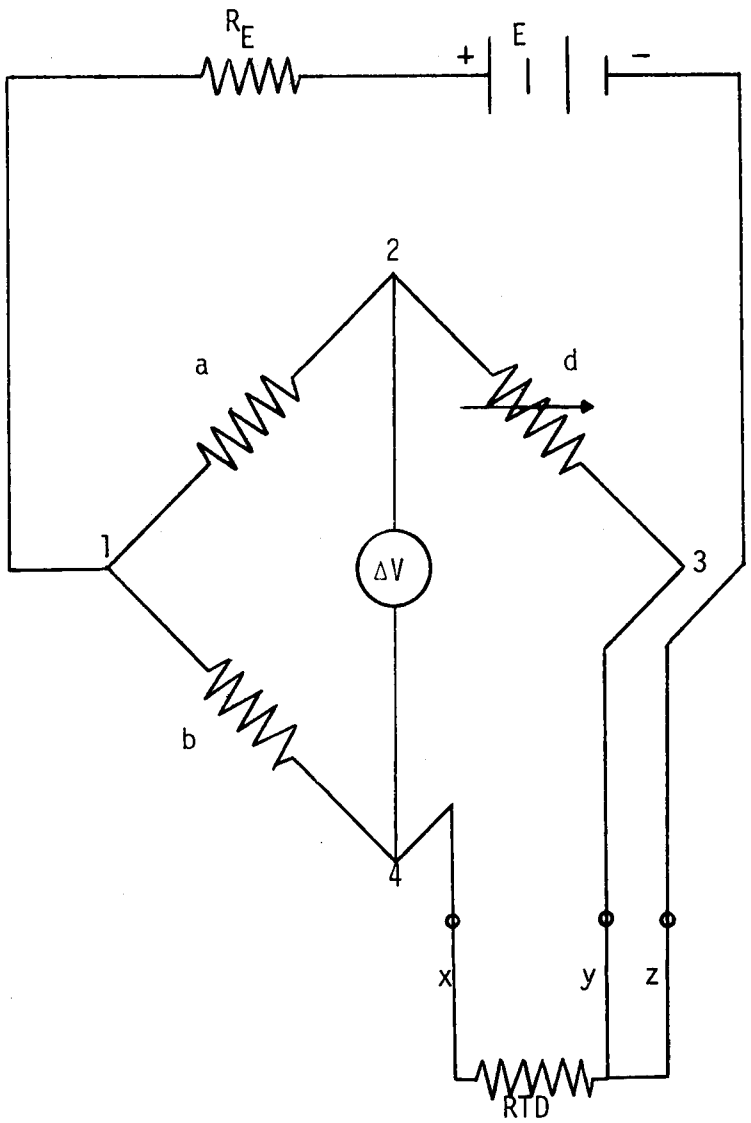


Figure 2.8 Three-Wire Bridge Circuit Diagram.

resistance element at a common point. The third lead x is connected to the other end of the winding. As a result, the resistance of lead x is added to the bridge arm b, while the resistance of lead y is added to d, thereby dividing the lead resistance and regaining a balance in the bridge circuit. This gives the effect of cancelling the lead wire resistance effect upon the bridge output voltage.

Although this method compensates for the effect of lead wire resistance, thus permitting the use of longer, higher resistance leads, the ultimate accuracy of the circuit depends upon x and y having equal resistance. For this reason, they should be identical in size, length, and material and should be placed side by side throughout their length so as to remain at the same temperature. Although their temperature conditions may change, their resistance remains equal, and such environmental perturbations have no effect on the bridge output reading. The circuit analysis of the three-wire bridge is given in Section 2.4.2.

2.4.1.3. Four-wire bridge. The four-wire bridge is used in measurements where a high degree of accuracy is needed such as in applications where the bridge is far removed from the sensor or the lead wires from the sensor to the bridge are unbalanced. Unbalanced lead wire resistance can occur if: (1) the lengths of each lead are not the same; (2) they do not traverse the same route to the bridge, thereby becoming susceptible to unequal environmental effects; or (3) they are not made of the same material. Figure 2.9 depicts a typical four-wire bridge. This bridge is used with an RTD that has four leads as shown in Figure 2.10. Another four-wire bridge is shown in Figure 2.11. This bridge is used

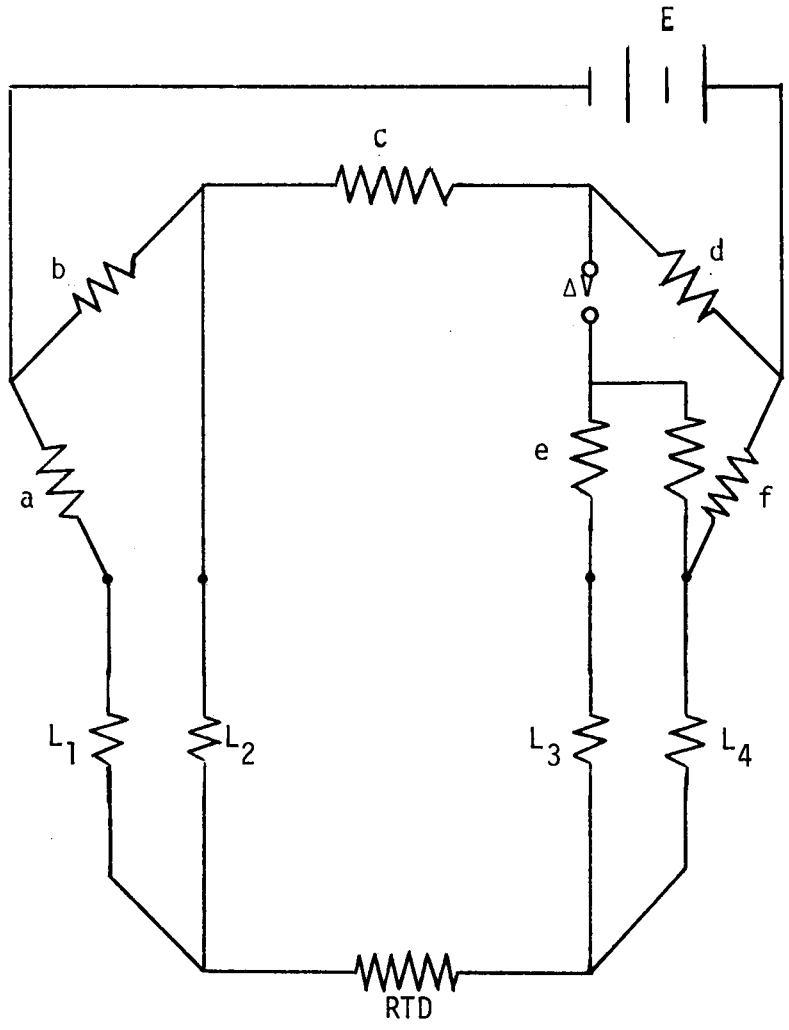


Figure 2.9 Four-Wire Bridge.

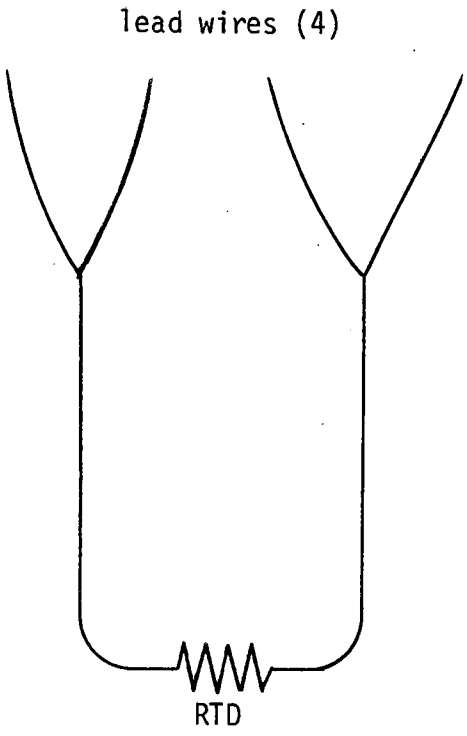


Figure 2.10 RTD Lead Wires for 4-Wire Bridge in Figure 2.9.

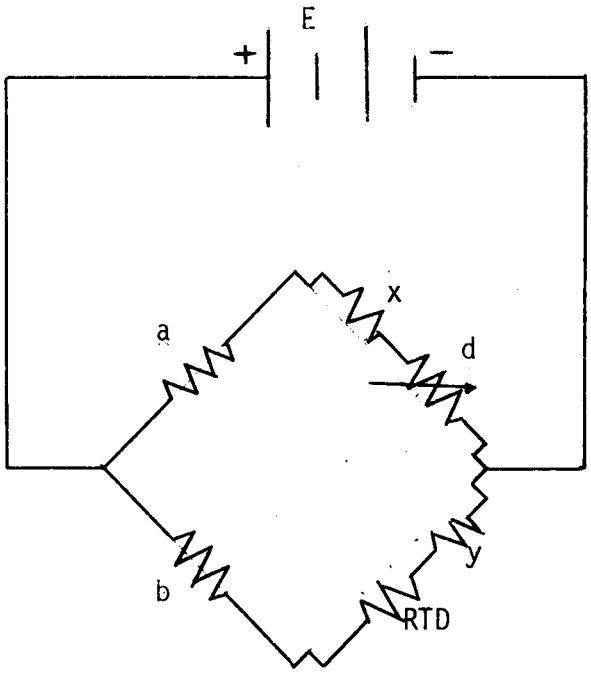


Figure 2.11 Alternative Four-Wire Bridge Configuration.

in conjunction with the RTD shown in Figure 2.12. The dummy lead wires are placed in series with R_d, thereby equalizing the element lead wire resistance in the other bridge arm.

2.4.1.4. Multiple bridge. Wheatstone bridge measurements can encounter errors due to random or systematic resistance variations occurring at the branch points where the unknown resistance is joined to the remainder of the bridge. Accurate measurements of resistance or of an incremental change in resistance requires particular attention to elimination of these errors. These random resistances, labeled "random contact resistances" (rcr's) by Warshawsky,[6] may be due to leads of variable temperature, terminals, connectors, switches, or slip rings.

The first-order effects of random resistance variations can be eliminated by employing multiple-bridge circuits. Multiple bridges add auxiliary resistor pairs at each bridge corner where variations might occur. A general discussion of multiple-bridge circuits is given by Warshawsky.[6] A form of the basic circuit is shown in Figure 2.13. The original Wheatstone bridge (A, B, S, and R) is highlighted by boldface lines. The bridge is assumed to possess random junction resistances r_{ab}, r_{cd}, r_{fg}, and r_{hk}. To eliminate first-order errors due to these resistances, the junction is "bridged" by an auxiliary resistor pair such as (a, b) or (c, d). This procedure is followed at each corner at which an undesirably large rcr might occur. In this way, the errors induced by random contact resistances can be added out.

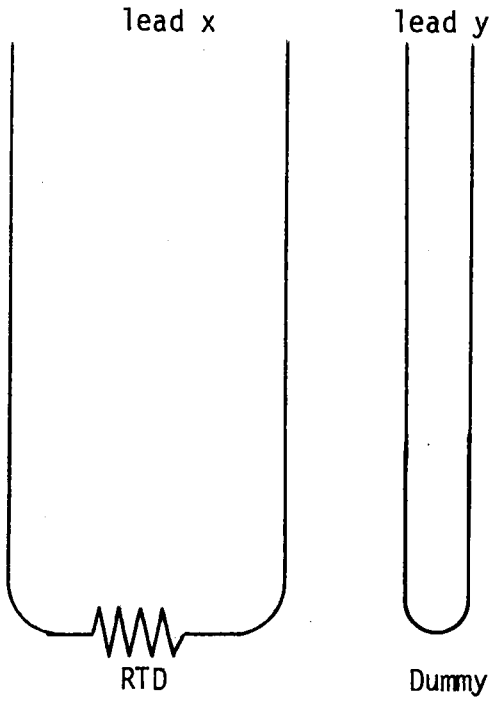


Figure 2.12 RTD Lead Wires for Alternative Four-Wire Bridge.

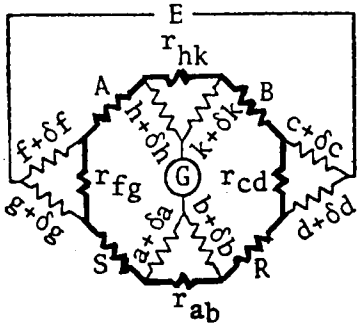


Figure 2.13 Multiple Bridge Circuit Diagram.

2.4.2. Results of Circuit Analysis for Two- and Three-Wire Bridges

It is helpful to derive the circuit equations when evaluating the merits of a particular electrical bridge. An equation relating the change in output voltage divided by the initial voltage ($\Delta V/V$) and the resistances in the bridge network can offer a comparison of the accuracy of each bridge.

2.4.2.1. Two-wire bridge. The circuit diagram for the two-wire bridge was given in Figure 2.7, page 24. The results of a circuit analysis of this basic two-wire bridge (Appendix A) are given below and lead wire resistance effects are discussed.

The equation from Appendix A giving the normalized change in voltage output of the bridge, with no lead wire resistance is,

$$\frac{\Delta V}{V} = \frac{R_b R_d - R_a R_{RTD}}{(R_a + R_d)(R_b + R_{RTD})} . \qquad (2.7)$$

This represents the true output of the bridge circuit (minus lead wire effects); that is, the response of the RTD.

If, however, there exists an appreciable resistance contribution in the lead wires, then the output of the bridge is affected. Replacing R_{RTD} by the sum of the sensor resistance and an arbitrary lead wire resistance in series, we obtain:

$$R_{RTD} = R_{RTD} + R_{Leads} . \qquad (2.8)$$

The resulting substitution of Eq. (2.8) into Eq. (2.7) after simplification (see Appendix A) gives

$$\frac{\Delta V}{V} = \left(\frac{\Delta V}{V}\right)_{RTD} \cdot \left[\frac{R_b+R_{RTD}}{R_b+R_{RTD}+R_d}\right] - \frac{R_a}{(R_a+R_d)} \cdot \left[\frac{R_{LEADS}}{R_b+R_{RTD}+R_{LEADS}}\right] . \qquad (2.9)$$

where $\left(\frac{\Delta V}{V}\right)_{RTD}$ is defined by Eq. (2.7).

The effects of lead wire resistance on the output of the bridge as the resistance of the RTD changes can be obtained from Eq. (2.9). Figure 2.14 shows the voltage change as a function of changes in R_{RTD} for several values of R_{LEADS}. For example, Figure 2.14 shows that for an increase in the sensing current of 50 mA (resulting in an increase in R_{RTD} of approximately 3 ohms) the relative error due to a lead wire resistance of 2% of the RTD resistance is less than 1%. Figure 2.15 shows the error in $\frac{\Delta V}{V}$ as a function of the lead wire resistance for a selected change in RTD resistance.

2.4.2.2. Three-wire bridge. The three-wire bridge, as shown in Figure 2.8, page 26, places lead wire resistances x and y in opposite arms of the resistance bridge. Lead wire resistance z is in series with the power supply and only affects the output of the power supply. In order to obtain a relation for $\frac{\Delta V}{V}$ we can use Eq. (2.7) and replace R_b and R_{RTD} by:

$$R_b = R_b + x \quad \text{and} \quad R_{RTD} = R_{RTD} + y .$$

Assuming the lead wire resistances to be equal (x=y=L) we obtain,

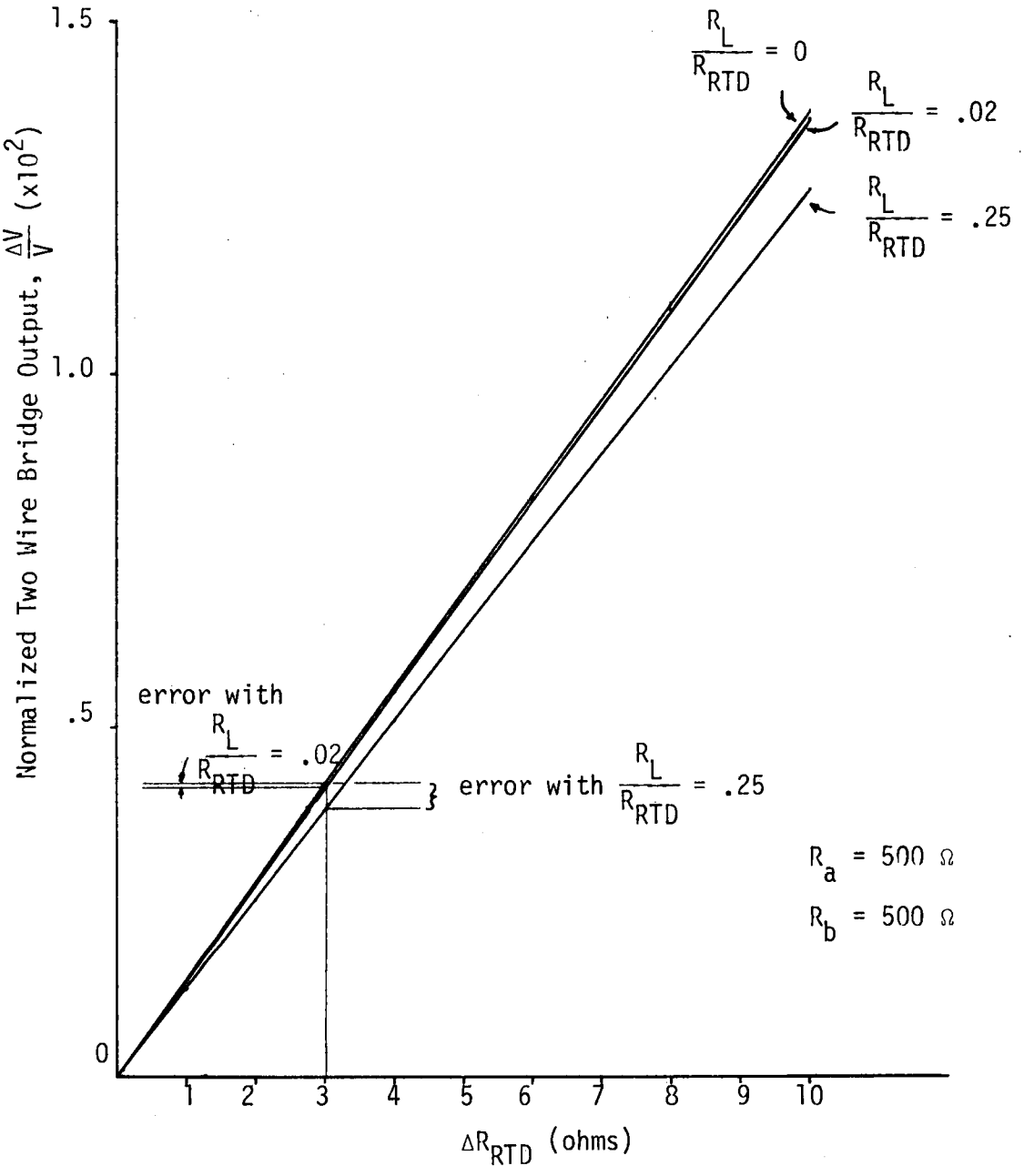


Figure 2.14 Lead Wire Resistance Effects on Two-Wire Bridge Output.

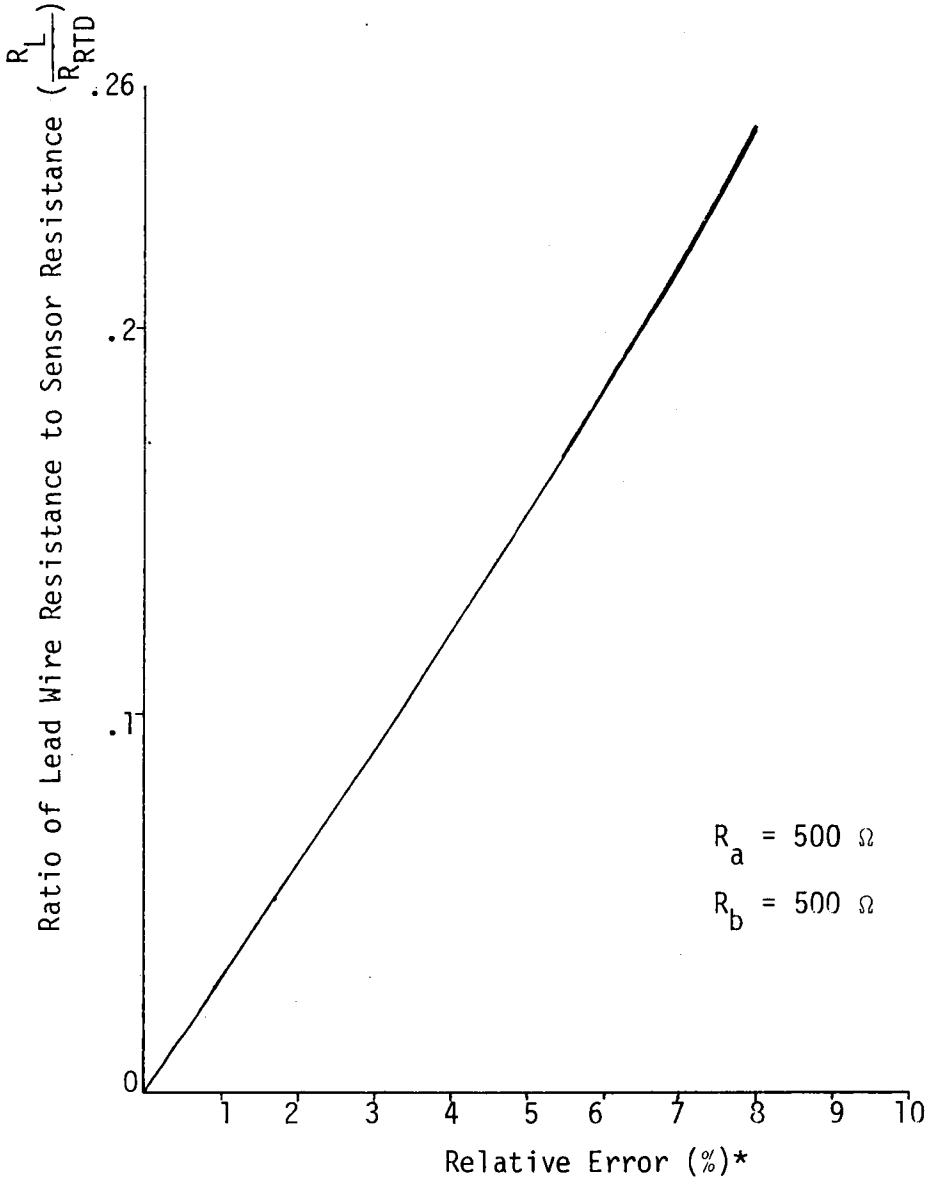


Figure 2.15 Two-Wire Bridge Error Versus R_L/R_{RTD}.

*For a change in resistance of the RTD of 3 ohms.

$$\frac{\Delta V}{V} = \frac{(R_b+L)R_d - (R_{RTD}+L)R_a}{(R_a+R_d)(R_b+R_{RTD}+2L)} \quad . \tag{2.11}$$

Simplifying,

$$\frac{\Delta V}{V} = \frac{R_bR_d - R_aR_{RTD}}{(R_a+R_d)(R_b+R_{RTD})} \cdot \frac{R_b+R_{RTD}}{(R_b+R_{RTD}+2L)} + \frac{(R_d-R_a)2L}{(R_a+R_d)(R_b+R_{RTD}+2L)} \cdot \tag{2.12}$$

Recognizing that

$$\frac{R_bR_d - R_aR_{RTD}}{(R_a+R_d)(R_b+R_{RTD})} = \left(\frac{\Delta V}{V}\right)_{TRUE} , \tag{2.13}$$

we obtain

$$\left(\frac{\Delta V}{V}\right)_{\substack{\text{three-}\\ \text{wire}\\ \text{bridge}}} = \left(\frac{V}{V}\right)_{TRUE} \cdot \frac{R_b+R_{RTD}}{(R_b+R_{RTD}+2L)} + \frac{R_d-R_a}{R_d+R_a} \cdot \left[\frac{2L}{R_b+R_{RTD}+2L}\right] \cdot \tag{2.14}$$

Equation (2.14) relates the output of the three-wire bridge to the response of the RTD. It can be shown that the effects of lead wire resistance are mitigated by this bridge configuration.

2.4.3. RTD Implementation in PWR's

Resistance temperature detectors of the type mentioned previously are used in pressurized water reactors. Normally, hot-leg and cold-leg temperature measurements are made for control and protection. The reactor control system uses the highest of the temperature measurements.

One of the main differences in resistance thermometry throughout the nuclear industry is the location of the temperature sensor in the coolant piping and the means by which it is installed. In Westinghouse plants, the sensors are located in a two-inch reactor coolant loop by-pass line.[16] The RTD's are installed circumferentially at approximately 120° intervals spaced along the length of a manifold welded to the by-pass line. Each of the temperature probes extend several inches into the coolant stream. The two-inch line leading to the RTD manifold provides adequate mixing to give an average temperature measurement.[16] A drawback of having the sensor placed in a by-pass line is that an added delay time is present in the overall system response. This is caused by the time it takes for the coolant to pass from the main stream to the sensor in the by-pass line.

The RTD's are installed directly into the main hot leg and cold leg piping in Combustion Engineering and in Babcock and Wilcox plants.[16] Four sensors are installed at 90° intervals spaced along the pipe in the hot leg. These RTD's are used for reactor protection. Another single RTD is placed also in the hot-leg for use in controlling the reactor (Reactor Regulating System). In the cold leg, there are two RTD's that are used for reactor protection and a single RTD used for control.

In each of the reactor systems mentioned above, several RTD's are used for reactor safety functions. One of the systems included a separate RTD for normal operation and control monitoring. Except for this case, there are no "installed spares" or backups available. If one or more of the RTD's fail, depending upon the particular vendor safety logic, the redundant two out of four logic is reduced to two out of three or less.[16] A reactor in such a condition might have to undergo a reduction in power to maintain operation, or in cases of more than one failure, might have to shut down to satisfy its technical specifications.

CHAPTER 3

THE LOOP CURRENT STEP RESPONSE (LCSR) TEST

3.1. DESCRIPTION OF TESTING METHOD

During normal operation of a resistance temperature detector (RTD) a small sensing current, typically 1-2 mA, is passed through the resistance element, and fluid temperature changes are determined by measuring the change in resistance of the element. The LCSR test procedure involves imposing a step change in the sensing current to 20-60 mA from the steady state value of 1-2 mA, to effectively increase the sensor internal temperature a few degrees above ambient temperature through ohmic heating. After a steady state condition is reached, the resistance heating is terminated by returning the sensing current to its original steady state value. The sensor output is monitored throughout the transient with the resistance measurement obtained using the two wire bridge.

3.2. THEORY AND PRINCIPLE OF METHOD

The sensor output from an LCSR test provides the response to a step change in the internal heating of the sensor. However, the response of interest is the response of the sensor when subjected to a change in fluid temperature outside the sensor assembly.

The difference between the LCSR test response and the desired response may be represented as solutions to a single differential equation with two different sets of boundary or initial conditions. The

response of every dynamic heat transfer system depends upon its heat transfer resistances, heat capacities, initial conditions, and forcing functions. The resistances and capacities are the same in each case, but the forcing functions for the LCSR test are different from those for a change in temperature of the surrounding fluid.[14]

Figure 3.1 depicts a typical signal measured during a LCSR test. If the two wire bridge is exactly balanced initially, $R_d = R_{RTD}$. The initial voltage output is given by (assuming $R_a = R_b$)

$$\Delta V = \left[\frac{(R_d - R_{RTD})R_a}{(R_a+R_d)(R_a+R_{RTD})}\right]_0 V_0 \qquad (3.1)$$

where

the subscript, 0, denotes conditions during initial low current operation.

When the current is stepped up, there should be an exponential change in the voltage output which reflects the response of a sensor and is given by,

$$\Delta V = C\ \Delta R_{RTD}\ V_N \qquad (3.2)$$

where

$C = \dfrac{R_a}{(R_a+R_d)(R_b+R_{RTD})}$ (assumed to be approximately constant)

ΔV = change in ΔV

V_N = voltage drop across the bridge.

The voltage output then settles out after a period of time and the bridge voltage, V_N, is stepped down to its original value at t_2. At this time, the voltage output decays exponentially to its original value.

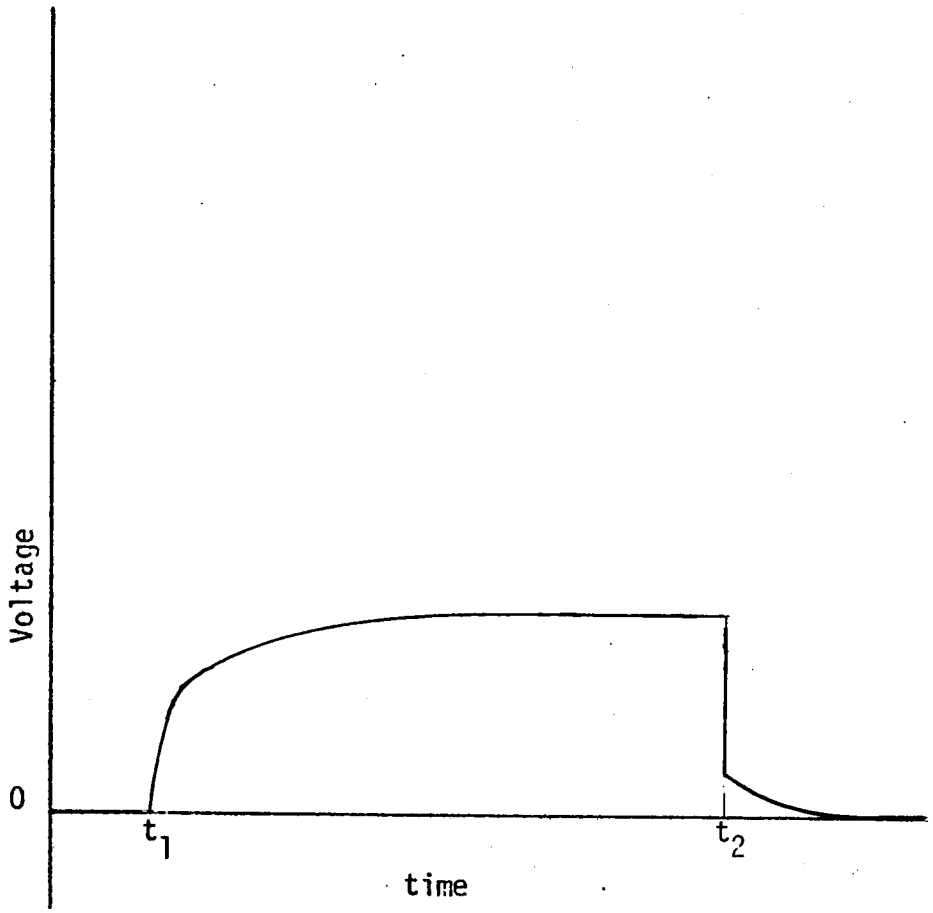


Figure 3.1 LCSR Test Result with $R_d = R_{RTD}$ Initially.

Actually, the resistance of the decade box, R_d, never exactly equals the resistance of the RTD. If the test is initiated with $R_d > R_{RTD}$, then the initial voltage output is not zero and the test proceeds as shown in Figure 3.2. The initial voltage is given by

$$\Delta V_0 = \left[\frac{(R_d - R_{RTD})R_a}{(R_a+R_d)\ (R_a+R_{RTD})}\right]_0 V_o > 0. \tag{3.3}$$

When the current is stepped up, there is an instantaneous rise in ΔV to a value

$$\Delta V_I = \left[\frac{(R_d - R_{RTD})R_a}{(R_a+R_d)\ (R_a+R_{RTD})}\right]_0 V_N \tag{3.4}$$

where

ΔV_I = instantaneous change in ΔV due to a change in V.

Then the signal begins its exponential rise to a steady state value of

$$\Delta V_F = \Delta V_I + \left[\frac{(R_d - R_{RTD})R_a}{(R_a+R_d)\ (R_a+R_{RTD})}\right]_N V_N \tag{3.5}$$

where

ΔV_F = final change in ΔV after change in V

N = subscript denoting new values after change in V.

When the current is lowered, the voltage output drops then begins its exponential decay back to the original steady state value.

It is not easy to discern the increase in voltage due to the current step from the increase due to the change in RTD resistance. This point is important to know in order to analyze the portion of the data that reflects only the response of the RTD.

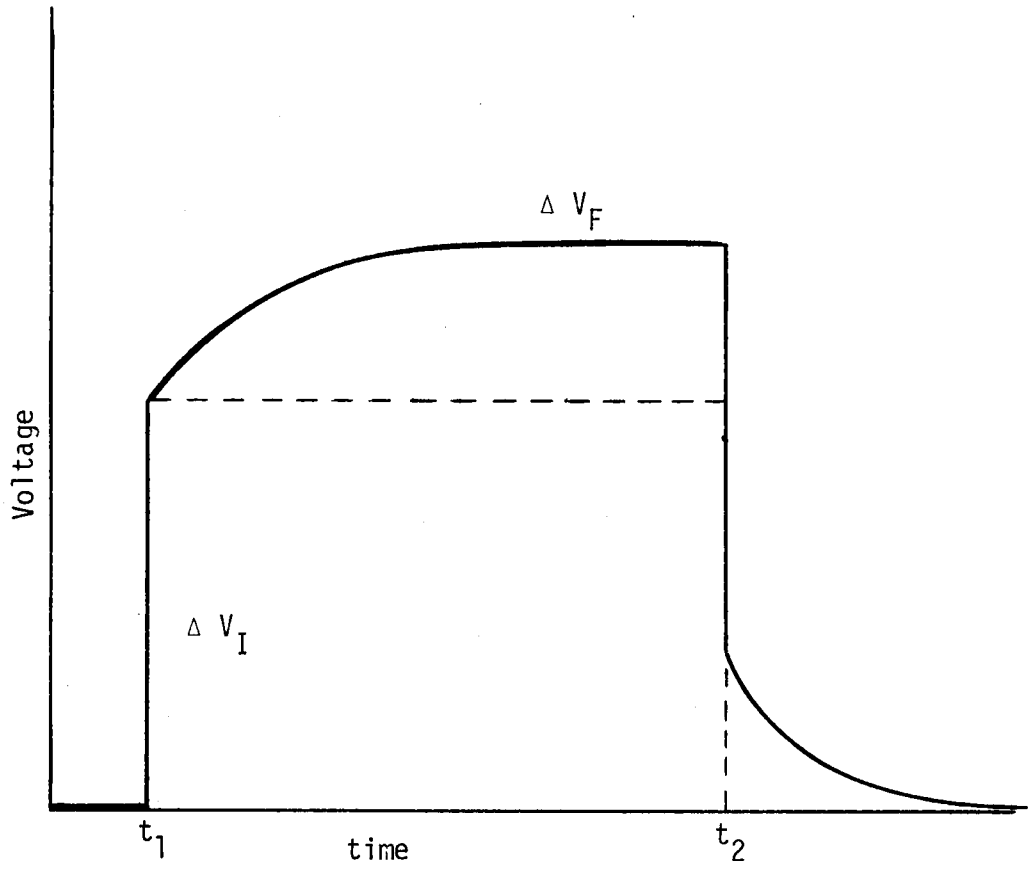


Figure 3.2 LCSR Test Result with $R_d > R_{RTD}$ Initially.

If an adjustment of the decade box is made so that initially $R_d < R_{RTD}$, then the initial steady state voltage output is given by

$$\Delta V_0 = \left[\frac{(R_d - R_{RTD})R_a}{(R_a+R_d)(R_a+R_{RTD})}\right]_0 V_0 < 0. \qquad (3.6)$$

If the LCSR test is begun with this initial condition, the response of the RTD is as shown by Figure 3.3. When the current is increased, there is an instantaneous negative voltage change given by Eq. (3.4).

When the change due to this effect is over, the sensor response effects begin and the exponential rise starts. After reaching the steady state condition at the higher current, the current is returned to its original value. There is an instantaneous drop in the voltage output and the response of the sensor decays exponentially to its original value.

When the test is executed with $R_{RTD} > R_d$, the presence of the negative spike allows one to see when the transient due to the current change is over and the response of the sensor begins. This assumes that the current change and the associated voltage drop occur in a negligible amount of time when compared to the sensor response time. Tests performed with the circuit nulled compared to tests with the spike indicate that the current transient effects occur in a very short time compared to the response time of any sensor and the effect of the spike is negligible.

It is important to note that, while a single LCSR test is performed and data are taken throughout, there are two sections of data over which the sensor time response may be determined (heating or cooling). However, because of the difficulty in determining the exact time when the bridge circuit transient ends and the sensor response begins, only the heating segment or the coolant segment can be analyzed in any single test. If the

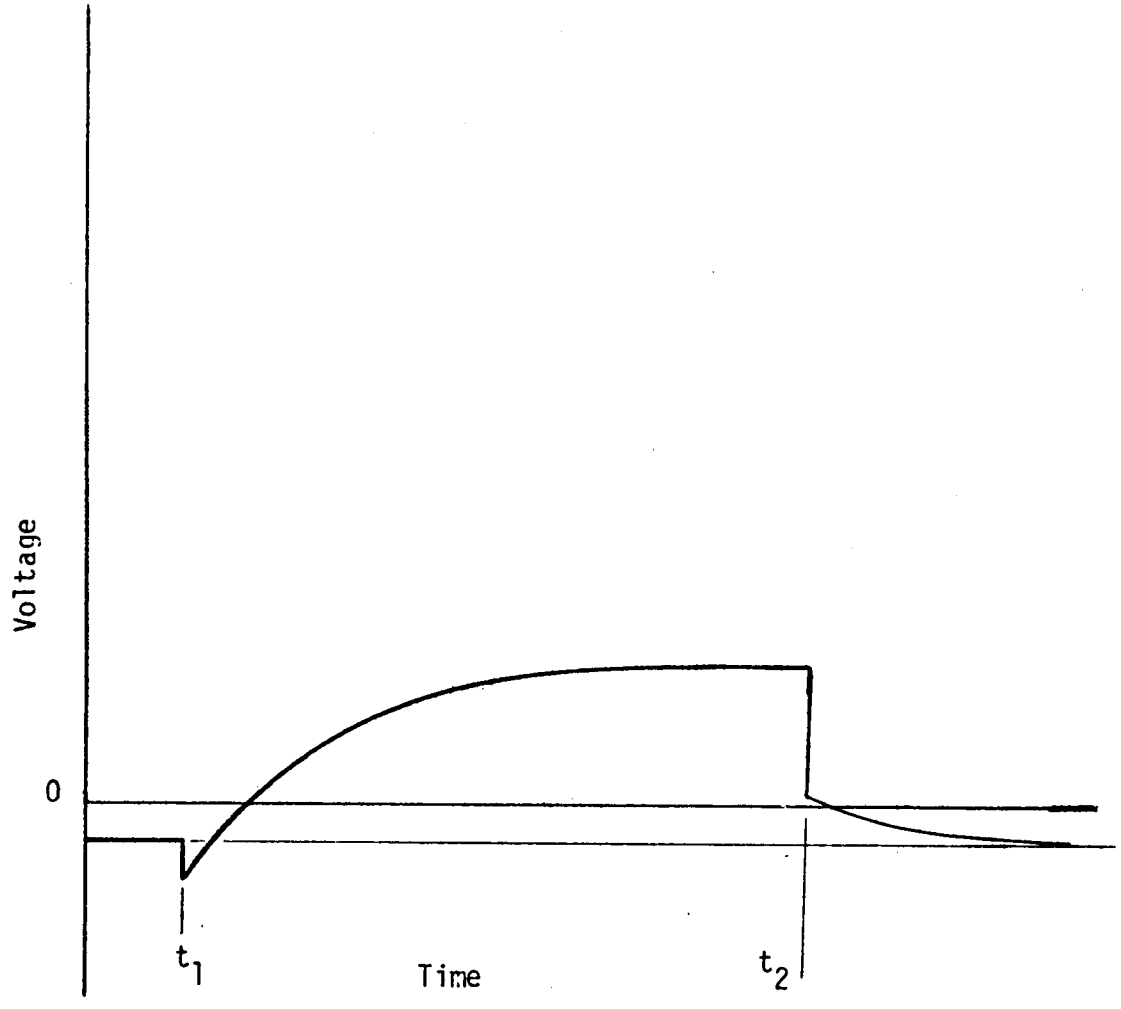


Figure 3.3 LCSR Test Result with $R_d < R_{RTD}$ Initially

circuit is exactly balanced before the test, it is difficult to determine the exact time when the voltage transient ends and the sensor response begins.

3.3. DISCUSSION OF ANALYTICAL TRANSFORMATION

In order to develop the analytical method required to convert LCSR results into responses equivalent to a step change in fluid temperature, a heat transfer model of the sensor system must be obtained. The transformation method must be insensitive to physical parameters inherent in the system and to the particular geometric details of the system. This is due to the requirement that the response time testing method should be usable in situ on all different types and configurations of sensors and also because the physical parameters (thermal conductivities, densities, and specific heat capacities) are usually not known accurately.

There are two choices for the basis of the analysis method; that is, using either a distributed-parameter model or a lumped-parameter model. A distributed-parameter model consists of the partial differential equations of heat conduction. Such a model as this would require detailed information on the physical properties and system geometry, and for this reason, it is judged to be impractical. For these reasons, a lumped-parameter model should be used.

The analytical transformation for converting LCSR results into equivalent fluid temperature step responses was developed by Kerlin.[14] Kerlin considered one- and two-dimensional lumped-parameter analysis and an application of distributed-parameter analysis. Of course, results from a lumped parameter model approach the results from a distributed

parameter model as the number of lumps increases. From this work, Kerlin concluded that use of a two-dimensional lumped-parameter model would require preliminary knowledge which is not available for LCSR applications. Therefore, the discussions of his transformation in this thesis will be limited to systems in which the assumption of one-dimensional geometry is valid.

A lumped-parameter heat transfer model in one-dimensional geometry can be represented by a series of nodes as shown in Figure 3.4. The temperatures are evaluated at the nodal points T_1, T_2, and T_3 and heat is transferred across thermal resistances R_{12} and R_{23}. The dynamic heat transfer equation governing the model heat transfer process for any node i is

$$MC \frac{dT_i}{dt} = \frac{1}{R_{12}}(T_{i-1} - T_i) - \frac{1}{R_{23}}(T_i - T_{i+1}) + Q_i \qquad (3.7)$$

where

M = mass of material in node i,

C = specific heat capacity of material in node i,

R_i = heat transfer resistance,

Q_i = heat generation rate in node i.

This can be rewritten in the more convenient form:

$$\frac{dT_i}{dt} = a_{i,i-1}T_{i-1} - a_{i,i}T_i + a_{i,i+1}T_{i+1} + b_iQ_i \qquad (3.8)$$

where

$$a_{i,i-1} = \frac{1}{MCR_{12}}$$

$$a_{i,i} = \frac{1}{MC}\left(\frac{1}{R_{12}} + \frac{1}{R_{23}}\right)$$

$$a_{i,i+1} = \frac{1}{MCR_{23}}$$

$$b_i = \frac{1}{MC}.$$

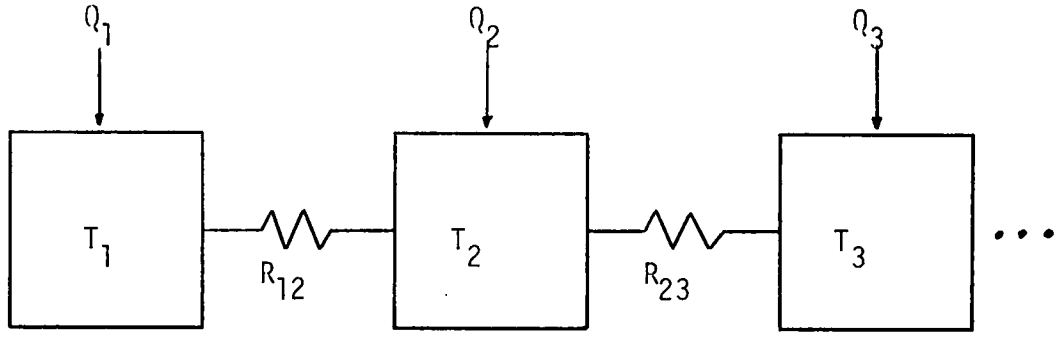


Figure 3.4 One-Dimensional Nodal Heat Transfer Model.

The nodal equation for the surface node is:

$$\frac{dT_n}{dt} = a_{n,n-1}T_{n-1} - a_{n,n}T_n + a_{NF}T_F + b_nQ_n \qquad (3.9)$$

where

T_N = temperature of the Nth node (with respect to the initial fluid temperature),

T_F = change in fluid temperature from its initial value.

These equations can be represented most easily in matrix form:

$$\frac{d\bar{x}}{dt} = A\bar{x} + \bar{f}\,T_F + B\bar{q} \qquad (3.10)$$

where

$$\bar{x} = \begin{pmatrix} T_1 \\ T_2 \\ T_3 \\ . \\ . \\ . \\ T_N \end{pmatrix} \quad A = \begin{pmatrix} -a_{1,1} & a_{1,2} & 0 & 0 & . & . & . \\ a_{2,1} & -a_{2,2} & a_{2,3} & 0 & 0 & . & . \\ 0 & a_{3,2} & -a_{3,3} & a_{3,4} & 0 & . & . \\ . & & & & & & \\ . & & & & & & \\ . & & & & & & \\ . & . & . & . & a_{n,n-1} & -a_{n,n} & \end{pmatrix} \quad \bar{f} = \begin{pmatrix} 0 \\ 0 \\ 0 \\ . \\ . \\ . \\ a_{NF} \end{pmatrix} \qquad (3.11)$$

$$B = \begin{pmatrix} b_1 & 0 & 0 & . & . & . \\ 0 & b_2 & 0 & . & . & . \\ 0 & 0 & b_3 & . & . & . \\ 0 & 0 & 0 & . & . & . \\ & & & & & b_N \end{pmatrix} \quad \bar{q} = \begin{pmatrix} Q_1 \\ Q_2 \\ Q_3 \\ . \\ Q_N \end{pmatrix} .$$

Transforming to the Laplace domain s gives

$$[sI - A]\bar{x}(s) = \bar{f}\, T_F(s) + B\,\bar{q} - \bar{x}(t = 0). \tag{3.12}$$

If only perturbations from steady state are considered, then $\bar{x}(t=0)$ can be set equal to zero. This equation can be solved using Cramer's rule which results in solutions for the central node $X_1(s)$:

$$T_1(s) = \frac{F(s)}{|sI-A|}\,. \tag{3.13}$$

For the LCSR case with internal heating the center with $T_F(s) = 0$, the F(s) matrix becomes:

$$F(s) = \begin{vmatrix} b_1 & -a_{12} & 0 & 0 & \cdots & \\ 0 & (s+a_{22}) & -a_{23} & 0 & \cdots & \\ \cdot & -a_{32} & (s+a_{33}) & -a_{34} & \cdots & \\ \cdot & \cdot & \cdot & \cdot & \cdots & \\ \cdot & \cdot & \cdot & \cdot & \cdots & \\ \cdot & \cdot & \cdot & \cdot & \cdots & \\ 0 & 0 & 0 & 0 & \cdots & -a_{n,n-1}(s+a_{n,n}) \end{vmatrix}\,. \tag{3.14}$$

Kerlin[13] has shown that after evaluation of the determinants F(s) and $|sI-A|$ gives a solution for the central node of the form

$$T_1(s) = \frac{(s-z_1)(s-z_2)\ldots(s-z_{N-1})}{(s-p_1)(s-p_2)\ldots(s-p_N)} \tag{3.15}$$

where z_i is a zero (a value that makes $T_1(s) = 0$), and p_i is a pole (a value that makes $T_1(s) = \infty$). After implementing the residue theorem, the solution obtained is

$$T(t) = \frac{(p_1-z_1)(p_1-z_2)\ldots(p_1-z_{N-1})}{(p_1-p_2)(p_1-p_3)\ldots(p-p_N)}\, e^{p_1 t} + \frac{(p_2-z_1)(p_2-z_2)\ldots(p_2-z_{N-1})}{(p_2-p_1)(p_2-p_3)\ldots(p_2-p_N)}\, e^{p_2 t} + \ldots \tag{3.16}$$

Note that this result is obtained only if the measured temperature is at the center-most node. Kerlin made the following important observations:

1. The coefficient in the exponents are determined only by the heat transfer characteristics of the sensor system and are independent of the initial temperature distribution.
2. The coefficients that multiply the exponential terms are determined by the zeroes as well as the poles and are thereby dependent upon the initial temperature distribution.

For the case of a step perturbation in fluid temperature, $T_F(s)$ is nonzero and $q(s) = 0$ for all nodes. The resulting F(s) matrix is:

$$F(s) = \begin{vmatrix} 0 & -a_{12} & 0 & 0 & 0 & \cdots & & \\ 0 & (s+a_{22}) & -a_{23} & 0 & 0 & \cdots & & \\ 0 & -a_{32} & (s+a_{33}) & -a_{34} & 0 & 0 \cdots & & \\ \cdot & \cdot & \cdot & \cdot & \cdot & \cdots & & \\ \cdot & \cdot & \cdot & \cdot & \cdot & \cdots & & \\ \cdot & \cdot & \cdot & \cdot & \cdot & \cdots & & \\ a_N T_F(s) & 0 & 0 & 0 & \cdot & \cdots & -a_{n,n-1} & s+a_{n,n} \end{vmatrix} .$$

The solution of the resulting equation again using Cramer's rule is given by Kerlin as

$$T_1(s) = \frac{a_{NF} T_F(s)(-1)^{N+1}}{(s-p_1)(s-p_2)\cdots(s-p_N)} \qquad (3.17)$$

using the residue theorem we obtain

$$T_1(t) = K\left\{\frac{1}{(-p_1)(-p_2)\ldots(-p_N)} + \frac{1}{p_1(p_1-p_2)(p_1-p_3)\ldots(p_1-p_N)}\, e^{p_1 t}\right.$$

$$\left. + \frac{1}{p_2(p_2-p_1)(p_2-p_3)\ldots(p_2-p_N)}\, e^{p_2 t} + \ldots\right\} \qquad (3.18)$$

where K = a constant. From Eq. (18), the following key observations can be made: (1) the exponential terms are the same in a plunge test and a LCSR test, and (2) a knowledge of the poles alone is sufficient to determine both the exponents and the coefficients for the plunge test.

In order to convert LCSR results into equivalent fluid temperature step responses, the only requirement is that the poles must be determined. This can be accomplished by fitting the following equation to LCSR data,

$$T(t) = (T_i - T_f)[Ae^{t/\tau_1} + Be^{t/\tau_2} + \ldots] + T_F \qquad (3.19)$$

where

T_i = initial temperature

T_f = final temperature

$\tau_i = \frac{1}{p_i}$ = time constants that describe the temperature T(t) at any time τ

A,B,... = constants

There are many methods available to the analyst for fitting Eq. (3.19) to experimental data. They include least squares (linear regression) analysis, exponential stripping, and others. The procedures used in each of these methods are well known[15] and will not be treated in detail in this thesis.

Once the poles are found, it is possible to construct the fluid temperature step response. After evaluation of as many poles (p_i) as possible, they are used in Eq. (3.18) to predict the sensor time response that would have occurred had a fluid temperature step been imposed on the sensor.

As mentioned earlier, the actual response of a sensor consists of an infinite series of exponentials as shown by Eq. (3.18). If a great "percentage" of the step response is contained in a few exponentials, then the response can be closely approximated by a truncated series of exponentials. For a two-cell, one-dimensional model, the response from Eq. (3.18) becomes:

$$T(t) = K\left[\frac{1}{(-p_1)(-p_2)} + \frac{1}{p_1(p_1-p_2)} e^{p_1 t} + \frac{1}{p_2(p_2-p_1)} e^{p_2 t}\right]. \qquad (3.20)$$

The time constant, defined in Section 1.1, can be determined from Eq. (3.20). It is the time required for the output of Eq. (3.20) to attain 63.2% of its asymptotic value.

3.4. RESTRICTIONS INHERENT TO THE ANALYTICAL TRANSFORMATION

The analytical transformation discussed in the previous section will predict the fluid temperature step response from the internal heating step response accurately provided the following restrictions are met.

1. The actual sensor heat transfer must be primarily one-dimensional. For multi-dimension cases Kerlin[14] has shown that a knowledge of the poles alone is inadequate to evaluate all of the coefficients needed to construct the equivalent fluid-temperature change result.

2. The sensing element must be located nearly in the center of the sensor. Otherwise the model used in the transformation cannot describe the actual heat transfer process.

In addition to breakdowns in the assumptions affecting the analytical part, it may be impossible or impractical to obtain the poles accurately. For instance, the identifiability of a pole depends upon whether the corresponding mode is excited strongly enough in the LCSR test. If an "important" mode of the fluid temperature perturbation response is small in the LCSR case, then it may be impossible to evaluate the p_i for that mode.

3.5. DEVELOPMENT OF AN EMPIRICAL TRANSFORMATION USING THE LCSR TEST

For cases where the assumptions apply, Kerlin's analytical transformation accurately predicts the sensor response to a fluid temperature step perturbation.[14] If either the analytical transformation fails for a particular sensor, or the method for implementing it fails because of difficulties in identifying the poles, another method is needed to interpret LCSR results. Because one of the objectives of this research was to develop an in situ test usable on all types of sensors, an effort was made to discover an empirical correlation to be used in cases where Kerlin's analytical transformation could not be applied.

Experimental results were investigated to determine whether a unique relationship existed between the fluid temperature step response and the response to a step increase in internal heating of the sensor. The two parameters of interest were the 63.2% time constants in the LCSR test and the plunge test. The LCSR time constant, τ_{LCSR}, is the time

required for the sensor to attain 63.2% of its final output after a step change in the internal heating in the sensor. The plunge test time constant, τ_{PL}, is defined as the time required by the sensor to attain 63.2% of its final output following the plunging of the sensor into a fluid at a temperature different from the original steady state temperature before the plunge.

As previously mentioned in Section 3.2, page 41, the time response of a sensor is dependent upon the heat transfer properties and characteristics of its environment. When the heat transfer resistance of a sensor increases, it follows that the response time of the sensor would increase. Likewise, when the heat transfer resistance of the sensor decreases, the response time of the sensor will decrease. It is possible to simulate heat transfer changes artifically in the sensor environment by placing insulating material of varying thicknesses around the thermometer bulb. LCSR and plunge tests can be performed in the laboratory and the resulting time constants measured.

The tests may be repeated under many differing simulated heat transfer environments. The associated time constants computed at each configuration constitute a point on an empirical curve. The resulting points when plotted yield an experimental correlation curve. From this empirical relationship, it is possible to predict the fluid temperature step response time constant given the LCSR time constant for any possible surface heat transfer condition. With this empirical transformation, it is possible to conduct tests before

installation of the sensor in the reactor and throughout the life of the plant, perform LCSR tests, determine their 63.2% response time, and verify whether the plunge test time constant has changed.

The major assumptions in this transformation include:

1. There is a unique relationship for each particular sensor type between the LCSR result and the plunge test result.
2. In conducting the laboratory testing, an adequate number of heat transfer environments must be imposed on the sensor. This is to assure that the full operating range of the sensor has be considered.
3. The tests in the laboratory must be performed under the same heat transfer environments during the LCSR, self-testing, and plunge tests.
4. Measurements made in the laboratory are consistent with ones made in the plant. This precludes any kind of dependence of the time response on temperature, pressure, or other conditions that could be different in the plant than in the laboratory.
5. All modes of time response degradation can be adequately simulated by changes in external heat transfer resistance.

Chapter 5 describes the procedures used in laboratory time response testing on a specific sensor. The resulting data are analyzed and the associated time constants are computed. An empirical transformation using the LCSR and plunge tests is discussed.

CHAPTER 4

THE SELF-HEATING TEST

4.1. DESCRIPTION OF TESTING METHOD

The self-heating test exploits the dependence of temperature rise in an RTD on the sensor-to-fluid heat transfer resistance during steady state internal ohmic heating to detect changes in heat transfer characteristics. The temperature rise in the sensor is a function of both the heat generated and the ability of the sensor to dissipate heat to its surroundings.

The normal sensing current passing through the resistance element is usually 1-2 mA. During the self-heating test, the current is incrementally increased from 1-2 mA to 60-80 mA. The electrical resistance of the element is measured for steady state conditions at each point and the power generated in the sensor is computed. The data may be analyzed using a least squares linear regression approach.

The result is a curve that shows the change in resistance of the sensing element as a function of the power generated in the sensor. The resistance change is proportional to the change in temperature of the resistance element. For elements made of platinum, the self-heating curve is linear.

4.2. THEORY AND PRINCIPLE OF METHOD

The parameter of interest in the self-heating test is the slope of the self-heating curve. A typical self-heating curve is shown in Figure 4.1 (results obtained for a platinum resistance sensor).

The heating in the sensor can be described by

$$Q = UA(T-\theta) \tag{4.1}$$

where

Q = heat generation developed in sensor by I^2R heating

T = sensor temperature

θ = fluid temperature

U = overall heat transfer coefficient

A = heat transfer area.

Equation (4.1) can be rewritten as

$$(T-\theta) = T = \frac{Q}{UA} . \tag{4.2}$$

Since the sensor electrical resistance is proportional to its temperature, and the fluid temperature is constant, then

$$\Delta R = \frac{\Delta T}{\alpha} = \frac{\Delta Q}{\alpha UA} \tag{4.3}$$

where

α = temperature coefficient of resistance in °C/Ω.

From Eq. (4.3), it can be seen that for constants α, U, and A, a change in internal heating, ΔQ, produces a corresponding change in resistance, ΔR. Since the heat generated in the sensor is proportional to the power generated in the sensor,

$$\frac{\Delta R}{\Delta P} = \frac{1}{\alpha UA} . \tag{4.4}$$

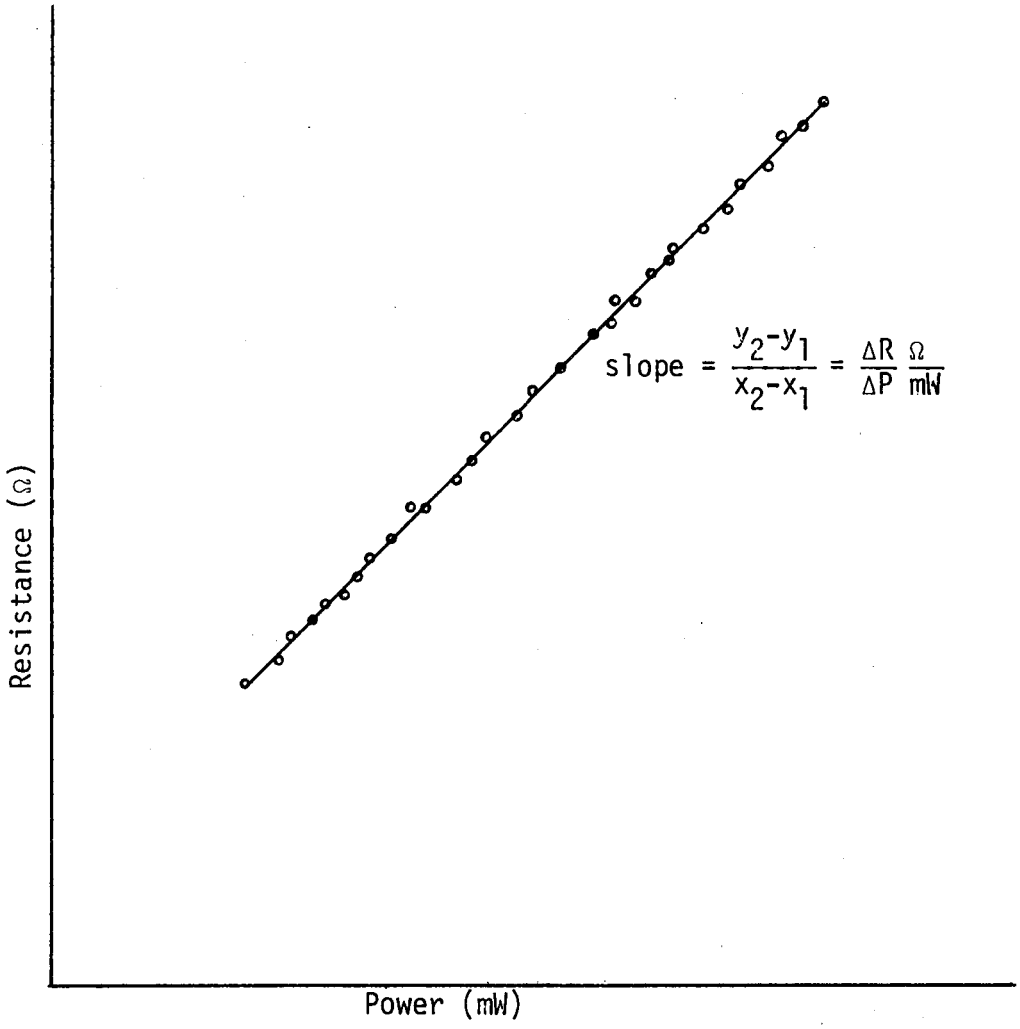


Figure 4.1 Typical Self-Heating Curve.

From Equation (4.4), it can be seen that for constant α and A, a change in the overall heat transfer coefficient U produces a corresponding change in the slope of the resistance versus heat generation rate curve ($\Delta R/\Delta P$). Thus, if a measurement reveals a change in $\Delta R/\Delta P$, a change in the heat transfer resistance is indicated.

4.3 DEVELOPMENT OF AN EMPIRICAL TRANSFORMATION USING THE SELF-HEATING TEST

From Equation (4.3), it was shown that there is a unique relationship between the slope of the self-heating curve and the heat transfer resistance of the sensor. It is possible to simulate changes in the sensor heat transfer resistance in laboratory tests. This is done by adding artificial heat transfer resistance (such as adhesive tape or short sections of rubber tubing) at the surface of the RTD. In doing so, an empirical relation can be obtained by performing plunge tests and self-heating tests on each heat transfer configuration.

The plunge test time constant is computed along with the value of the slope of the self-heating curve for each heat transfer condition. The tests are repeated in different environments in the laboratory. After installation in a reactor, the fluid temperature step response can be predicted by performing a self-heating test in situ, computing the value for $\Delta R/\Delta P$ for that environment, and determining the corresponding plunge test time constant from the empirical curve.

The assumptions that were stated in Section 3.5 also apply for this empirical transformation. The laboratory implementation of the self-heating test is described in Chapter 5 along with experimental determination of the self-heating empirical transformation for a specific sensor.

CHAPTER 5

LABORATORY TIME RESPONSE TESTING OF AN RTD USED IN WESTINGHOUSE PWR's

5.1. INTRODUCTION

The LCSR and self-heating methods were tested in the laboratory. An analytical transformation was used to convert measured LCSR results into equivalent fluid temperature step perturbation results. These results were compared to plunge test results (which approximate the fluid temperature perturbation case).

Self-heating, LCSR, and plunge tests were performed for many different heat transfer conditions. Empirical transformations using these results were developed for use in cases where the analytical transformation failed.

5.2. EXPERIMENTAL EQUIPMENT DESCRIPTION AND SETUP

The experimental work was performed in the Thermometry Laboratory of the Nuclear Engineering Department at the University of Tennessee. Testing of the sensors was conducted in a stirred bath at room temperature ($\sim$ 72 °F) in order to maintain constant heat transfer conditions. The bath,* shown in Figure 5.1, consists of a square tubular frame with a 5/8 inch thick stainless steel working surface. A washing machine tub mounted on casters was connected underneath to a shaft with

---

*Furnished on loan by R. R. Shepard, Oak Ridge National Laboratory.

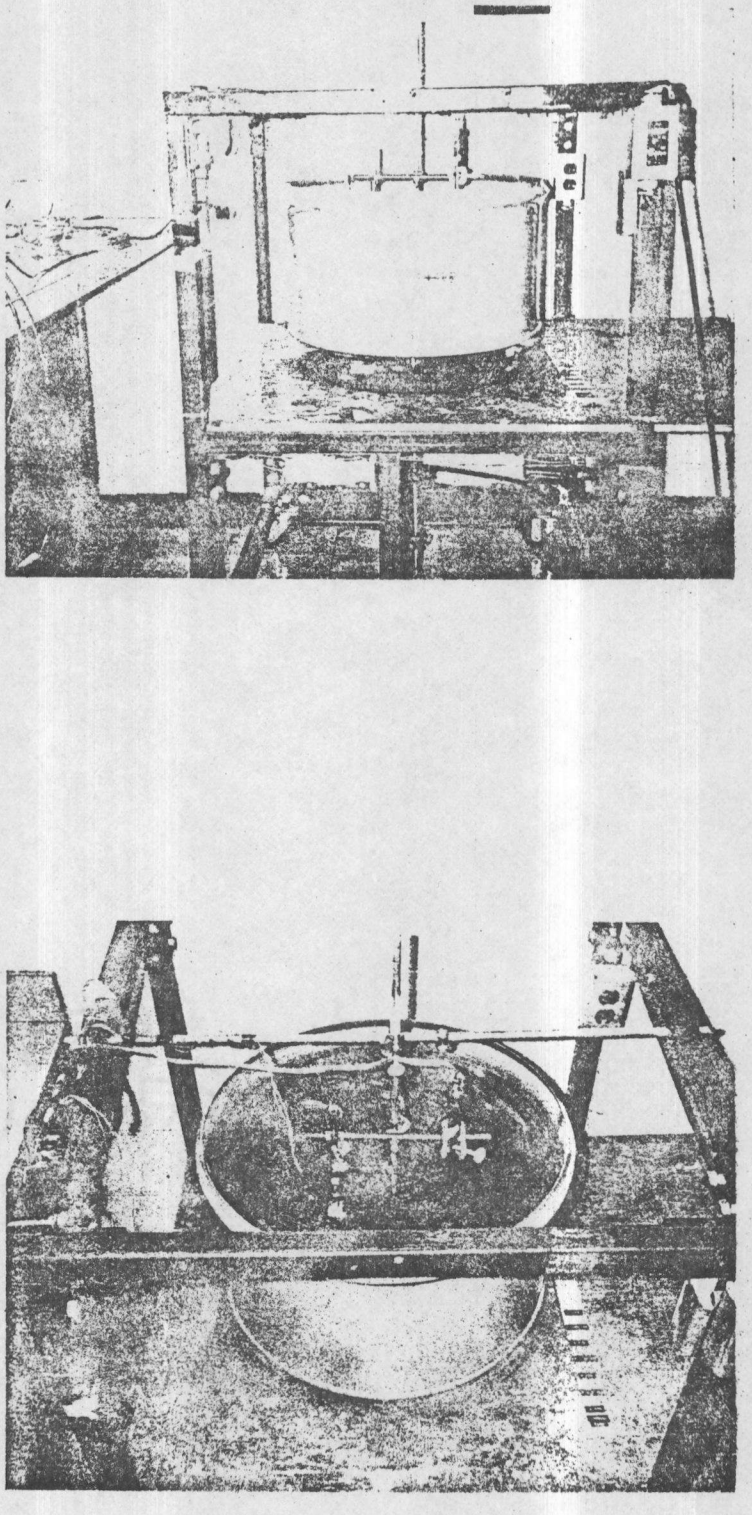


Figure 5.1 Stirred Bath.

a V-belt pully. A geared 1/12 H.P., 1725 rpm, single-phase induction motor provided the driving force via the belt drive. The maximum water velocity at the perimeter of the tub was 120 cm per second. A stainless steel shaft was mounted horizontally over the tub and was used to hold the testing RTD in place. The maximum immersion depth in the tub was 28 cm.

The circuit used for resistance measurements is shown in Figure 5.2. It is a modified two-wire Wheatstone bridge in which the current through the sensor can be changed incrementally or in a stepwise manner. Resistors R_a, R_b, R_d, and the sensor R_{RTD} comprise the two-wire bridge whose operation was explained in Chapter 2, page 22. R_1 is used in conjunction with a relay switching circuit, denoted in this diagram by a switch, to change the sensing current passing through the RTD in a stepwise fashion.

The two-wire bridge was selected for use in the laboratory for two reasons: (1) steady state lead wire resistance errors would not affect the transients or deviations from steady state that occur during the laboratory testing; and (2) the two-wire bridge was simple.

The circuit analysis of the laboratory bridge circuit is given as follows. From Ohm's law we know that for the circuit

$$V = I_{circ} R_{circ} \tag{5.1}$$

where

V = voltage potential of circuit

I_{circ} = total current in circuit

R_{circ} = total resistance of the equivalent circuit.

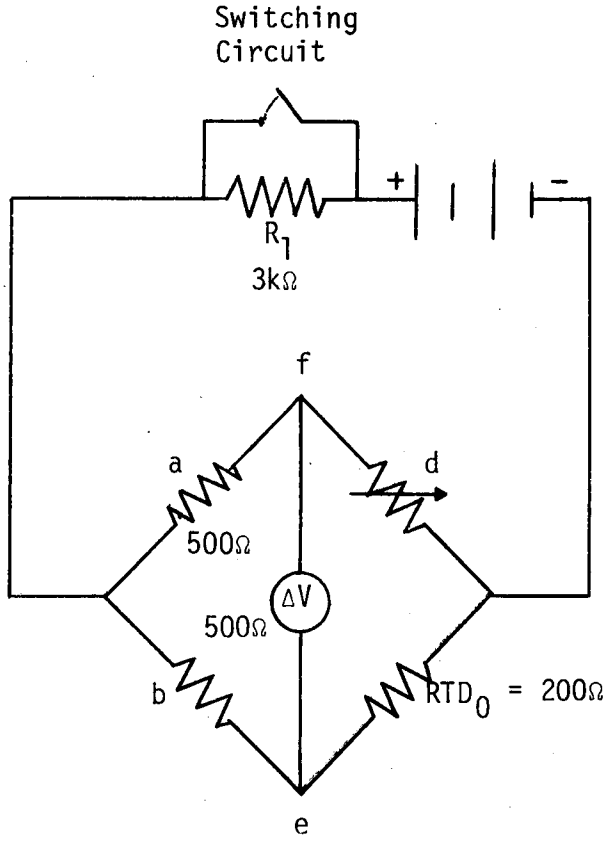


Figure 5.2 Laboratory Testing Bridge Circuit Schematic.

The switching resistance is given by R_1. When the switch is open, the current passing through the sensor is approximately 2 mA. Closing the switch allows the 3K resistors to be by-passed and a higher current is passed through the sensor.

The equivalent bridge resistance can be found using

$$\frac{1}{R_{bridge}} = \frac{1}{R_a+R_d} + \frac{1}{R_b+R_{RTD}}, \tag{5.2}$$

$$\frac{1}{R_{bridge}} = \frac{R_a+R_d+R_b+R_{RTD}}{(R_a+R_d)(R_b+R_{RTD})}, \tag{5.3}$$

therefore

$$R_{bridge} = \frac{(R_a+R_d)(R_b+R_{RTD})}{(R_a+R_d+R_b+R_{RTD})}. \tag{5.4}$$

The equivalent total circuit resistance with the switch closed is given by

$$R_{circ} = R_1 + R_{bridge}. \tag{5.5}$$

The current in the circuit can be obtained from Eq. (5.1).

$$I_{circ} = \frac{V}{R_{circ}}. \tag{5.6}$$

When the switch is closed, the total current is

$$I_{\substack{\text{circ with}\\ \text{switch closed}}} = V\left(\frac{R_a+R_b+R_d+R_{RTD}}{(R_a+R_d)(R_b+R_{RTD})}\right). \tag{5.7}$$

With the switch open, we have

$$I_{\substack{\text{circ with}\\ \text{switch open}}} = V\left(\frac{1}{R_1 + \dfrac{(R_a+R_d)(R_b+R_{RTD})}{(R_a+R_b+R_d+R_{RTD})}}\right) . \tag{5.8}$$

The size of the resistors in the bridge circuit were chosen so that when the bridge is balanced, points e and f are at the same potential. The current through the upper path must equal the current through the lower path.

$$I_{upper} = \left(\frac{R_b+R_{RTD}}{R_a+R_b+R_d+R_{RTD}}\right) I_{circ} \tag{5.9}$$

$$I_{lower} = \left(\frac{R_a+R_d}{R_a+R_b+R_d+R_{RTD}}\right) I_{circ} . \tag{5.10}$$

For $I_{upper} = I_{lower}$, the governing relation is:

$$\frac{R_a}{R_b} = \frac{R_d}{R_{RTD}} . \tag{5.11}$$

The bridge arm resistors R_a and R_b are chosen to be equal so that when the bridge is balanced the reading of the decade box equals the resistance of the RTD. This measure of the sensor resistance is used in the self-heating test.

Measurement of the resistance of the sensor in the LCSR test and the plunge test requires continuous monitoring of the bridge-sensor output. When the balance of the bridge is upset by a change in the sensor

resistance, R_{RTD}, a potential difference is created between bridge points e and f. The voltage difference between these points, ΔV_{EF}, is approximately proportional to the change in resistance of the sensor, ΔR_{RTD} (see Eq. (2.7)).

The measurement of the time varying voltage difference across the bridge was obtained by passing the signal through a low noise amplifier. The results were recorded either by a strip chart recorder, voltmeter, or computer.

The bridge circuit resistors have high power ratings (25 watts) to insure that their resistance would not change appreciably when a current of up to 80 mA is passed through it. The circuit was checked before testing by inserting a normal 100 ohm resistor in place of the RTD. The current was stepped up and the bridge output was recorded. If the bridge circuit was not "heating up" due to I^2R heating of the circuit resistors, the response would be a simple step. Figure 5.3 shows that this was the case, indicating that the heating effect on the bridge resistors is negligible.

Two Wanless Electric Company Maverick II variable voltage 18 volt direct current power supplies wired in series were used as the power source. The maximum current available with the 3K resistor by-passed was 80 mA. During the self-heating test which requires incremental current changes, the 3K resistor remains by-passed and the current is varied using the power supply output voltage adjustment.

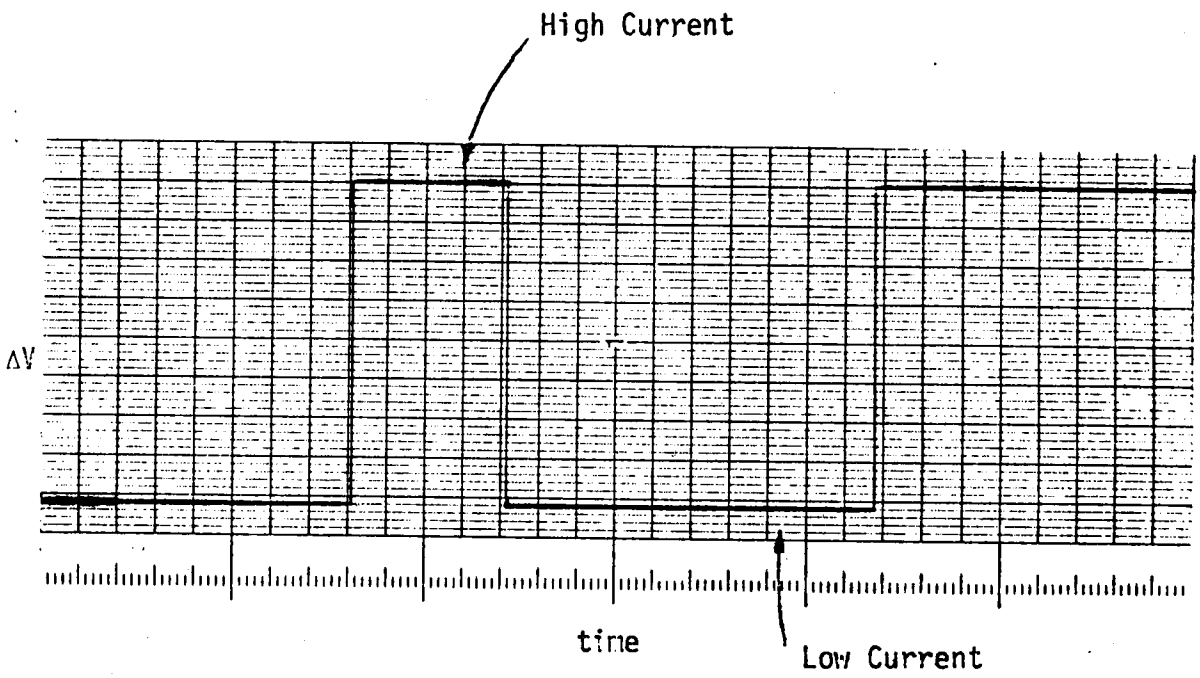


Figure 5.3 Resistor Response to Step Change in Current.

5.3. LABORATORY TESTING

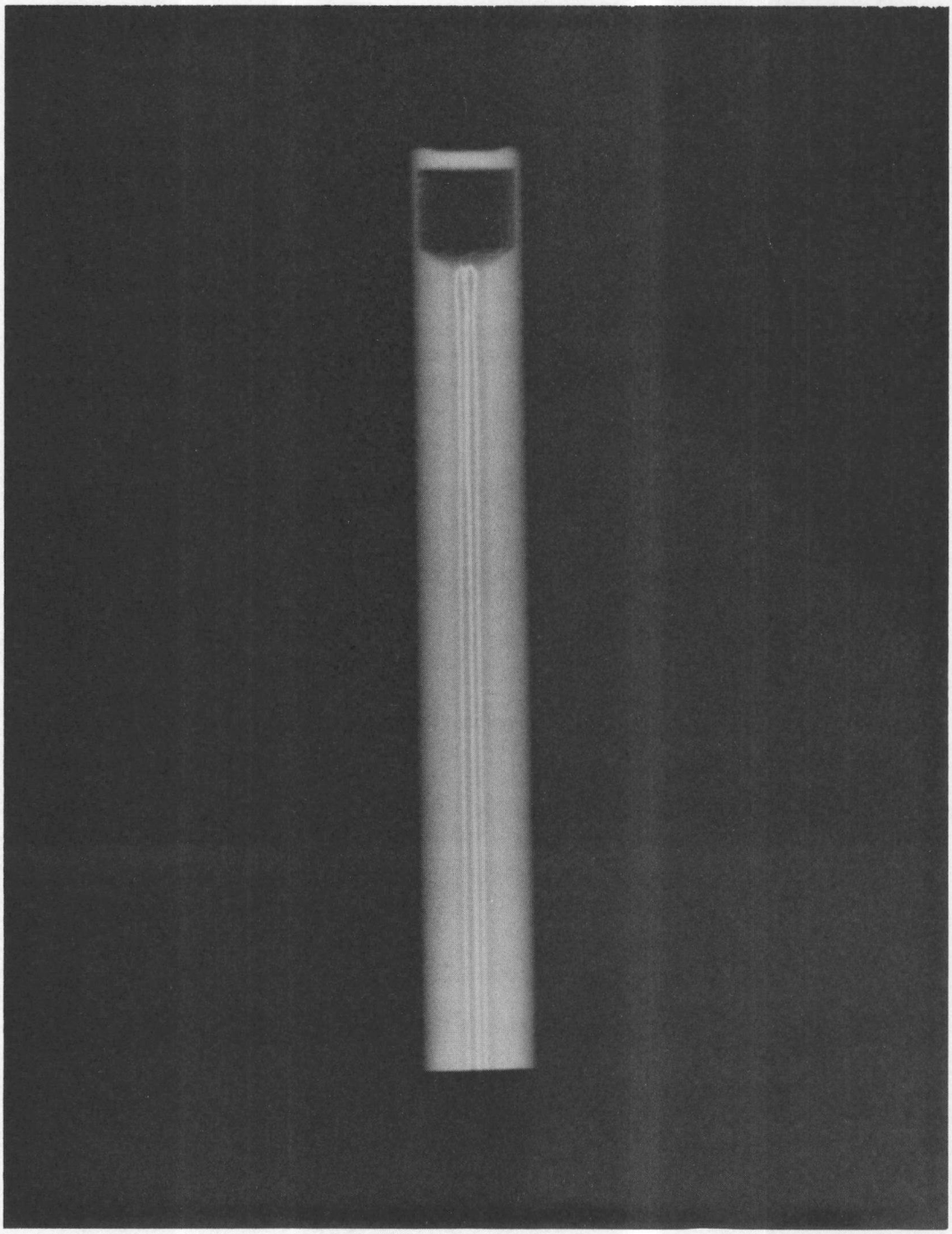
A Rosemount model number 176-KF platinum resistance temperature sensor was obtained from Florida Power and Light Company. This type sensor is used in the reactor coolant system at Turkey Point Nuclear Plant Units 3 and 4. Laboratory time response testing was conducted using this sensor.

An x-ray was taken of the sensor to determine its internal makeup. The x-ray and a photograph of the RTD are shown in Figure 5.4. The platinum element is a helical coil wound around the perimeter of a cylindrical support core placed in the bottom of the sheath. The diameter of the element is very nearly equal to the inside diameter of the sheath. The very close proximity of the element to the inside surface of the sheath minimizes the heat transfer resistance and thereby improves the response time of the sensor.

5.3.1. Plunge Test

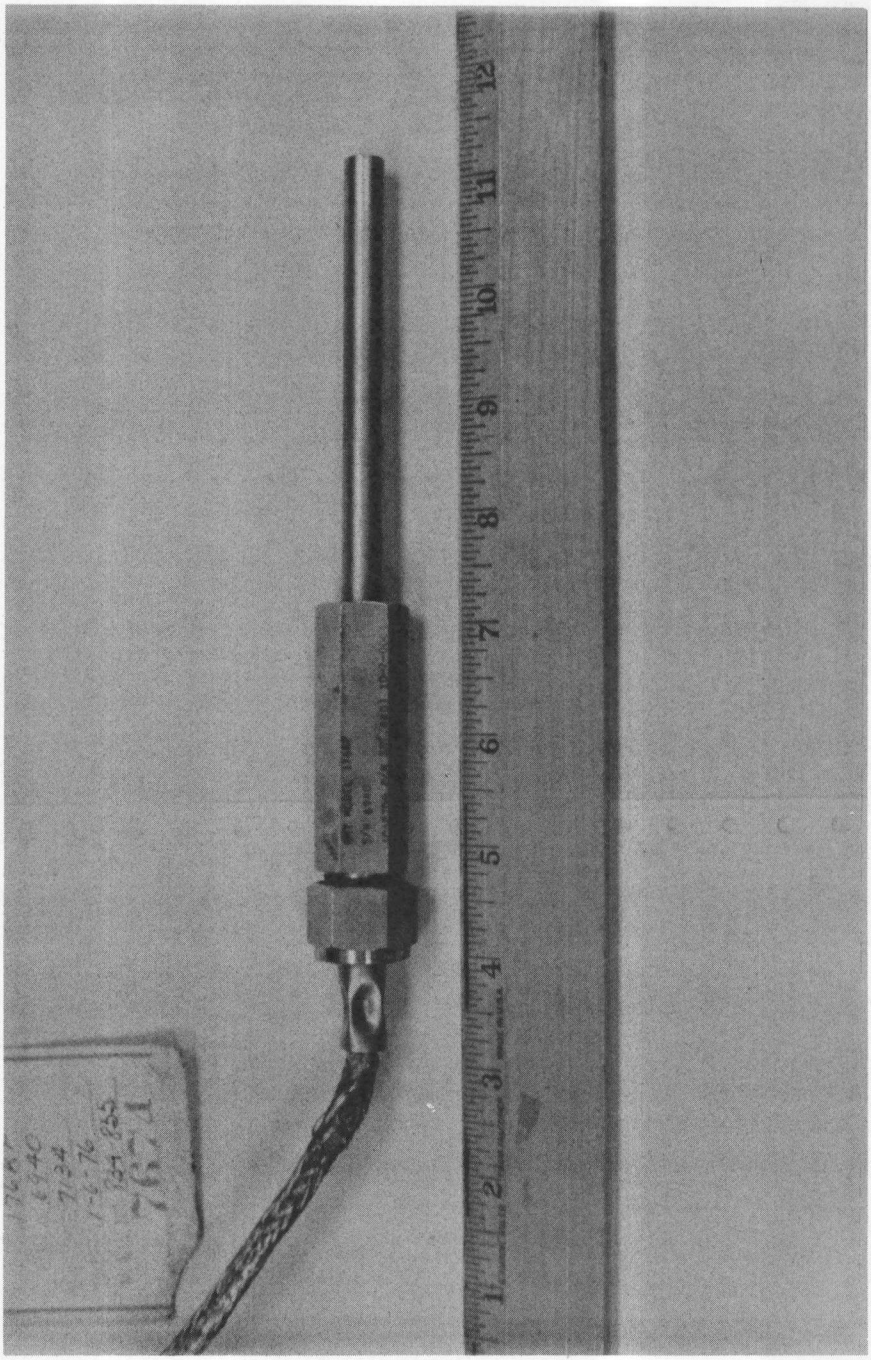
The testing method used to simulate a step change in fluid temperature outside an RTD is the plunge test. In a plunge test, a sensor that is at steady state conditions, operating at its normal sensing current, is suddenly immersed into a stirred bath at a different temperature. The response of the sensor is monitored on a strip chart recorder until it again reaches the steady state. A typical plunge test response of the 176-KF sensor is shown in Figure 5.5.

The bridge circuit configuration used during the plunge test is shown in Figure 5.6. The relay switch remains open allowing the sensing current to maintain its normal operating value of 1-2 mA. The time at



a) X-Ray

Figure 5.4 Rosemount Model 176-KF RTD.



b) Picture

Figure 5.4 (Continued).

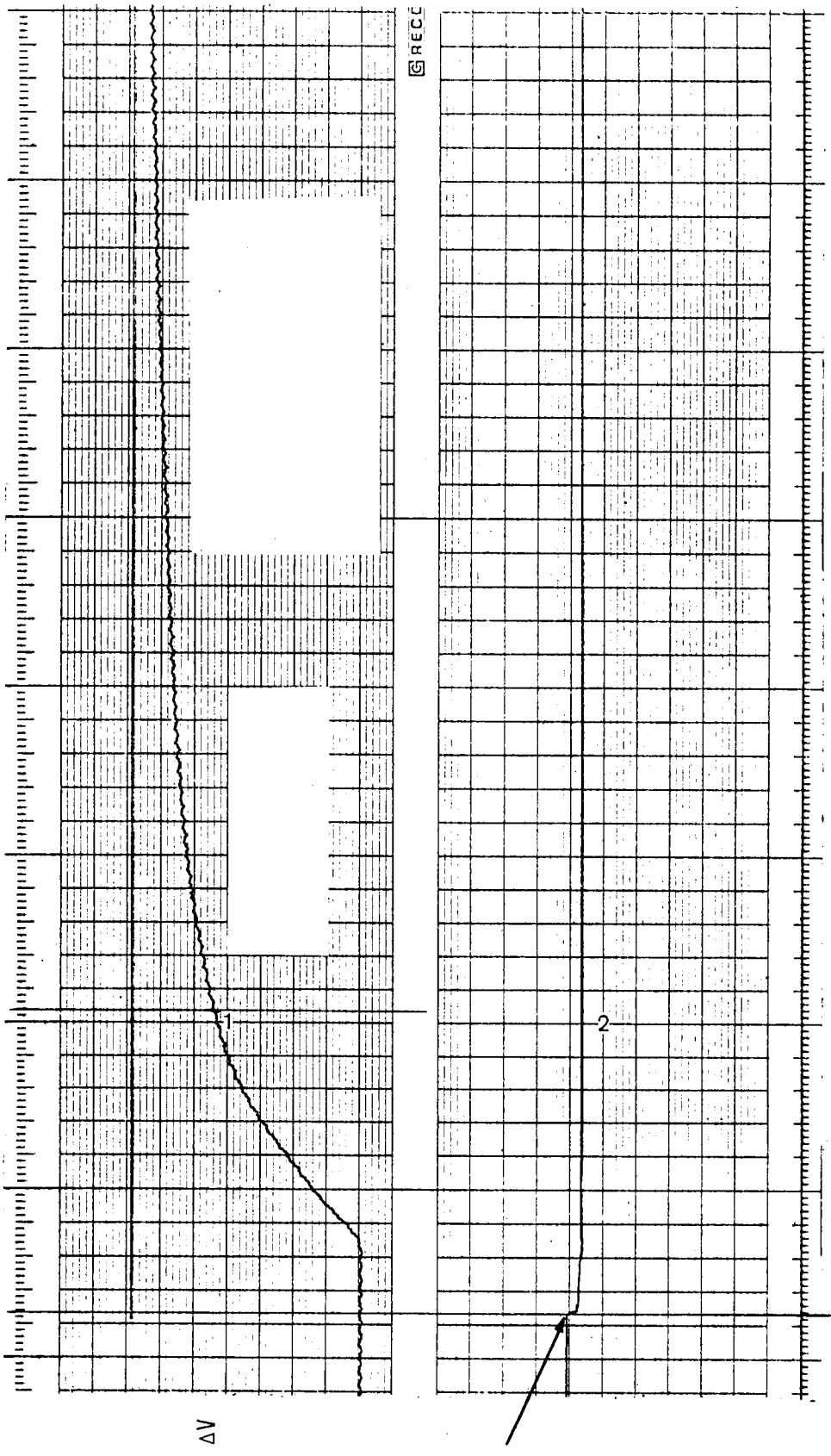


Figure 5.5 Plunge Test Response for Bare 176-KF Sensor.

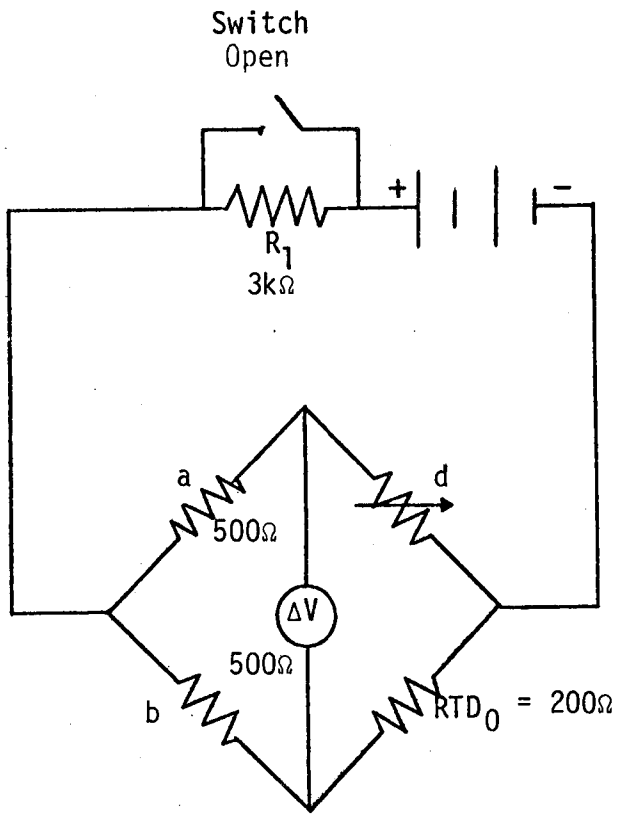


Figure 5.6 Laboratory Plunge Test Bridge Circuit.

which the sensor enters the water is noted by the arrow in Figure 5.5. This point is marked by the recorder by attaching one of the input channels of the strip chart recorder to a battery circuit connected to the sensor holder, shown in Figure 5.7. When the RTD and its holder enter the water, the circuit is closed and the point is marked on the strip chart.

This plunge test time constant is determined as shown in Figure 5.8. A line is drawn denoting the point at which the sensor responded to 63.2% of its final output. At this point, a vertical line is drawn down to the x-axis (time axis). The number of spaces between this point and the time point when the sensor touched the water are counted. The time constant is calculated using the conversion factor appropriate to the strip chart recorder scale used. The plunge test time constant for the bare 176-KF sensor in this test 0.36 seconds.

5.3.2. Loop Current Step Response Test

The theory behind the loop current step response (LCSR) test was discussed in Section 3.2. The following is a discussion of the laboratory implementation of this technique.

The LCSR test was implemented in two ways: (1) a fully automated process in which a PDP-11/20 was used to coordinate and control data acquisition, and to process the data using an analytical transformation,[13] and (2) a manual implementation of the test by stepping the sensing current up or down, and recording the results with a strip chart recorder. The sensor-bath setup remained the same regardless of the procedure used.

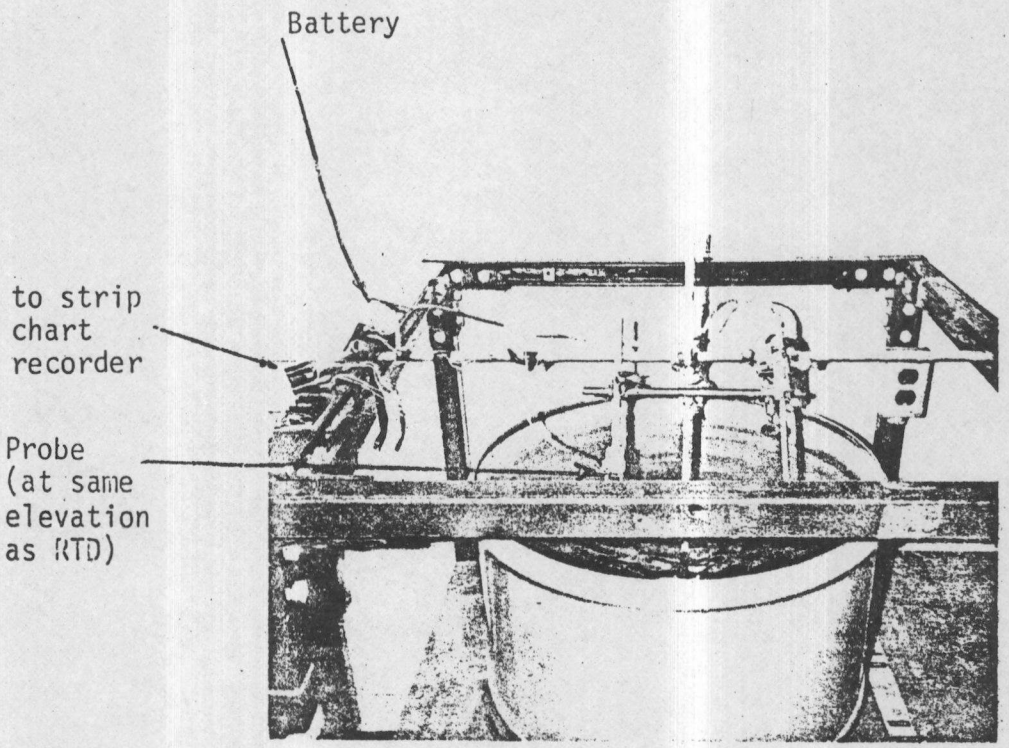


Figure 5.7 Plunge Test Battery Circuit.

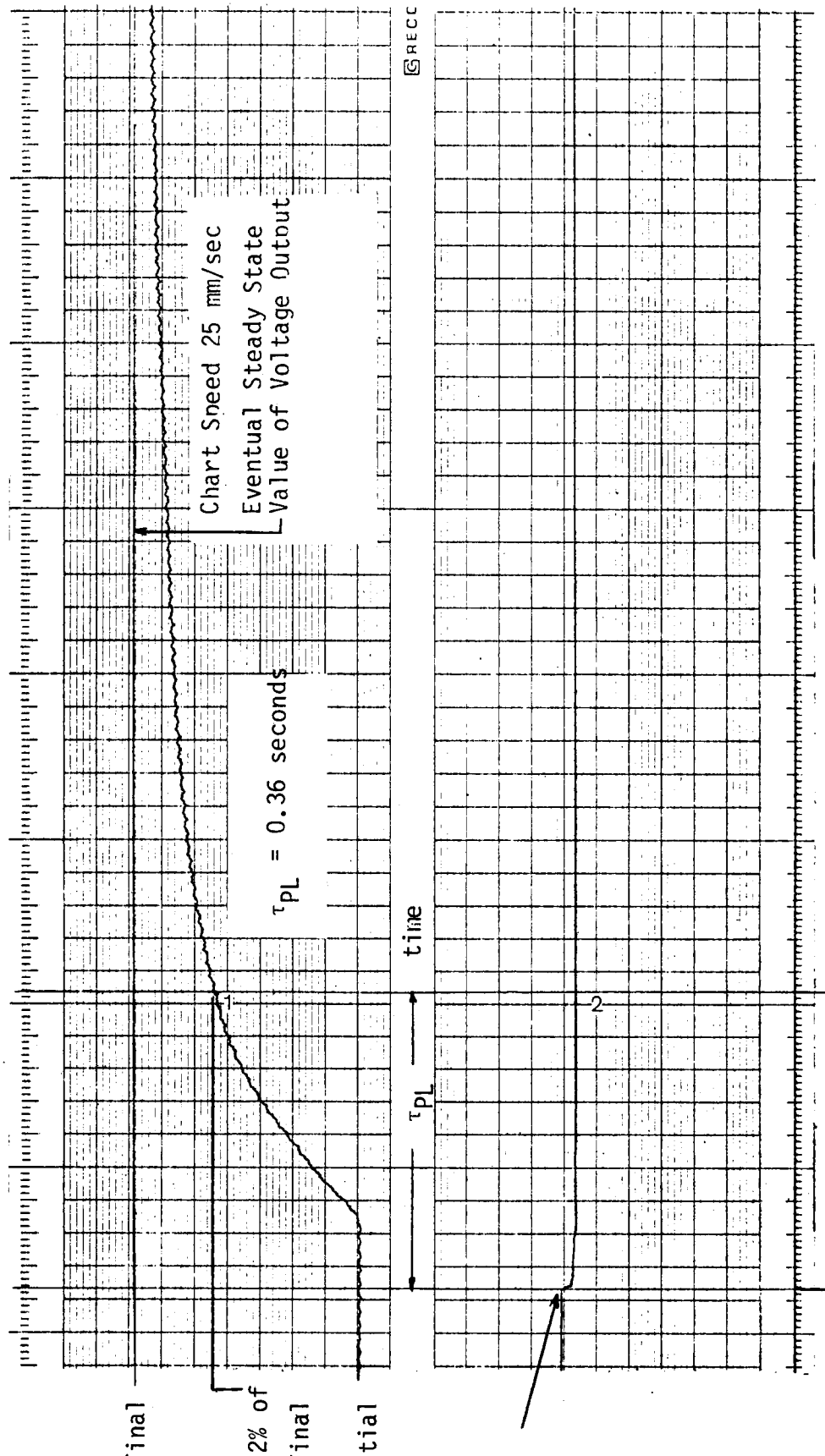


Figure 5.8 Determination of Plunge Test Time Constant for Bare 176-KF Sensor.

The bridge circuit configuration used in the LCSR test is the same as shown in Figure 5.6, page 75, except the switch is opened and closed. The operation of the relay switching circuit can be done manually or triggered by the computer. The output of the bridge circuit is routed to an amplifier to increase the voltage level. The signal is then sent either to a strip chart recorder or to the computer where an analog to digital (A/D) converter digitizes the continuous time-varying voltage output signal. The signal input to the computer is sampled at desired time intervals using an external clock pulser. Each time the clock emits a pulse, a sample is taken and an A/D conversion is made. The LCSR data acquisition setup is shown in Figure 5.9.

The current management using the relay circuit is also controlled by the computer. A five volt pulse initiated by the computer is sent through a digital to analog (D/A) converter to the relay. Each time a pulse is received, the relay changes state (opens or closes). The timing is managed by the internal clock of the computer. When the specified sampling period is over, the data record may be analyzed using the transformation described in Section 3.3, page 48. Discussion of the computer program that complements the LCSR test will be treated in Section 5.4.

The manual implementation of the LCSR test uses basically the same experimental setup. A strip chart recorder is substituted for the computer system and the current management is accomplished through a manual switch. Figure 5.10 shows the equipment setup.

The current is initially at about 2 mA with the sensor at steady state. The current is then switched and the current is stepped to

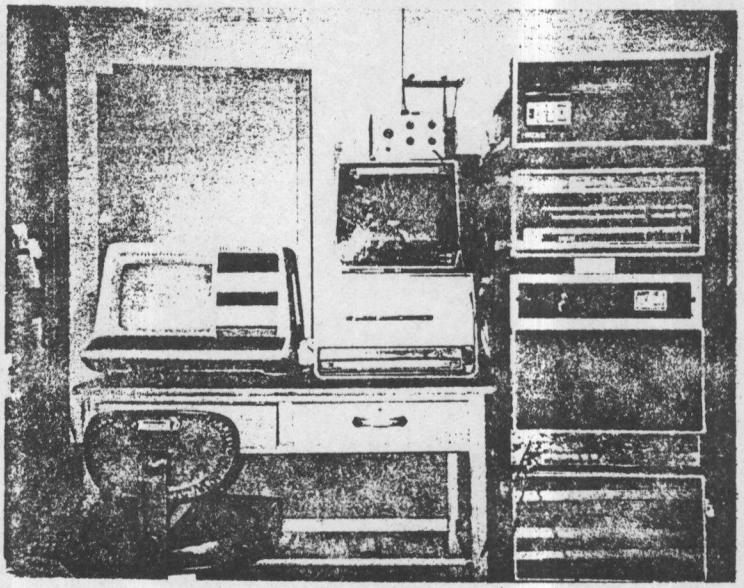


Figure 5.9 LCSR Computer Data Acquisition Setup.

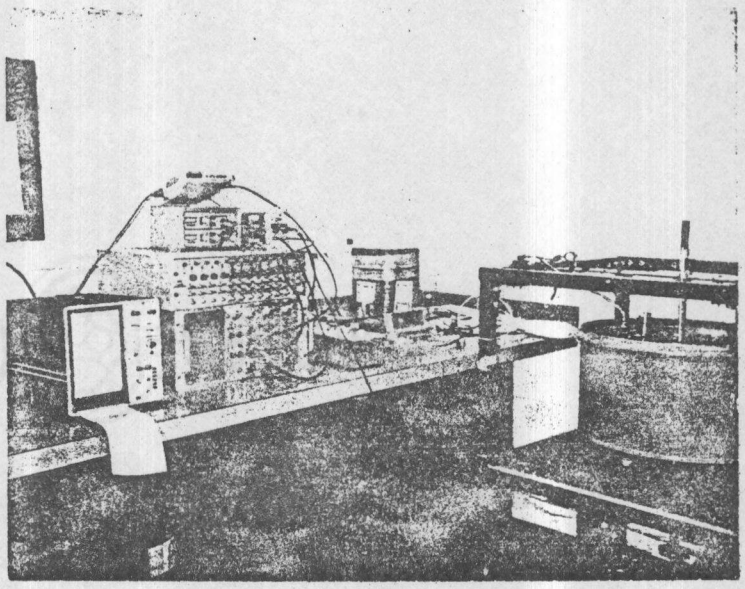


Figure 5.10 LCSR Manual Data Acquisition Setup.

20 to 60 mA. The sensor is allowed to reach steady state; then, the current is stepped down to its original value and the sensor is again allowed to settle out.

The output of the bridge-sensor circuit is continuously monitored during both the heating and cooling portions of the test. The LCSR time constant during the heating portion is determined from the strip chart recorder output by measuring the time required to reach 63.2% of the final value. The LCSR result for the bare 176-KF sensor is shown in Figure 5.11. The LCSR time constant for this test is 0.026 seconds.

5.3.3 Self-Heating Test

The self-heating test is performed on the sensor immersed in the stirred bath. The sensing current in the sensor is increased incrementally from its normal value of 1-2 mA to 40-60 mA using the bridge circuit configuration shown in Figure 5.6, page 75, with the swith closed. The power supply voltage is varied to adjust the current through the sensor. The power generated in the sensor-system as the current increases is proportional to the square of the current. After the current is increased, the system is allowed to return to steady state before an observation is made. Then, the change in resistance of the element associated with the change in temperature of the sensor-system is recorded at each interval. The resistance measurement is made by balancing the bridge circuit using a seven decade resistance box.

The power generated in the sensor is determined by multiplying the resistance of the sensing element (the resistance of the decade box), times the square the current flowing through it. In the balanced bridge circuit, the current flowing through the upper path is equal to the current flowing in the lower path. A measurement of the voltage drop across R_a or R_b is made. This value divided by the resistance of the

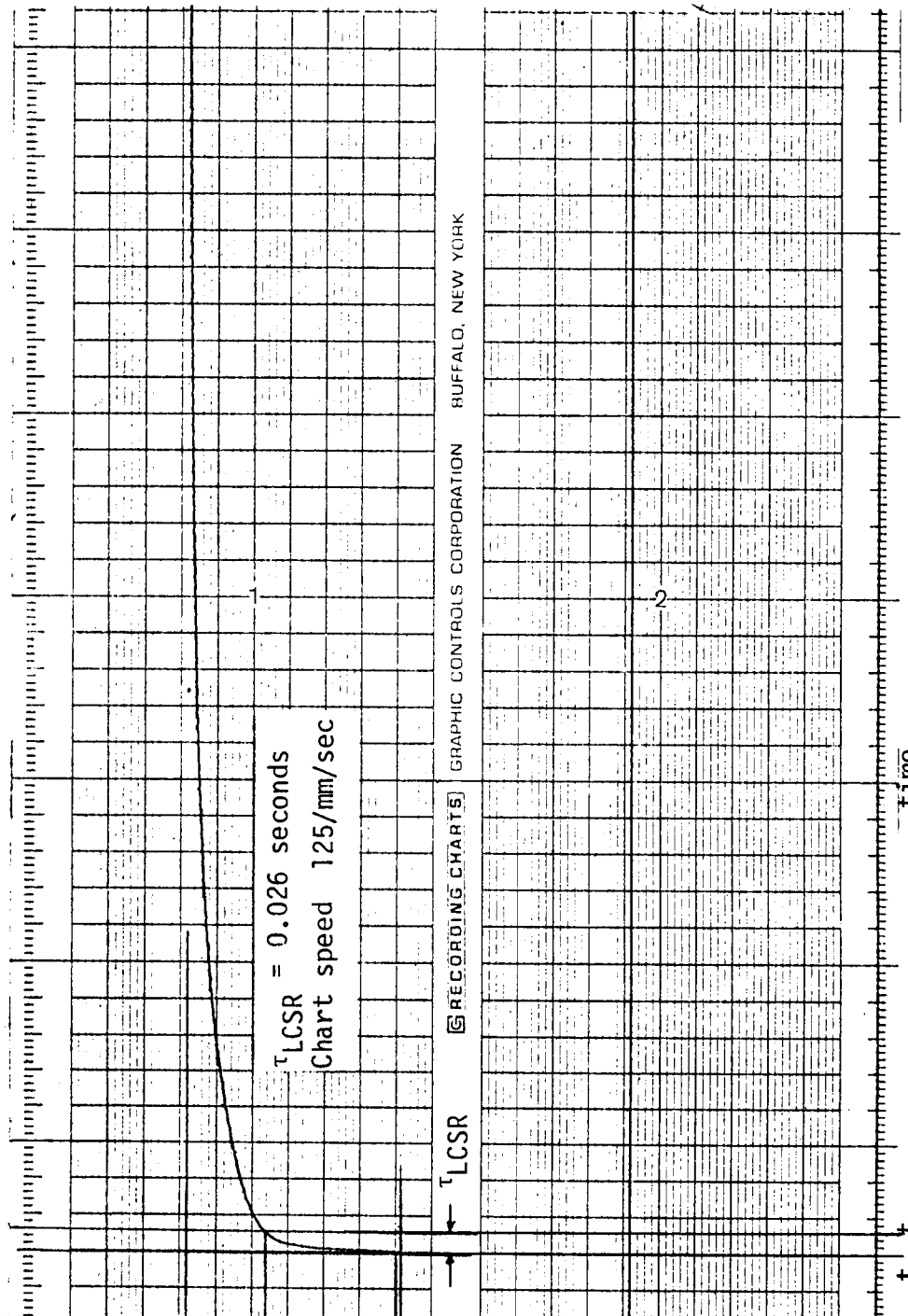


Figure 5.11 LCSR Test on Bare 176-KF Sensor.

resistor yields the value of the current flowing in the path. This value is equal to the current flowing in the RTD.

The power generated at each current increment is plotted versus the resistance of the sensor at that current. The result for the bare 176-KF sensor is approximately a linear relationship as shown in Figure 5.12. The slope may be evaluated through use of a least square linear regression approach or it may be approximated by

$$\frac{y_2-y_1}{x_2-x_1} = \frac{\Delta R}{\Delta P}\,\frac{\Omega}{mW} \,. \qquad (5.12)$$

For each milliwatt of power generated in the sensor in this test, the resistance of the sensing element increases 0.00584 ohms.

5.4. RESULTS OF COMPUTER AIDED ANALYSIS AND TRANSFORMATION OF LABORATORY TEST DATA

A FORTRAN program which controls LCSR data acquisition and analytical transformation of results was written by D. C. Warner for use with a PDP-11/20 computer. Numerous LCSR tests on different types of sensors have been analyzed. The results of the computer aided transformation compared favorably with results from associated plunge tests (see Appendix B) for sensors that have construction characteristics that satisfy the assumptions used in developing the transformation.

The equipment setup for LCSR testing using the computer was discussed in Section 5.3.2. LCSR tests were performed on the Rosemount 176-KF RTD and equivalent fluid temperature perturbation responses were constructed using the transformation. The time constants obtained from the transformed

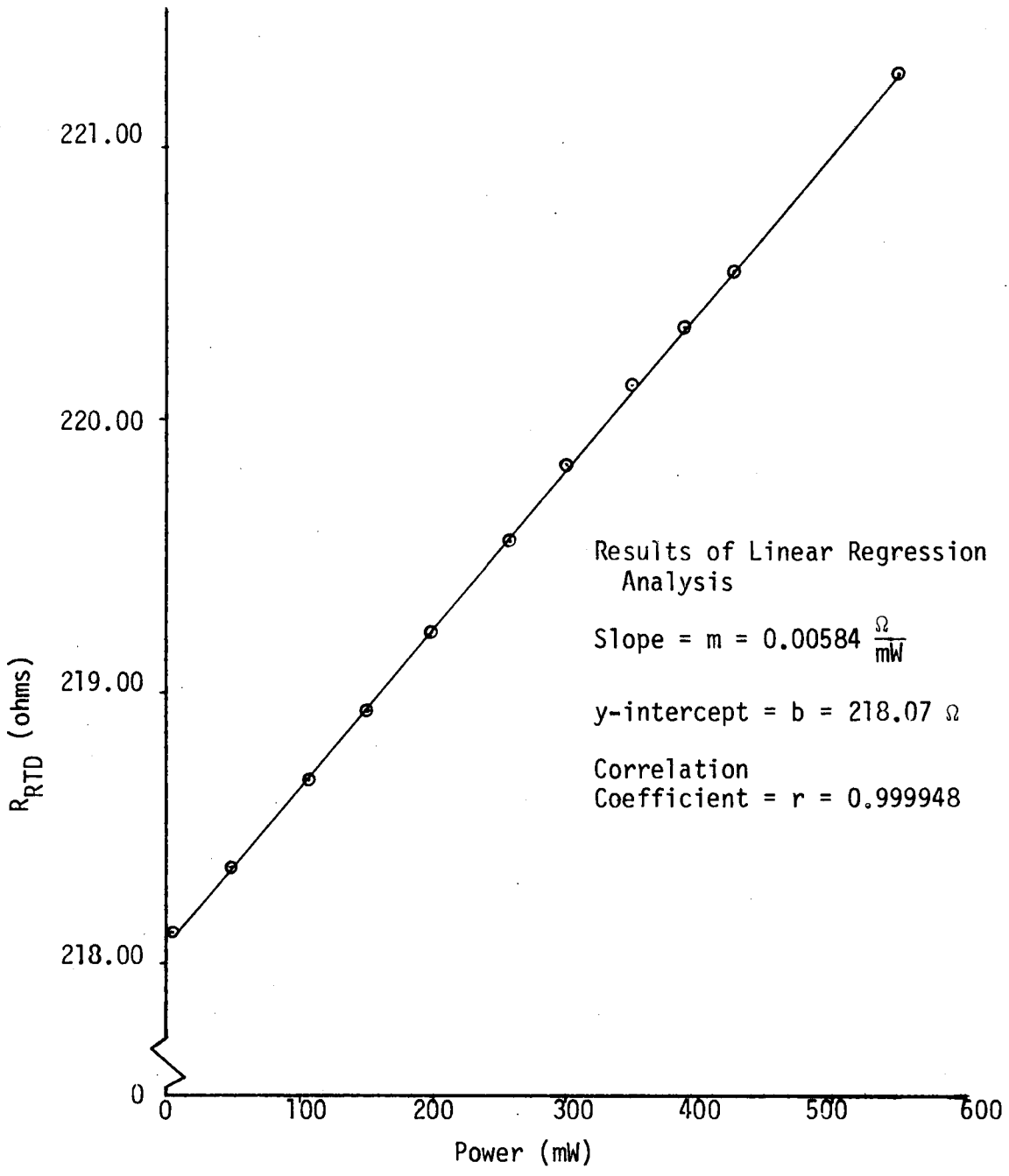


Figure 5.12 Self-Heating Test Result for Bare 176-KF Sensor.

LCSR responses varied over a wide range (from 0.20 to 10.63 seconds).. These values were consistently greater than values of the plunge test time constant (0.34 to 0.39 seconds). This discrepancy or failure of the transformation to predict the correct response accurately was attributed to the physical makeup of the RTD. Implicit in the analytical transformation is the assumption that the sensing element is centrally located. From the x-ray print in Figure 5.4, page 72, it was seen that the sensing element was "distributed" more around the perimeter of the sheath. This violates one of the important assumptions and invalidates the analytical transformation for use on sensors with this characteristic. Failure to predict the correct response response accurately was attributed to the physical makeup of the RTD.

5.5. DISCUSSION OF EMPIRICAL RELATIONSHIPS OBTAINED FROM EXPERIMENTAL RESULTS

Possible methods for manual data acquisition were listed in Section 5.3, page 71. This section describes a means of interpreting in situ RTD test results to predict corresponding sensor plunge test time constants.

Empirical transformations were developed using LCSR, plunge, and self-heating test results. The sensor was tested in many different simulated surface heat transfer configurations. This was accomplished by either placing 3/4 inch fiber glass tape and electrical tape in varying thicknesses securely around the side and/or on the bottom of the

sensor, or by securing lengths of rubber tubing around the outside of the sensor sheath. At each configuration, a series of tests was performed; nominally, four plunge and LCSR tests, and a single self-heating test involving 20-30 data points.

A typical heat transfer configuration is shown in Figure 5.13. The corresponding plunge and LCSR test data are shown in Figures 5.14 and 5.15 with their 63.2% time constants. Table 5.1 lists data obtained from the self-heating test for this configuration. The associated self-heating curve is plotted in Figure 5.16.

The results from laboratory time response testing are tabulated in Table 5.2. Plunge test results, τ_{PL}, varied over the range of 0.34 seconds to 24.2 seconds. Corresponding LCSR results, τ_{LCSR}, varied from 0.026 seconds to 7.16 seconds. Values for the self-heating slope, $\Delta R/\Delta P$, ranged from 5.84×10^{-3} Ω/mW to 1.79×10^{-2} Ω/mW.

The LCSR time constant plotted versus the plunge test time constant is shown in Figures 5.17 and 5.18. The result is a quadratic or exponential relationship that is concave upward. Figures 5.19 and 5.20 show the plunge test time constant versus the self-heating curve slope. The curve rises quadratically or exponentially concave downward.

The sample means and sample standard deviations were computed for each set of LCSR and plunge tests at each heat transfer configuration. The self-heating test was performed only once for each condition. To obtain good statistical results, four or five groups of five data points each were fitted using linear regression analysis. The resulting values of $\Delta R/\Delta P$ were used to compute the mean and standard deviation for that particular self-heating test.

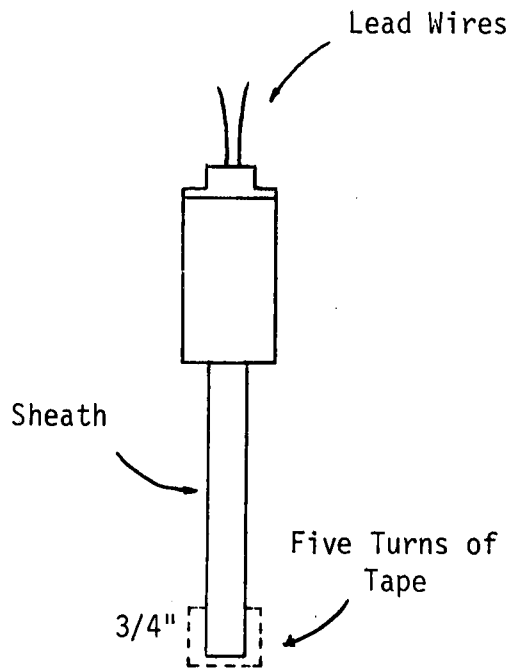
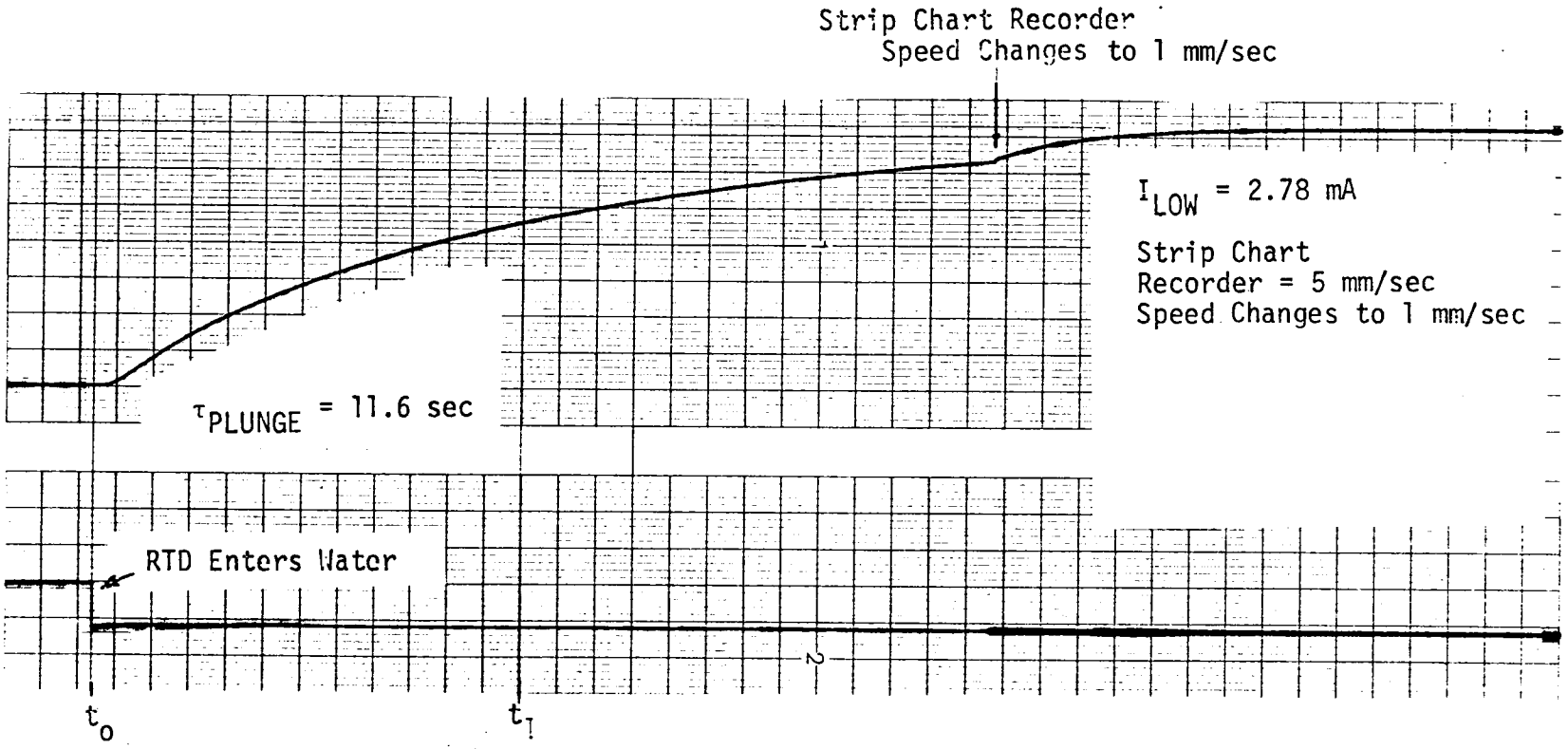


Figure 5.13 Typical Simulated Heat Transfer Configuration.



5.14 Plunge Test for Rosemount 176-KF RTD with Augmented Surface Resistance.

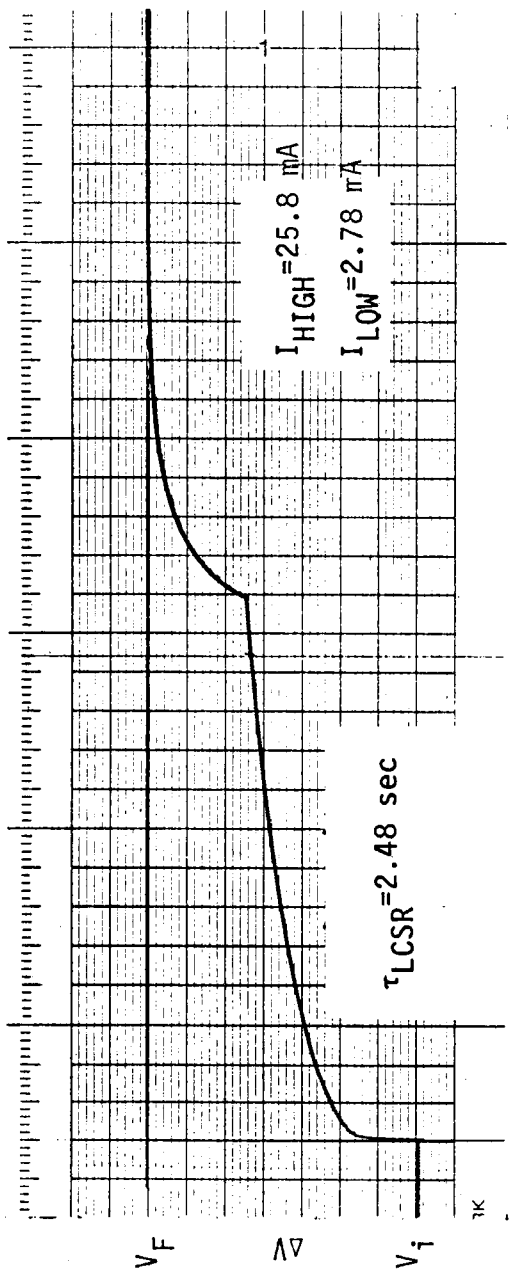


Figure 5.15 LCSR Test for Rosemount 176-KF RTD with Augmented Surface Resistance.

TABLE 5.1

SELF-HEATING TEST DATA FOR RTD WITH AUGMENTED SURFACE RESISTANCE

Voltage (V)	$R_d=R_{RTD}$ (ohms)	Current (mA)	Power (mW)
22.2	223.47	44.4	440.5
21.5	227.08	43.0	412.5
20.3	222.47	40.6	366.7
18.8	221.78	37.6	313.5
17.3	221.09	34.6	264.7
16.1	220.62	32.2	228.7
15.4	220.35	30.8	209.0
14.7	220.10	29.4	190.2
14.0	219.87	28.0	172.4
13.1	219.57	26.2	150.7
12.2	219.29	24.4	130.6
11.0	218.97	22.0	106.0
9.93	218.70	19.9	86.3
9.11	218.52	18.2	72.5
8.27	218.34	16.5	59.7
7.03	218.12	14.1	43.1
6.38	218.01	12.8	35.5
5.46	217.88	10.9	26.0
4.89	217.81	9.78	20.8
3.99	217.72	8.0	13.9
3.02	217.64	6.0	7.9
2.18	217.59	4.36	4.1
1.38	217.55	2.76	1.7

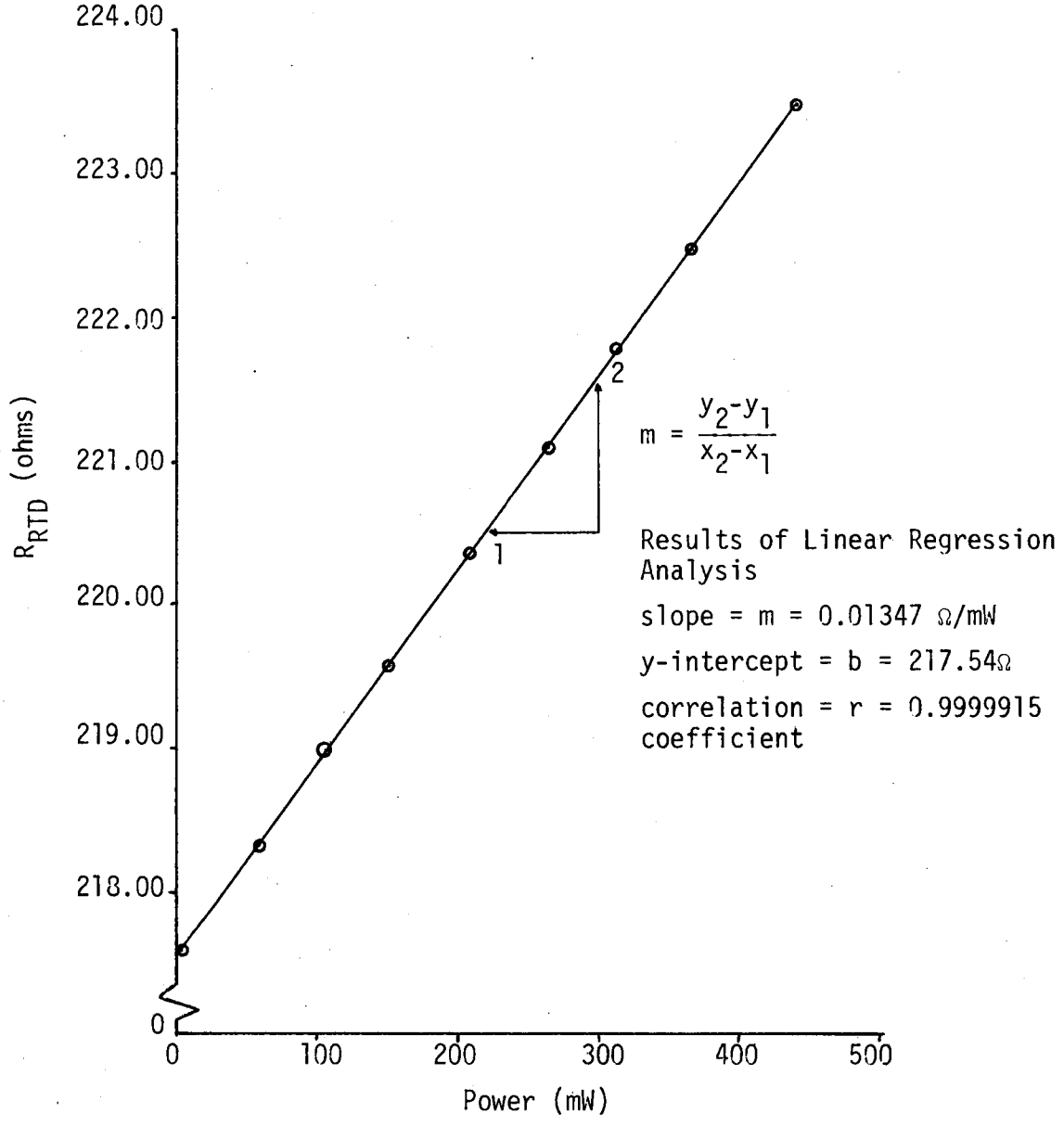


Figure 5.16 Self-Heating Test for Rosemount 176-KF RTD with Augmented Surface Resistance.

TABLE 5.2

LABORATORY TIME RESPONSE TEST DATA

Sample No. \ Trial No.	Plunge Test Results (sec)						LCSR Results (sec)						Self-Heating Results
	1	2	3	4	Mean	Std. Dev.	1	2	3	4	Mean	Std. Dev.	Slope (Ω/mW)
1	0.4	0.38	0.36	0.34	0.362	0.029	0.028	0.030	0.026	0.028	0.028	0.003	0.00584
2	3.91	3.93	3.72	4.02	3.90	0.126	0.8	0.8	0.8	0.82	0.8	0.011	0.0109
3	18.2	17.3	18.7	16.7	17.7	1.27	4.17	4.04	5.61	4.94	4.69	0.601	0.1554
4	9.29	9.48	9.32	9.12	9.3	0.15	1.74	1.68	1.72	1.64	1.69	0.041	0.1248
5	11.75	12.08	11.6	11.6	11.76	0.226	2.48	2.44	2.56	2.36	2.46	0.083	0.01347
6	13.4	12.8	12.6	12.5	12.83	0.40	3.8	3.86	4.0	3.88	3.87	0.082	0.01448
7	24.2	24.4	24.2	24.0	24.2	0.16	6.4	6.3	6.6	6.5	6.48	0.13	0.01776
8	9.64	9.7	9.56	9.6	9.63	0.06	2.26	2.16	2.24	2.20	2.22	0.044	0.01339
9	5.60	5.64	5.58	5.66	5.62	0.04	1.08	1.08	1.06	1.06	0.07	0.012	0.01127
10	20.8	20.88	21.4	20.8	20.97	0.29	5.10	5.12	5.08	5.08	5.1	0.02	0.01633
11	3.2	3.08	3.16	3.24	3.17	0.07	0.62	0.62	0.63	0.60	0.62	0.013	0.0098
12	2.16	2.14	2.15	2.32	2.19	0.09	0.4	0.41	0.41	0.41	0.41	0.005	0.00888
13	1.6	1.7	1.62	1.6	1.63	0.05	0.344	0.32	0.3	0.33	0.33	0.016	0.00864
14	13.6	13.4	13.48	13.5	13.49	0.08	2.72	2.84	2.70	2.66	2.73	0.077	0.01400
15	16.1	16.2	16.0	16.0	16.1	0.087	4.0	4.12	3.98	3.96	9.02	0.072	0.01547
16	15.2	15.18	15.3	15.2	15.22	0.054	3.44	3.68	3.6	3.72	3.61	0.124	0.01498
17	17.3	17.0	17.0	16.9	17.05	0.513	3.6	3.56	3.58	3.52	3.57	0.034	0.01497
18	25.1	25.6	25.0	25.7	25.6	0.374	6.9	7.16	7.12	7.04	7.06	0.115	0.01794
19	16.0	15.7	15.6	15.6	15.73	0.189	4.4	4.42	4.44	4.5	4.44	0.043	0.01585
20	19.84	19.9	19.5	20.1	19.84	0.25	4.56	4.48	4.6	4.54	4.57	0.069	0.01601
21	21.4	21.3	21.4	21.2	21.33	0.096	5.24	5.18	5.12	5.2	5.17	0.058	0.01654
22	22.7	22.6	22.0	22.2	22.4	0.33	5.52	5.52	5.5	5.56	5.53	0.025	0.01681

TABLE 5.2 (Continued)

Sample No. \ Trial No.	Plunge Test Results (sec)						LCSR Results (sec)						Self-Heating Results
	1	2	3	4	Mean	Std. Dev.	1	2	3	4	Mean	Std. Dev.	Slope (Ω/mW)
23	0.450	0.460	0.480	0.552	0.486	0.046	0.036	0.036	0.040	0.040	0.038	0.002	0.00641
24	2.42	2.44	2.40	2.42	2.42	0.02	0.476	0.424	0.444	0.464	0.446	0.026	0.00931
25	1.39	1.54	1.40	1.66	1.50	0.13	0.234	0.246	0.242	0.230	0.238	0.007	0.00835
26	1.70	1.80	1.84	1.98	1.83	0.12	0.302	0.314	0.318	0.314	0.311	0.005	0.00883
27	2.06	2.12	2.08	2.16	2.11	0.04	0.374	0.364	0.384	0.372	0.373	0.008	0.00914
28	0.91	0.95	0.86	0.94	0.92	0.04	0.140	0.152	0.144	0.147	0.146	0.005	0.00738
29	1.17	1.25	1.23	1.07	1.18	0.08	0.189	0.180	0.190	0.184	0.188	0.050	0.00778
30	0.664	0.665	0.670	0.663	0.665	0.003	0.069	0.068	0.083	0.076	0.074	0.007	0.00675
31	2.99	2.95	3.03	2.93	2.97	0.044	0.559	0.558	0.570	0.566	0.563	0.006	0.00973

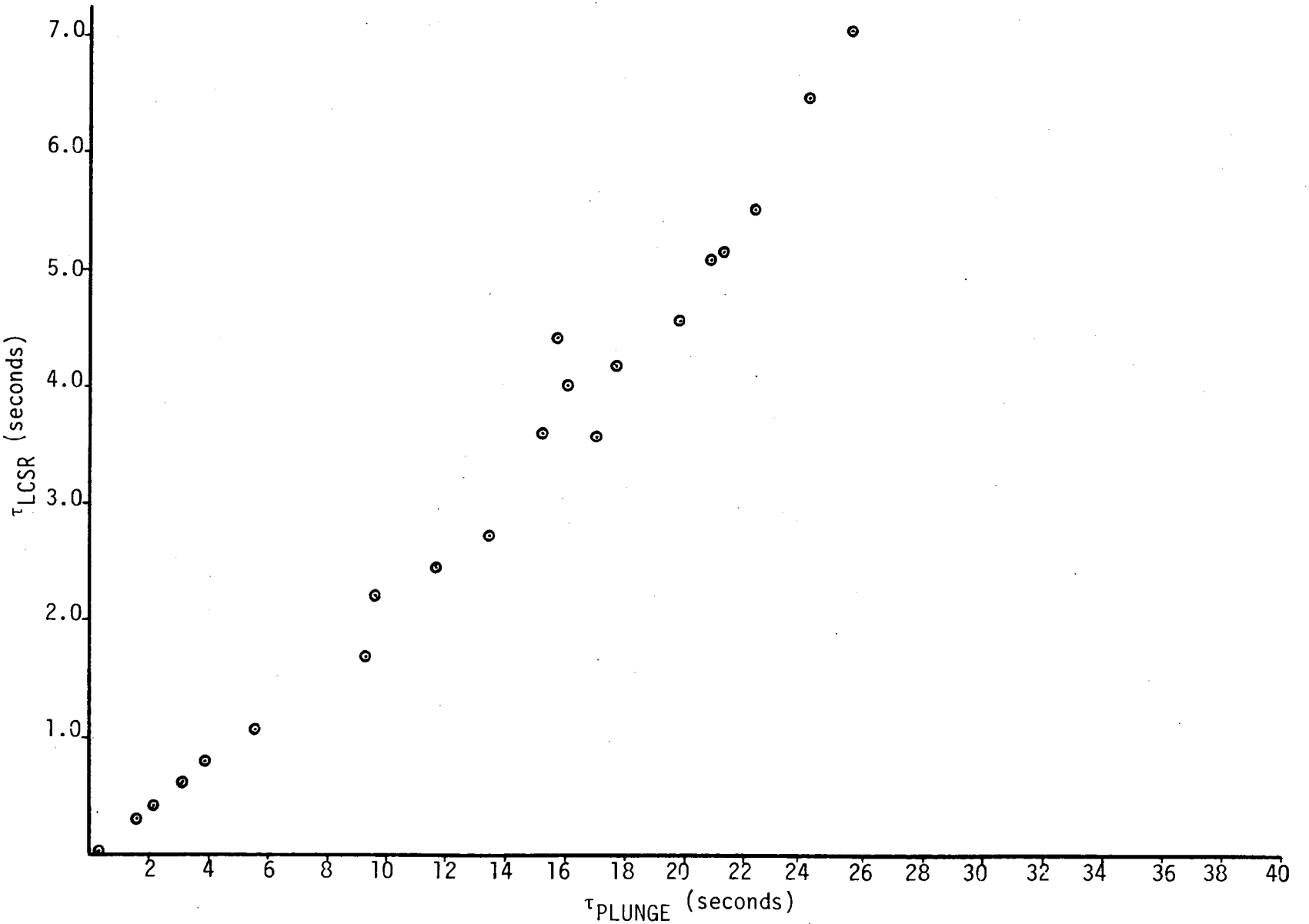


Figure 5.17 τ_{LCSR} versus τ_{PLUNGE}.

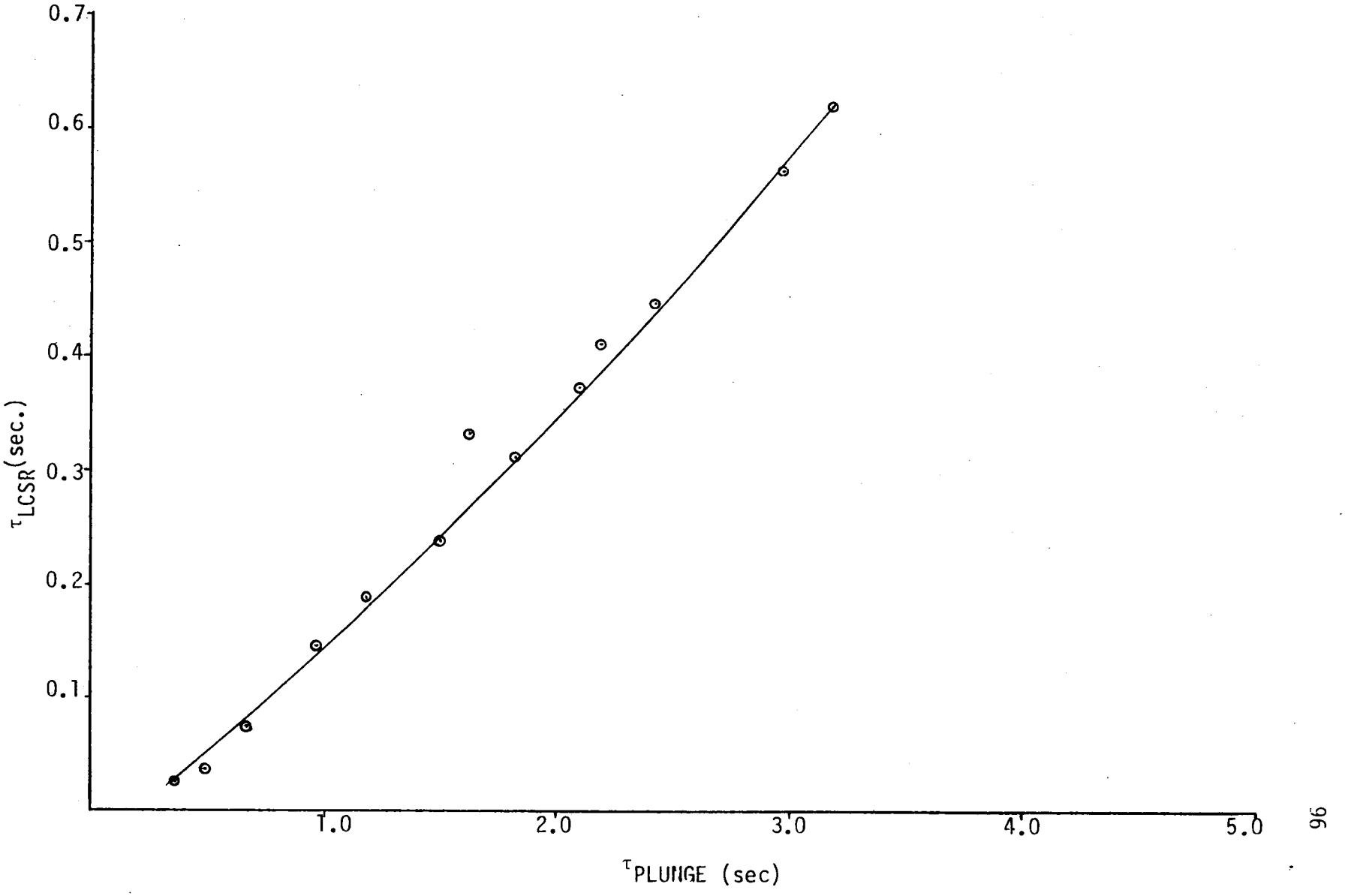


Figure 5.18 τ_{LCSR} Versus τ_{PLUNGE}: Lower Region.

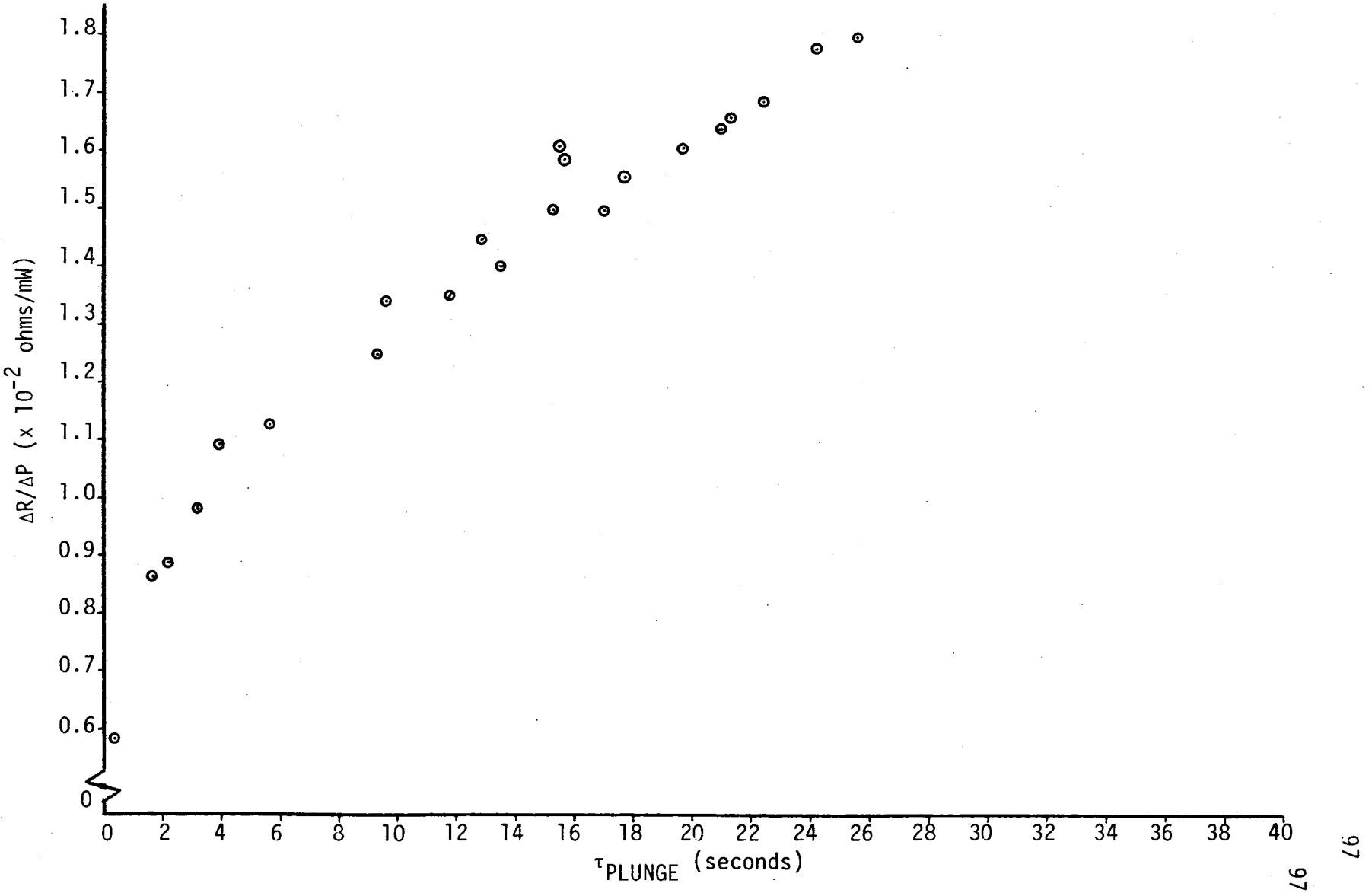


Figure 5.19 Self-Heating Slope versus τ_{PLUNGE}.

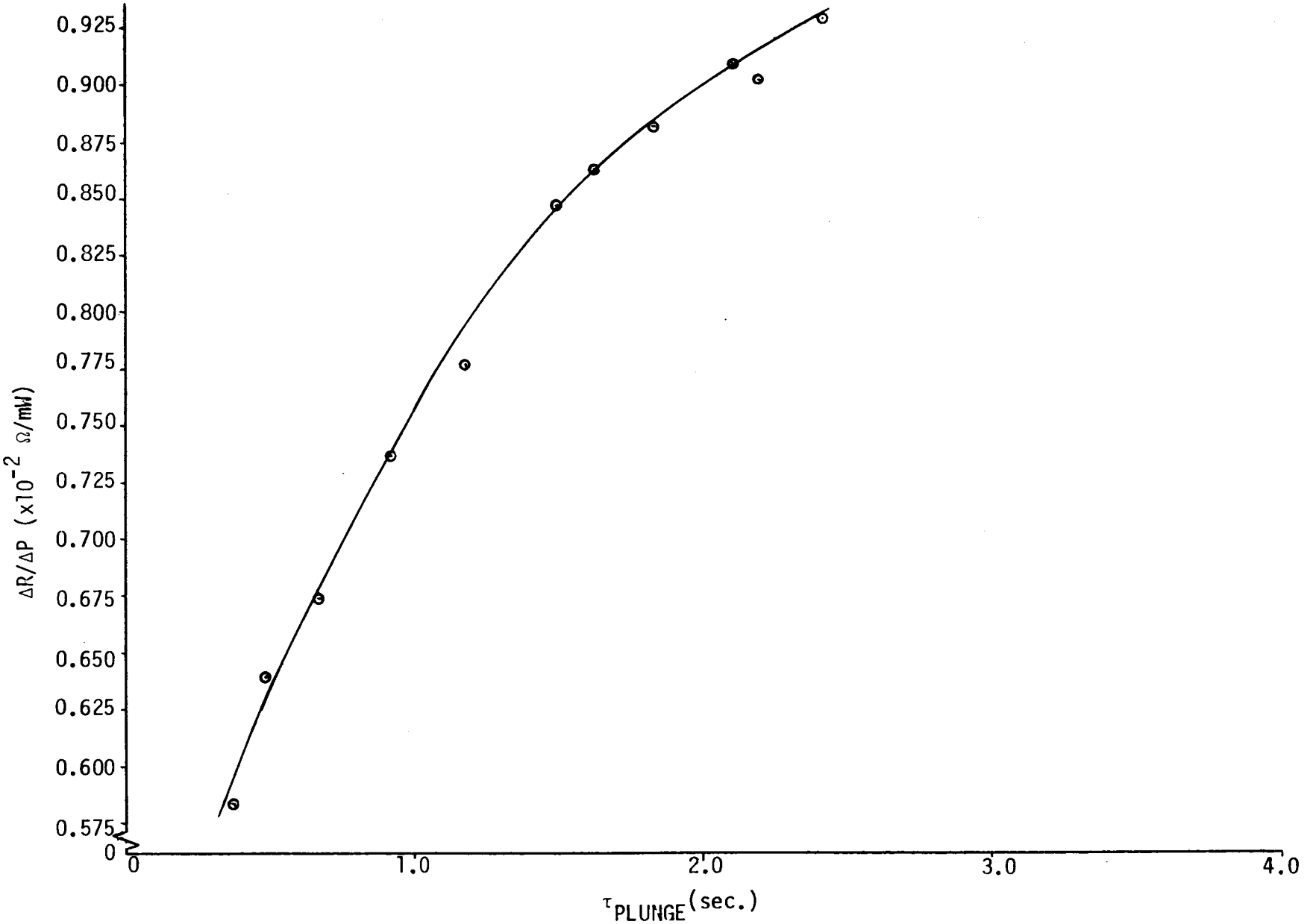


Figure 5.20 Self-Heating Slope Versus τ_{PLUNGE}: Lower Region.

At this point in the research, the error analysis was combined with a statistical effort to assure a conservative interpretation of the results. A one-sided 99% upper bound confidence interval was calculated using the t-distribution (Appendix C). Error bounds were obtained for each data point. These error limits were plotted and curves containing the outermost limits were drawn.

Figures 5.21 and 5.22 show the curves representing the empirical correlation to τ_{LCSR} versus τ_{PL} with a 99% confidence interval. Correspondingly, a one-sided 99% upper bound confidence interval curves for $\Delta R/\Delta P$ versus τ_{PL} are shown in Figures 5.23 and 5.24.

Conservative conclusions can be drawn using Figures 5.21, 5.22, 5.23, and 5.24 in conjunction with in situ experimental response time test data. Given a mean value of τ_{LCSR} or $\Delta R/P$ from a series of tests weighted by the appropriate number of standard deviations, one can be 99% confident that the actual value of the plunge test time constant, τ_{PL} is less than or equal to the corresponding value read off the appropriate graph.

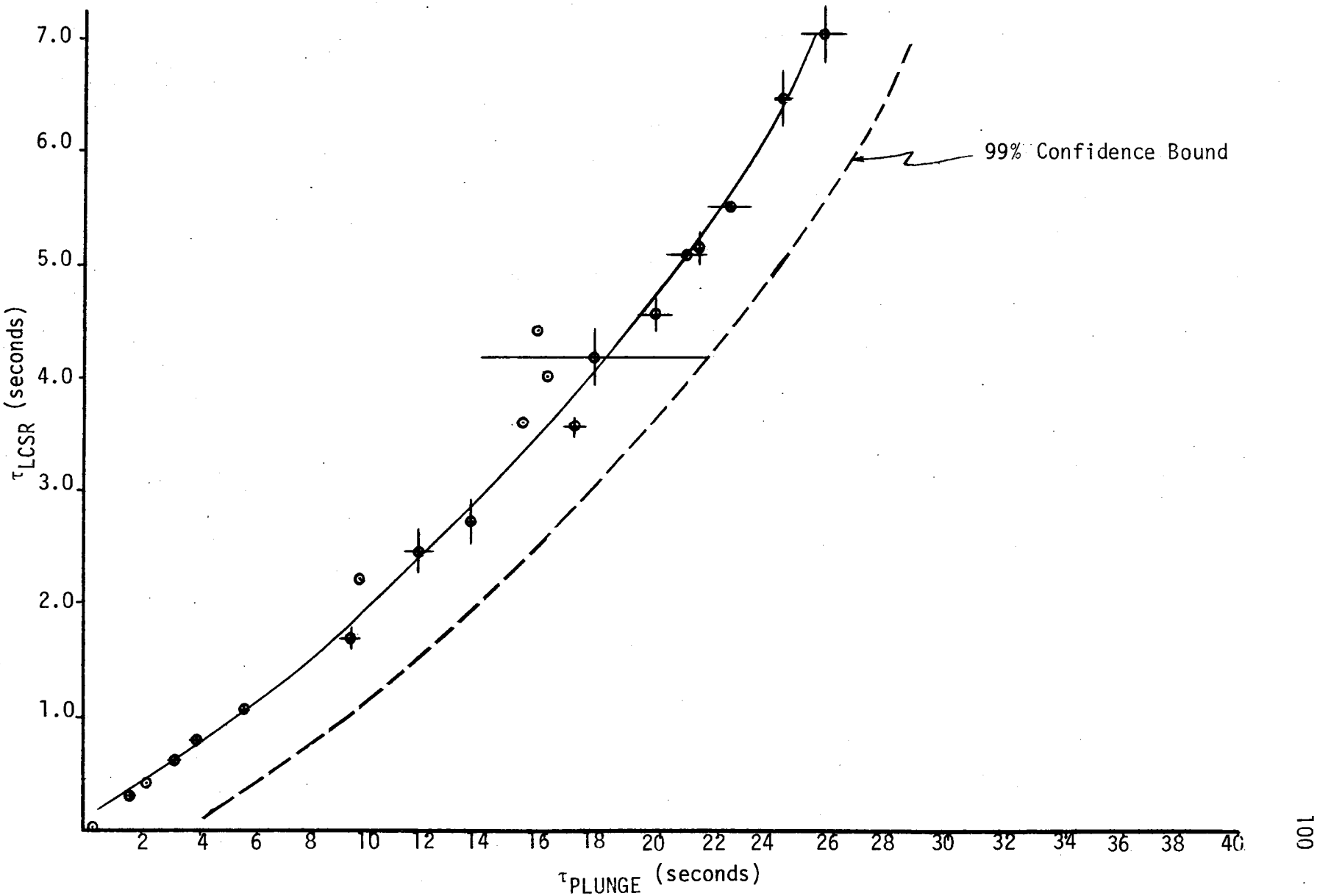


Figure 5.21 τ_{LCSR} versus τ_{PLUNGE} with a 99% Upper Confidence Bound.

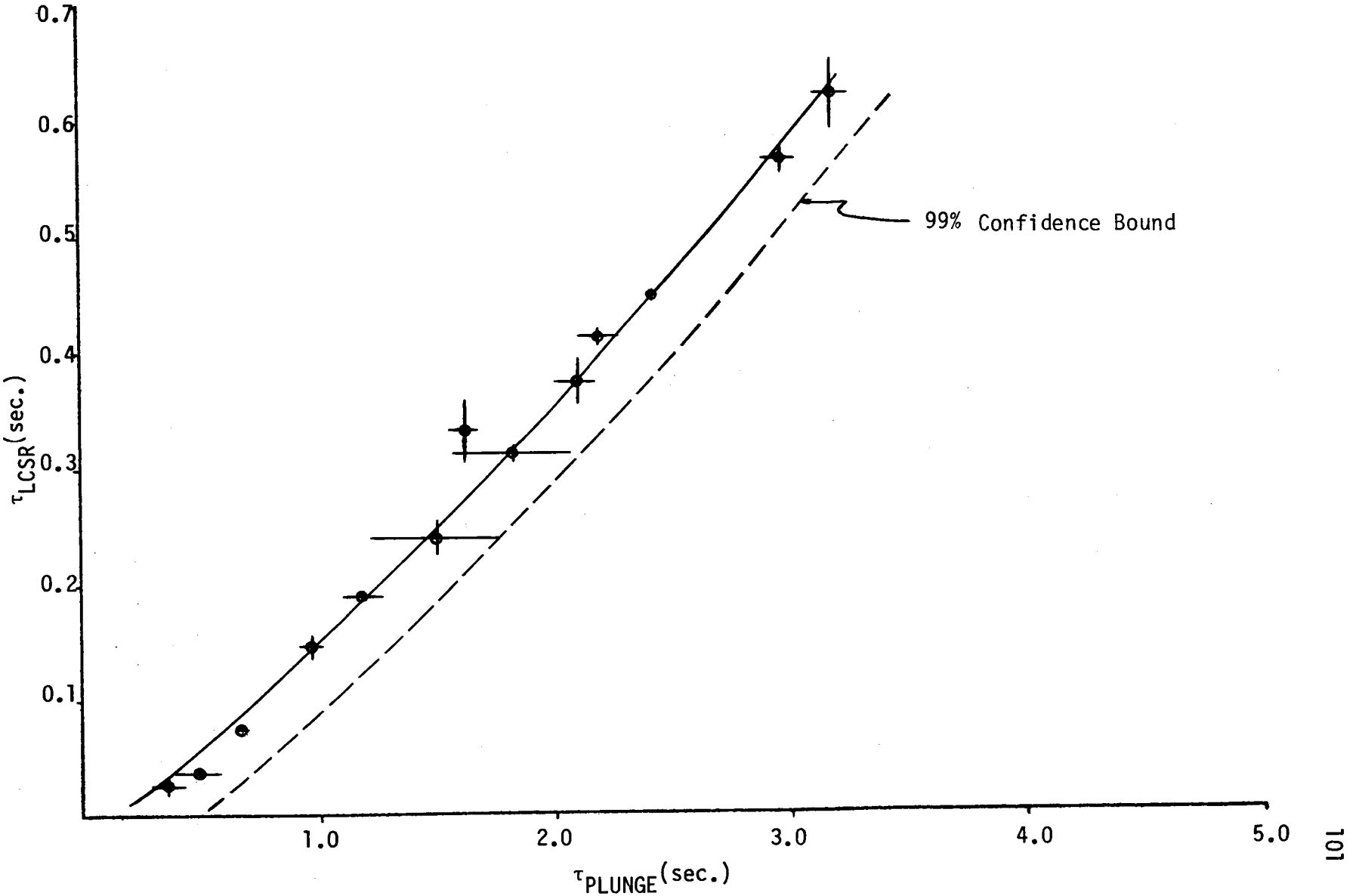


Figure 5.22 τ_{LCSR} Versus τ_{PLUNGE}: Lower Region with a 99% Upper Confidence Bound.

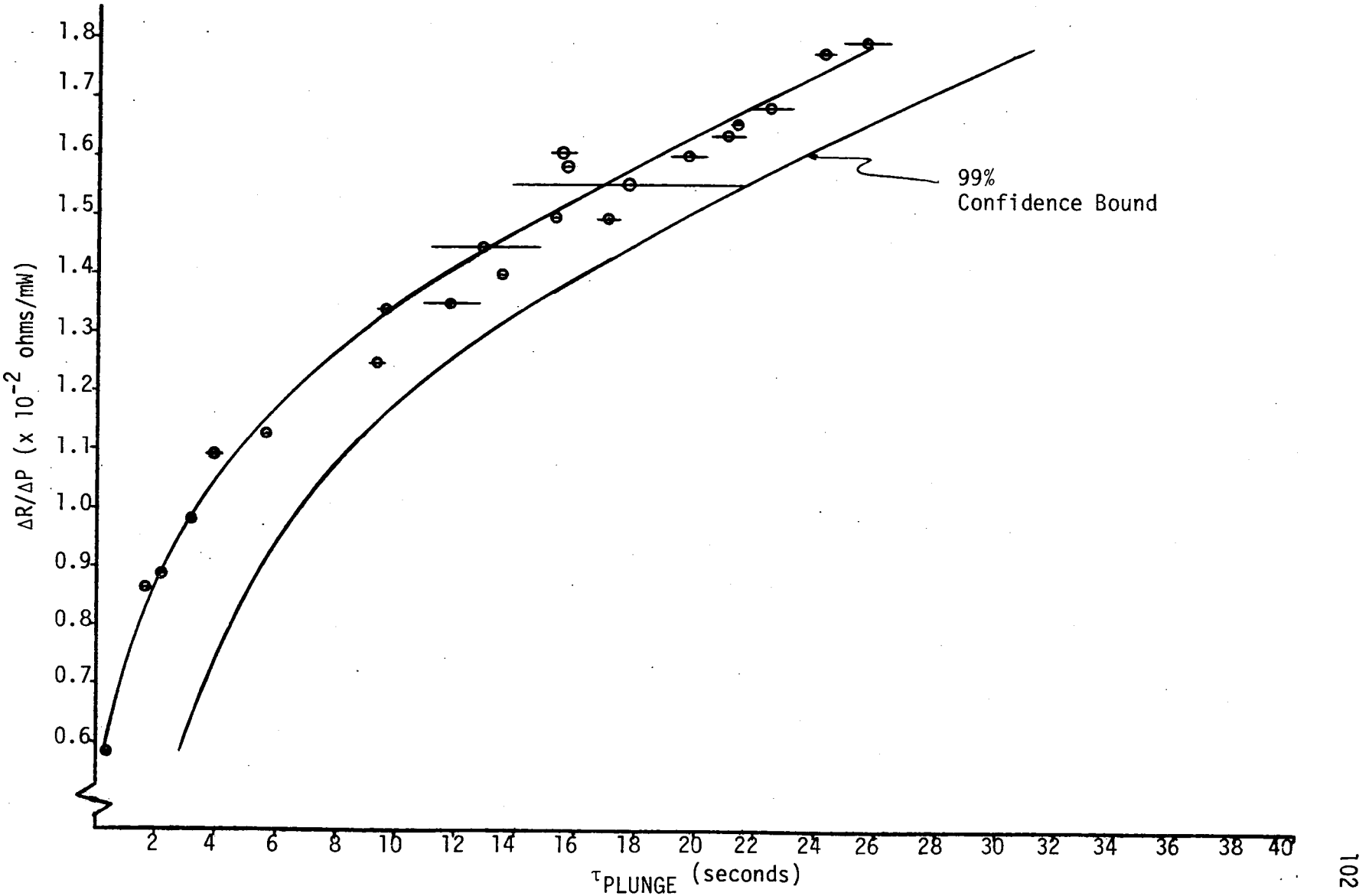


Figure 5.23 Self-Heating Slope versus τ_{PLUNGE} with a 99% Upper Confidence Bound.

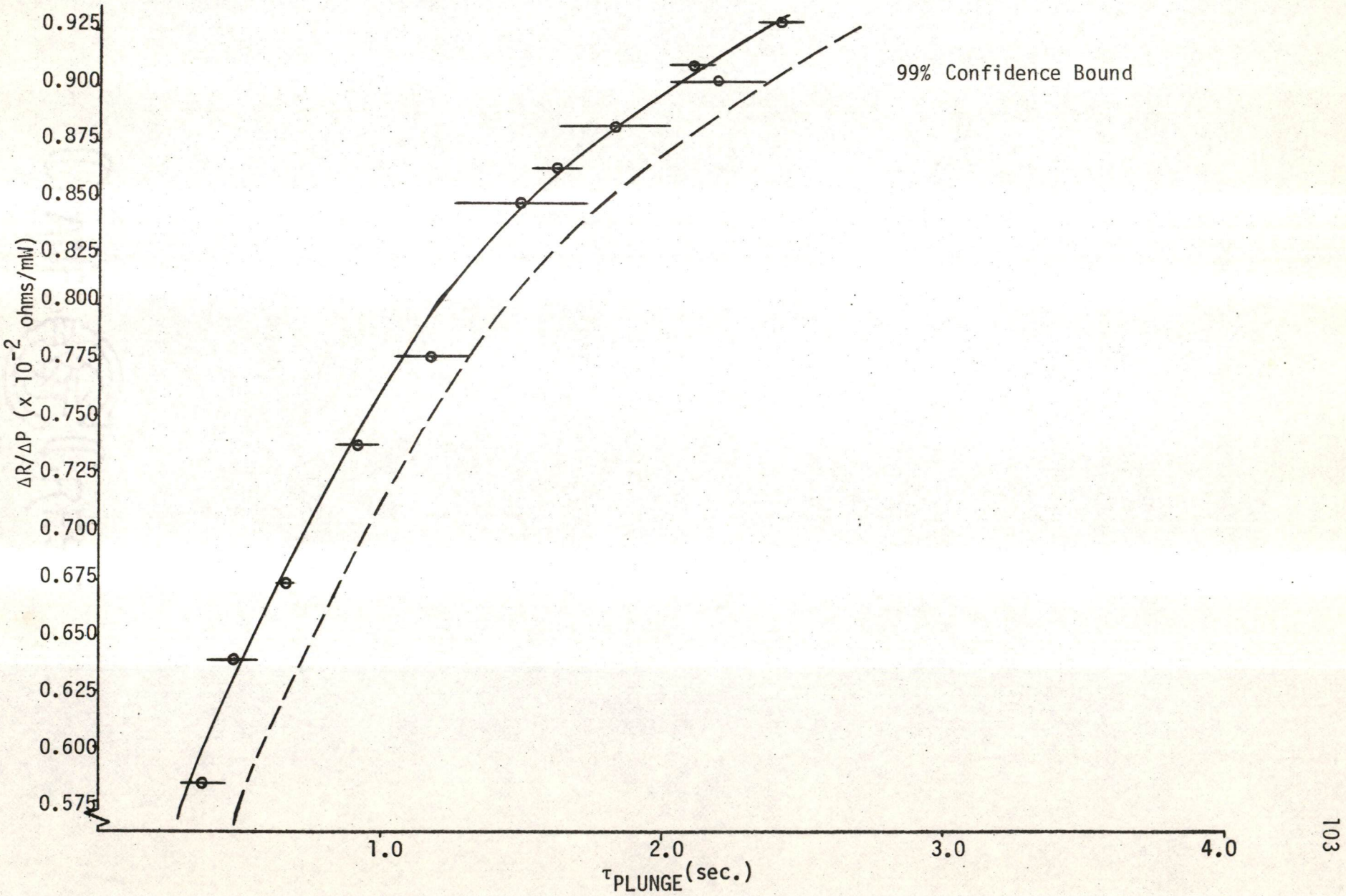


Figure 5.24 Self-Heating Slope Versus τ_{PLUNGE}: Lower Region with a 99% Upper Confidence Bound.

CHAPTER 6

IN-PLANT TIME RESPONSE TESTING

Preliminary time response testing was conducted in March 1976 at Florida Power and Light Company's Turkey Point Nuclear Plant Unit 3. The purpose of this visit was to perform in situ loop current step response tests in an operating reactor and to determine resistance temperature detector time constants.

6.1. DESCRIPTION OF TESTING APPARATUS

The equipment used in the testing was assembled in the cable spreading room directly beneath the Unit 3 control room. The two-wire bridge described in Section 5.2, page 63, was used for the resistance measurement. The bridge output was routed to a low noise amplifier where the signal voltage was increased. A PDP-11/20 computer was used to collect the data and later analyze the results. Two voltmeters were used: a Vallhalla Scientific Company Model 4440 Digital Multimeter and a Systron-Donner Model 7004 Digital Multimeter. They were used to monitor the bridge-amplifier output and to monitor the current through the RTD. Connection to the RTD was made through terminals located in a reactor instrumentation cabinet.

A checkout of the testing set up revealed that the relay circuit which switches the current was not functioning properly. The relay would not change state (open or close) when actuated. In order to perform the tests, the current was switched manually using a banana

plug to shunt around the 3K resistor. This method of current management may have resulted in a problem when the plug did not make proper contact with its "seat." This appears to have resulted in "clatter" or "spiking" in the voltage signal when the current was switched improperly. This effect is shown in Figure 6.1.

6.2 TEST DESCRIPTION AND PROBLEMS ENCOUNTERED

A control or baseline test was performed at Turkey Point on the same sensor that was used in the laboratory testing described in Chapter 5, page 63. The RTD was placed in a bucket of water. The LCSR data record that was taken, shown in Figure 6.2, indicated that the testing setup was operating properly except for the relay.

Twenty-five LCSR tests were performed. However, it was found that only six of the resulting data records were useable. All of the thers were so contaminated with spurious spikes as to be useless. The six data records were found to have a single spike near the beginning of the test. Figures 6.3 through 6.8 show the affected regions of the data shortly after the step change in current.

After returning to the lab, LCSR tests were run with the Systron-Donner voltmeter connected across the 500 ohm resistor to measure the current to the RTD. This resulted in a spike in the bridge output much like what was experienced at Turkey Point. Figure 6.9 shows a transient with the suspected voltmeter included for voltage drop measurement in a LCSR test in the laboratory. Numerous tests were conducted and the spike occurred in each one with the Systron-Donner

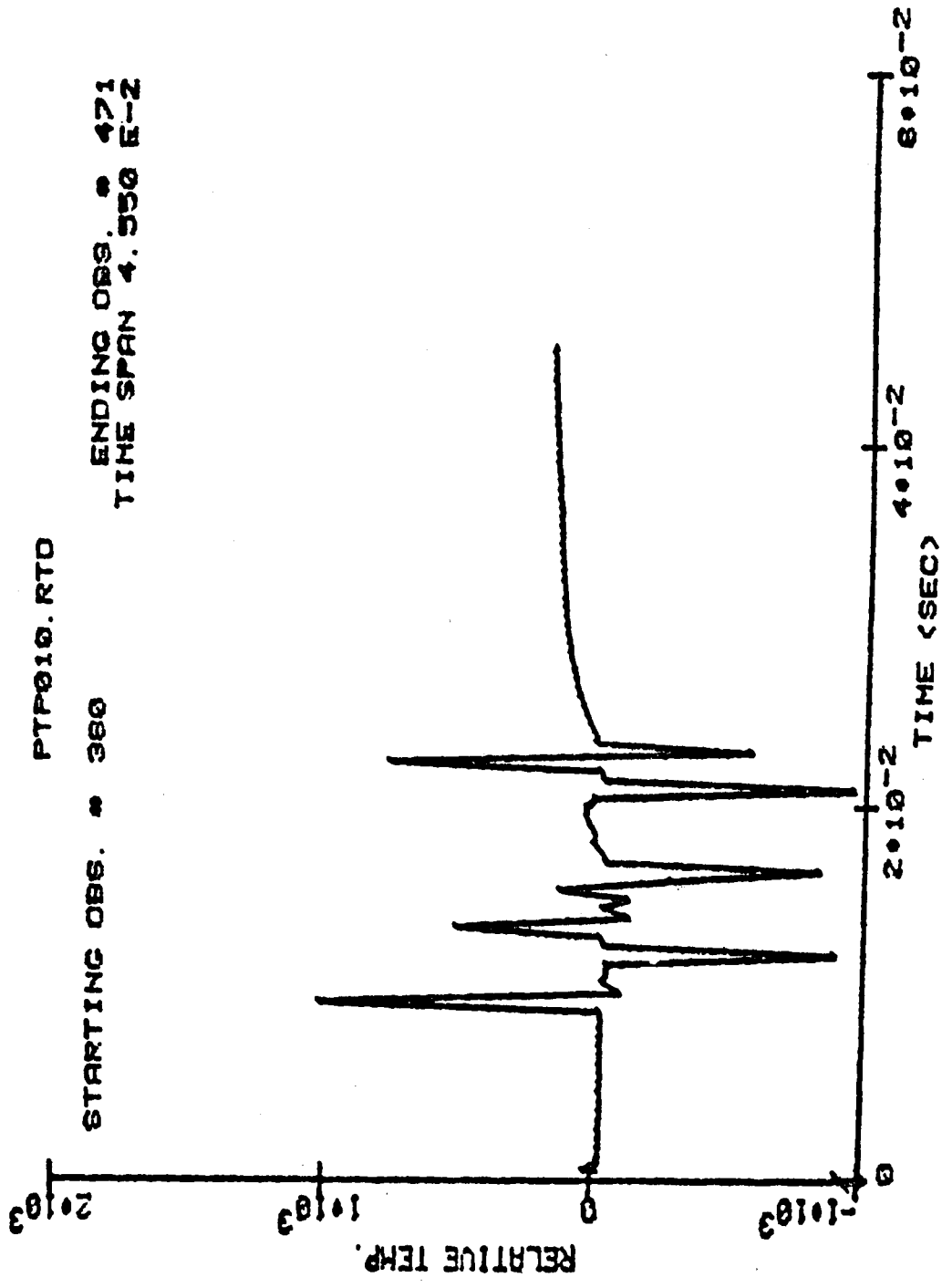


Figure 6.1 Possible LCSR Test Switching Clatter.

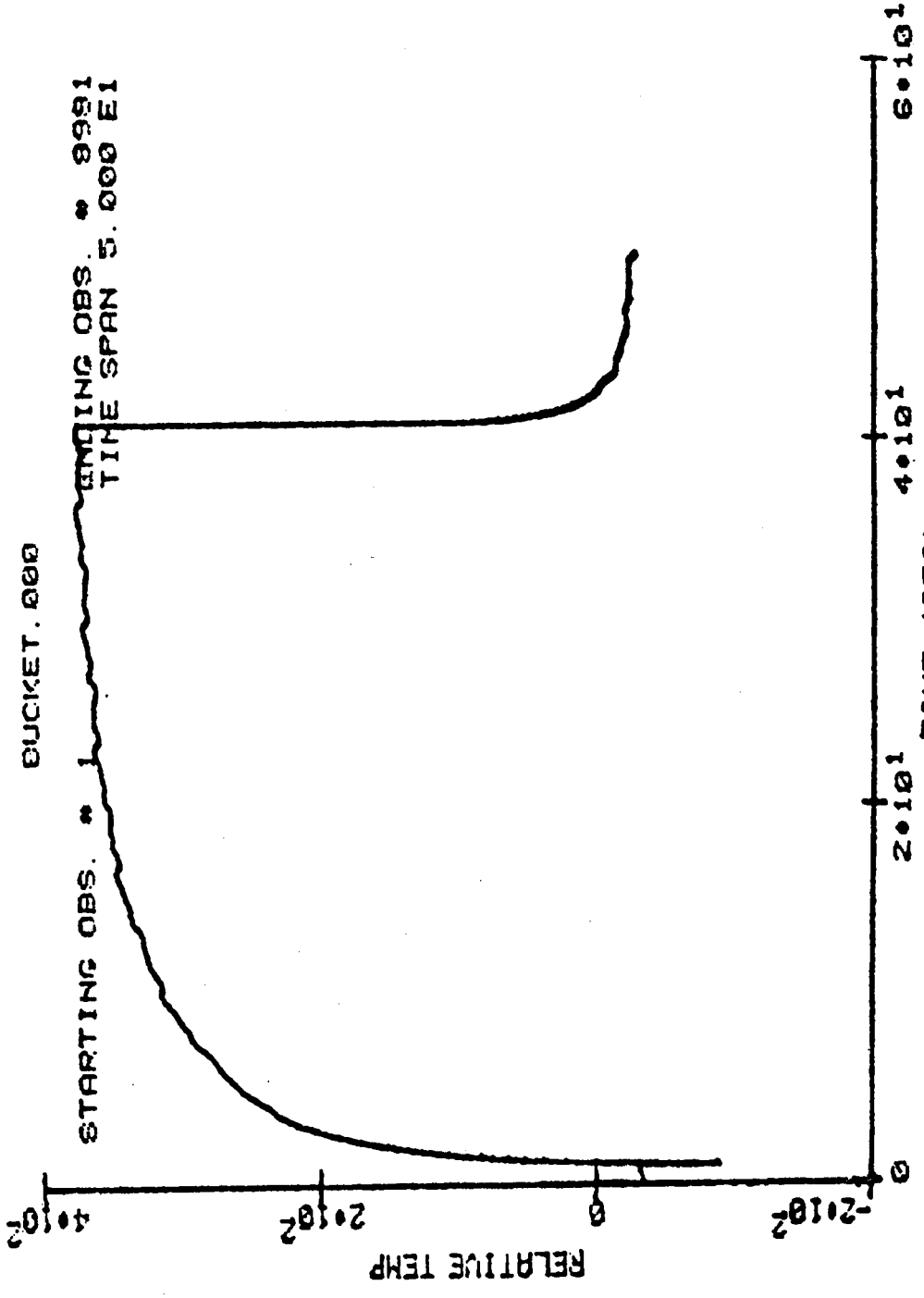


Figure 6.2 LCSR Data on Sensor in Bucket.

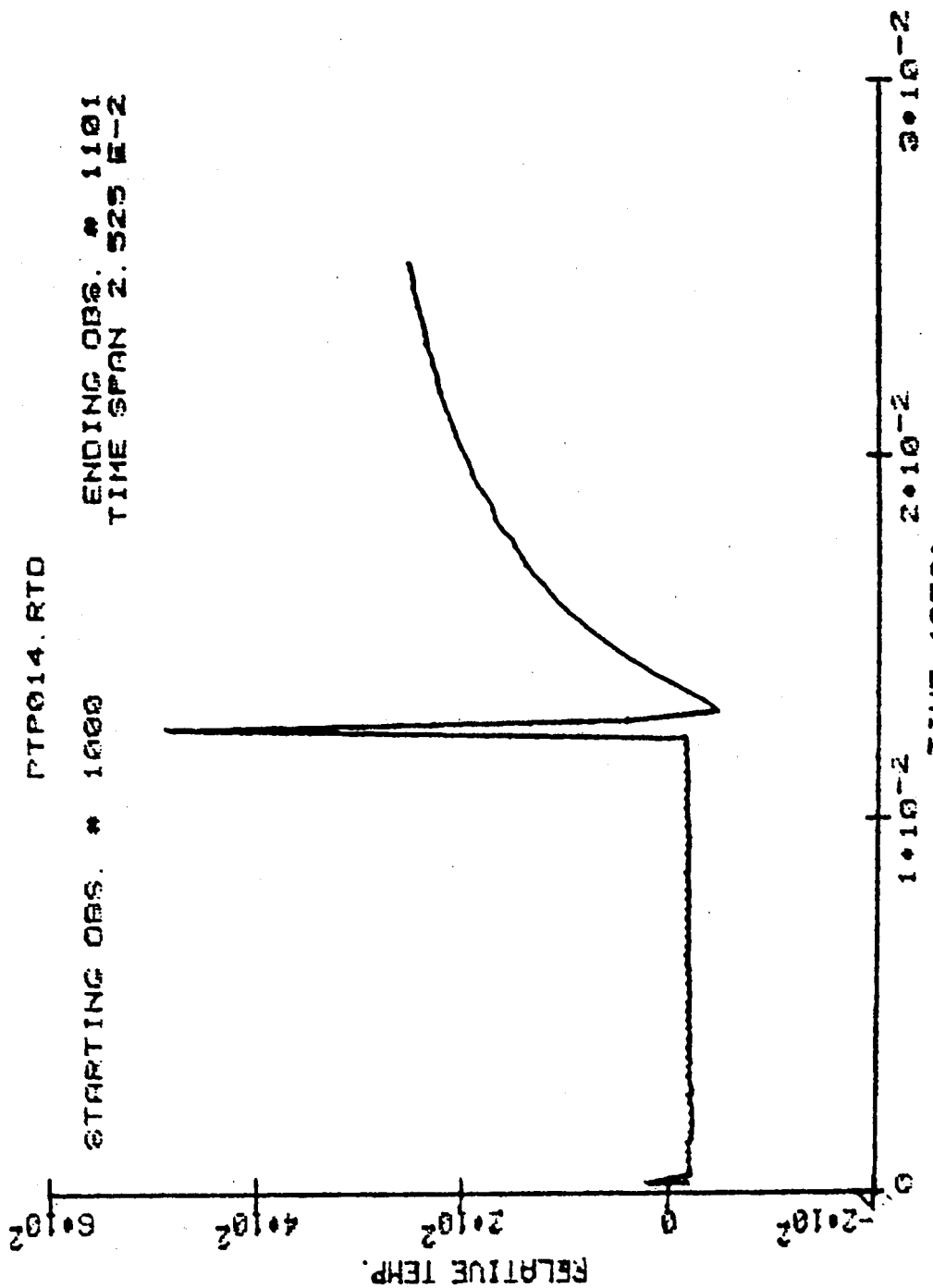


Figure 6.3 LCSR Test PTP014 RTD Data.

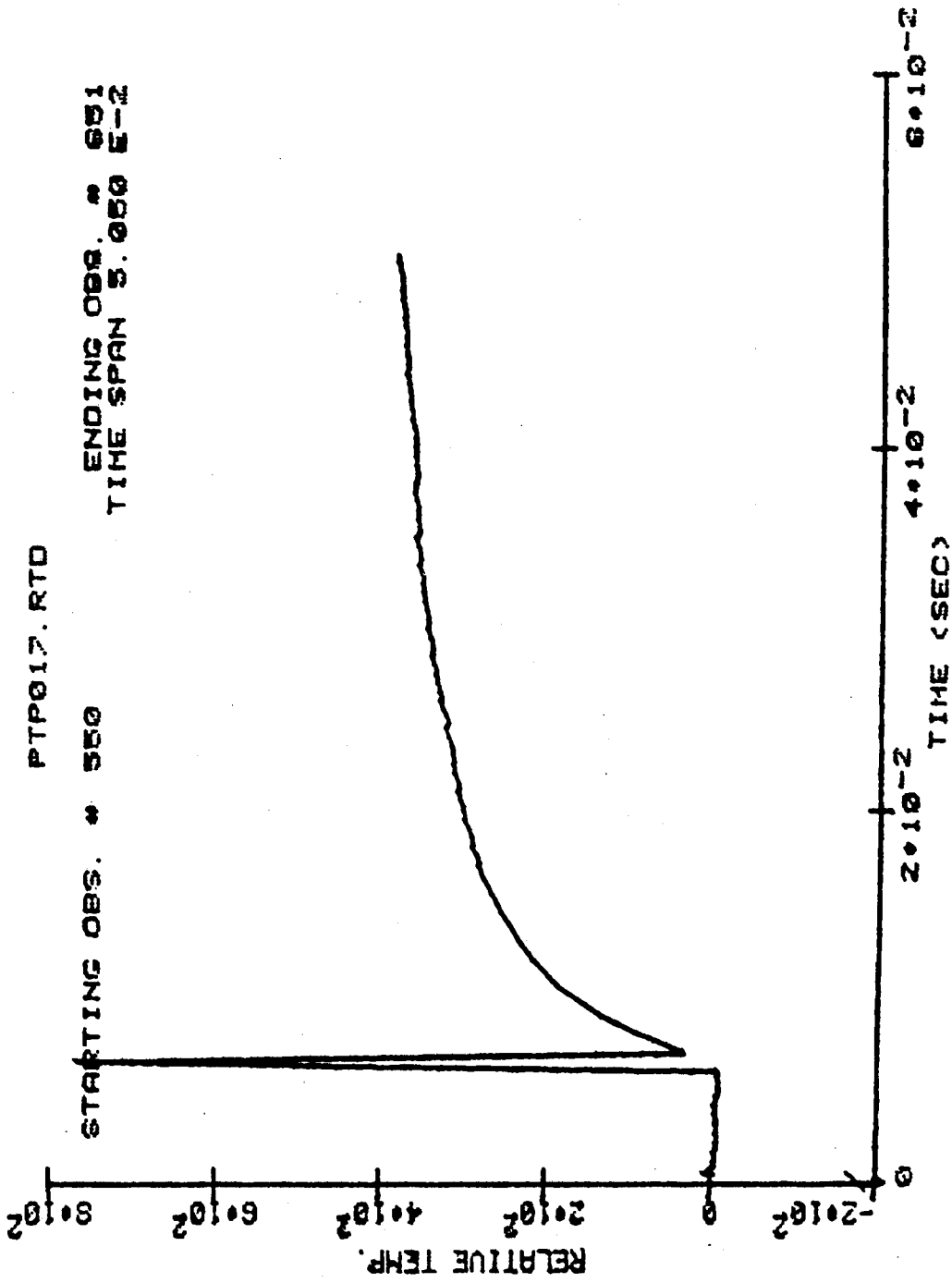


Figure 6.4 LCSR Test PTP017 RTD Data.

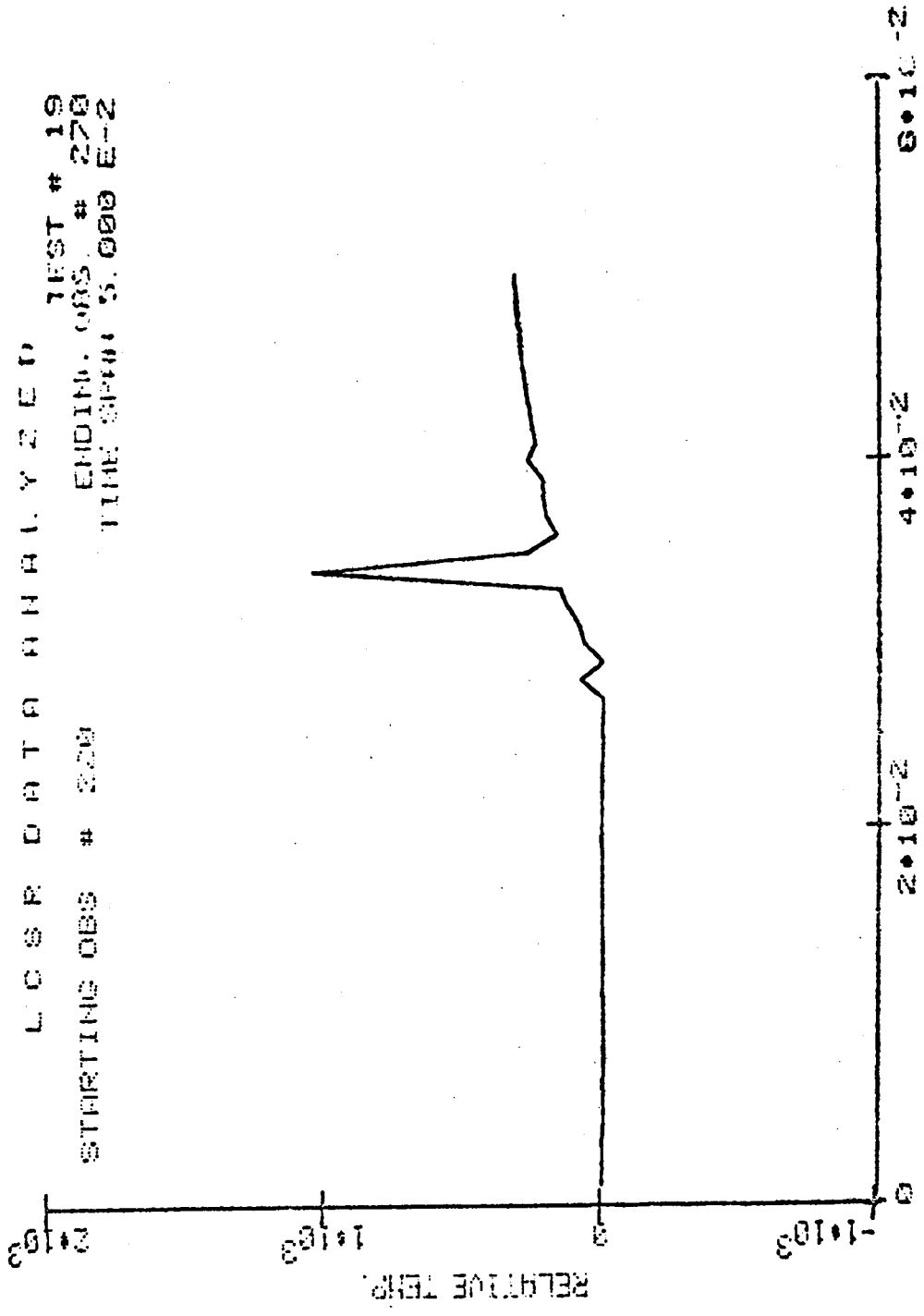


Figure 6.5 LCSR Test PTP019 RTD Data.

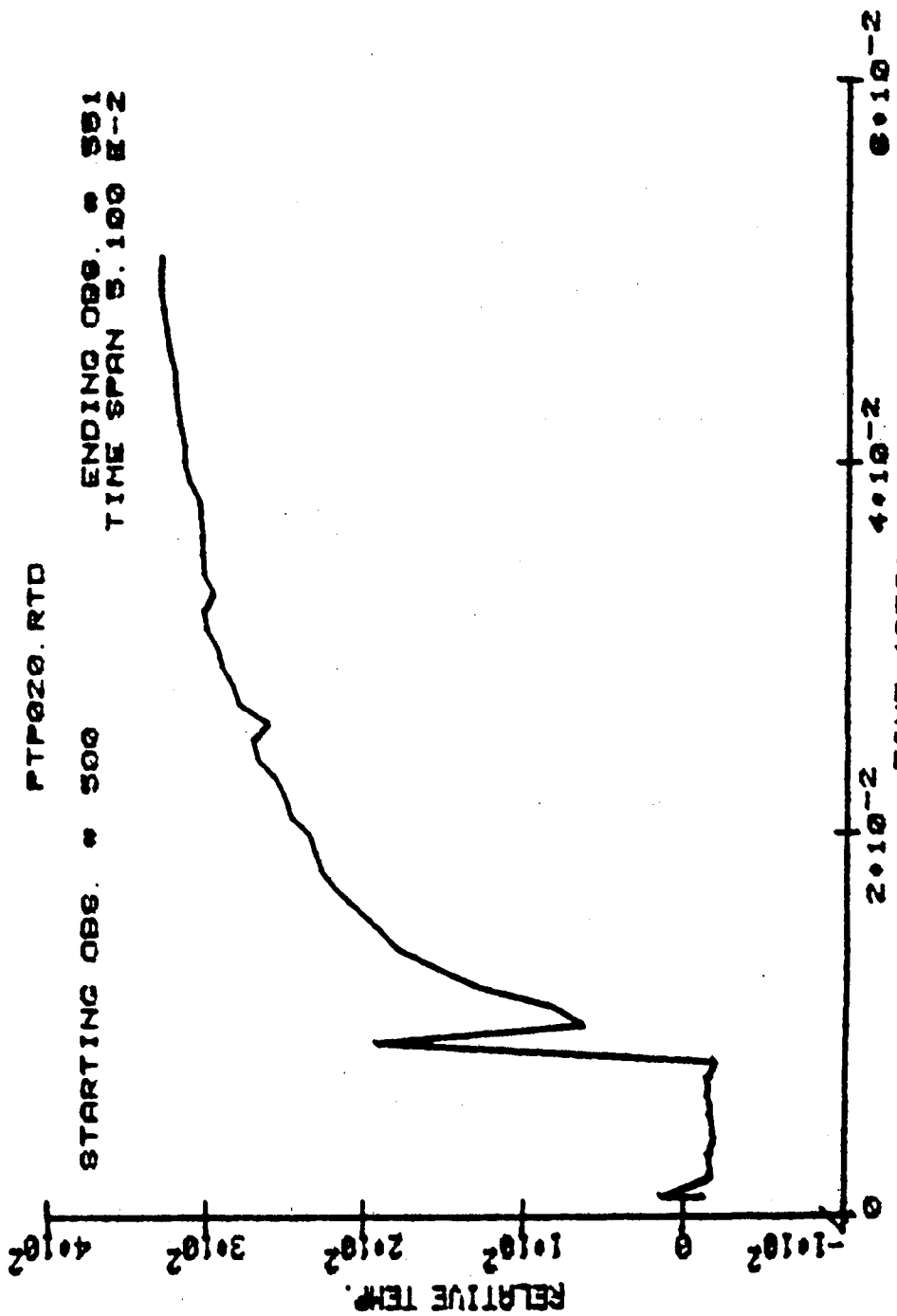


Figure 6.6 LCSR Test PTP020 RTD Data.

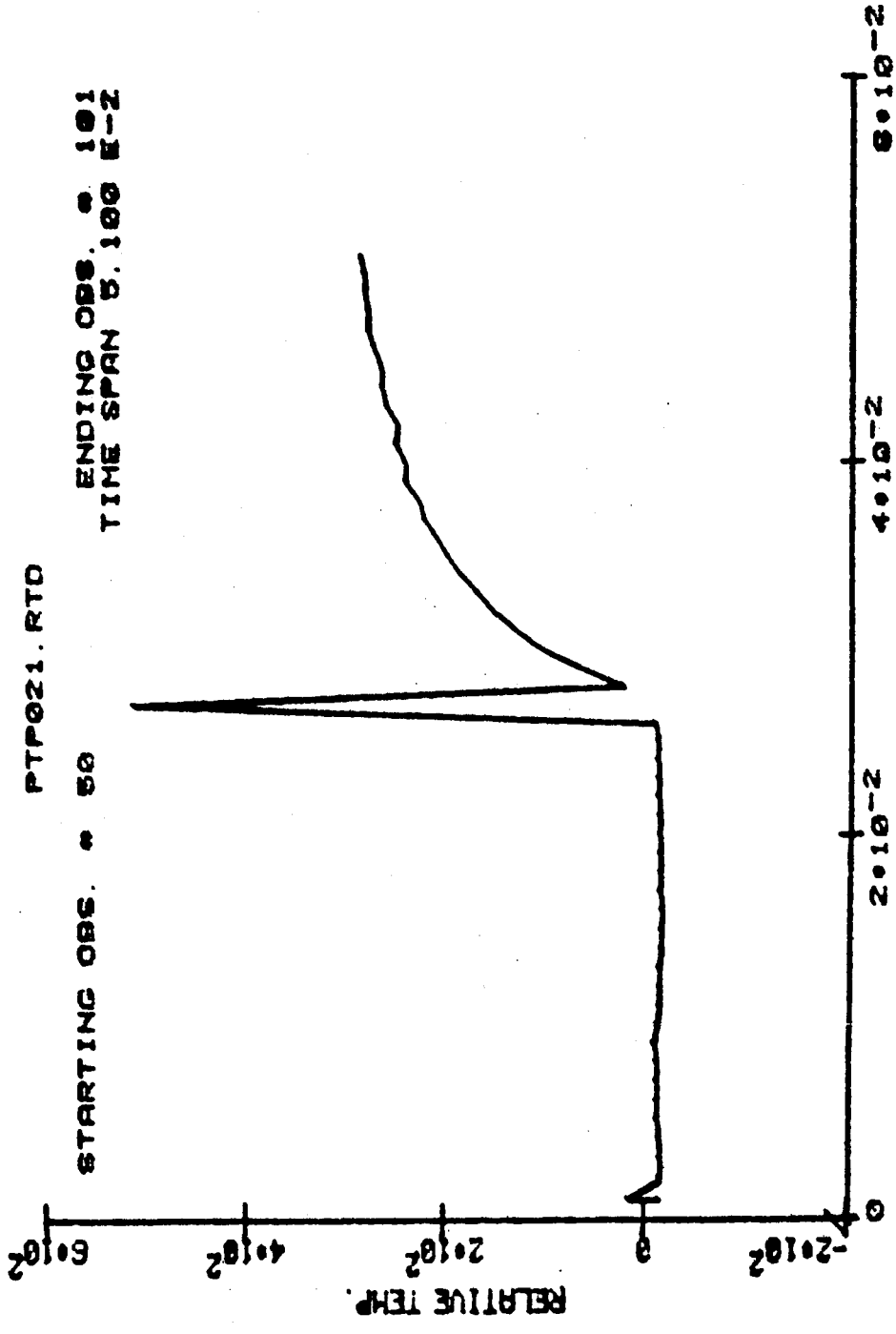


Figure 6.7 LCSR Test PTP021 RTD Data.

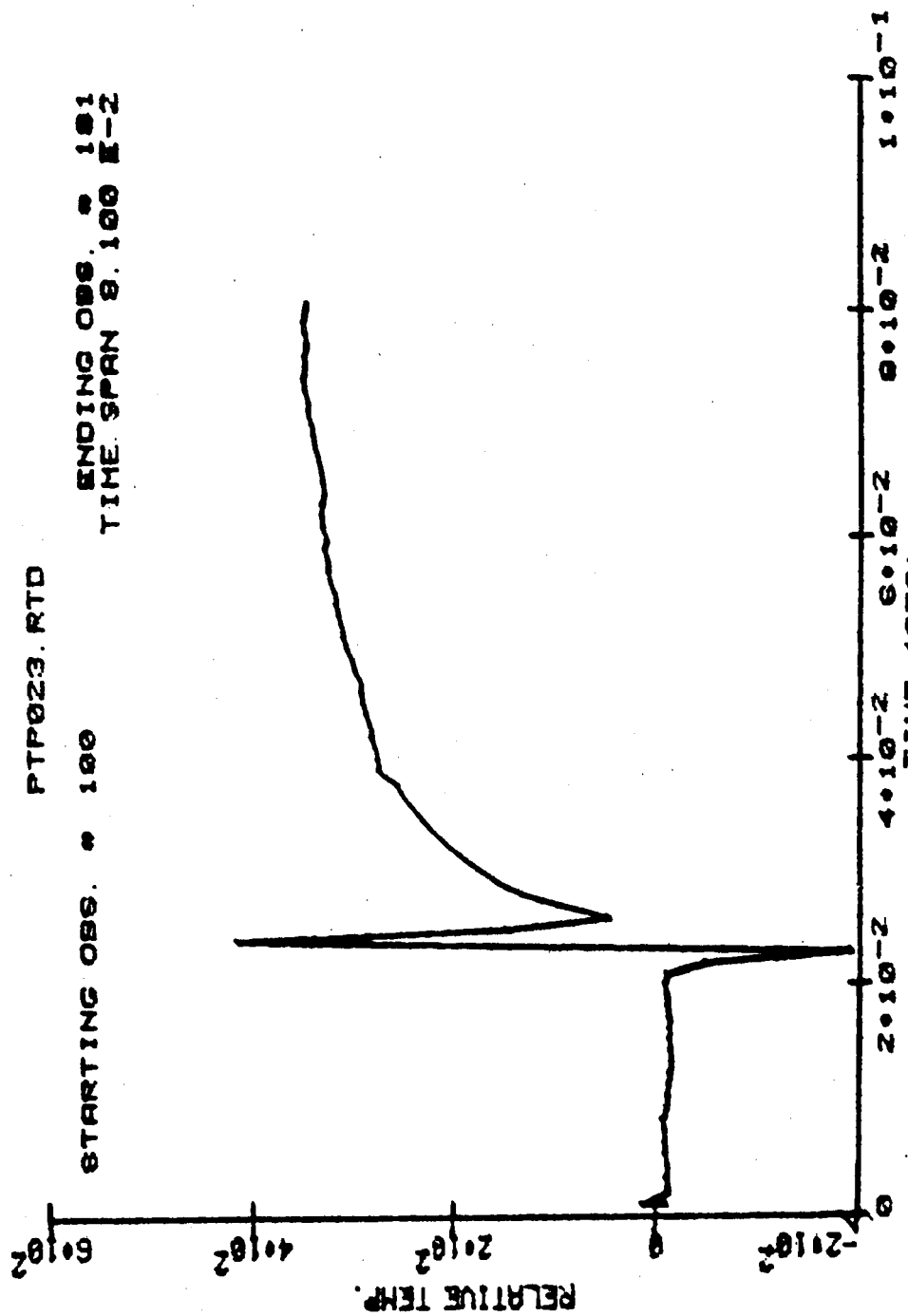


Figure 6.8 LCSR Test PTP023 RTD Data.

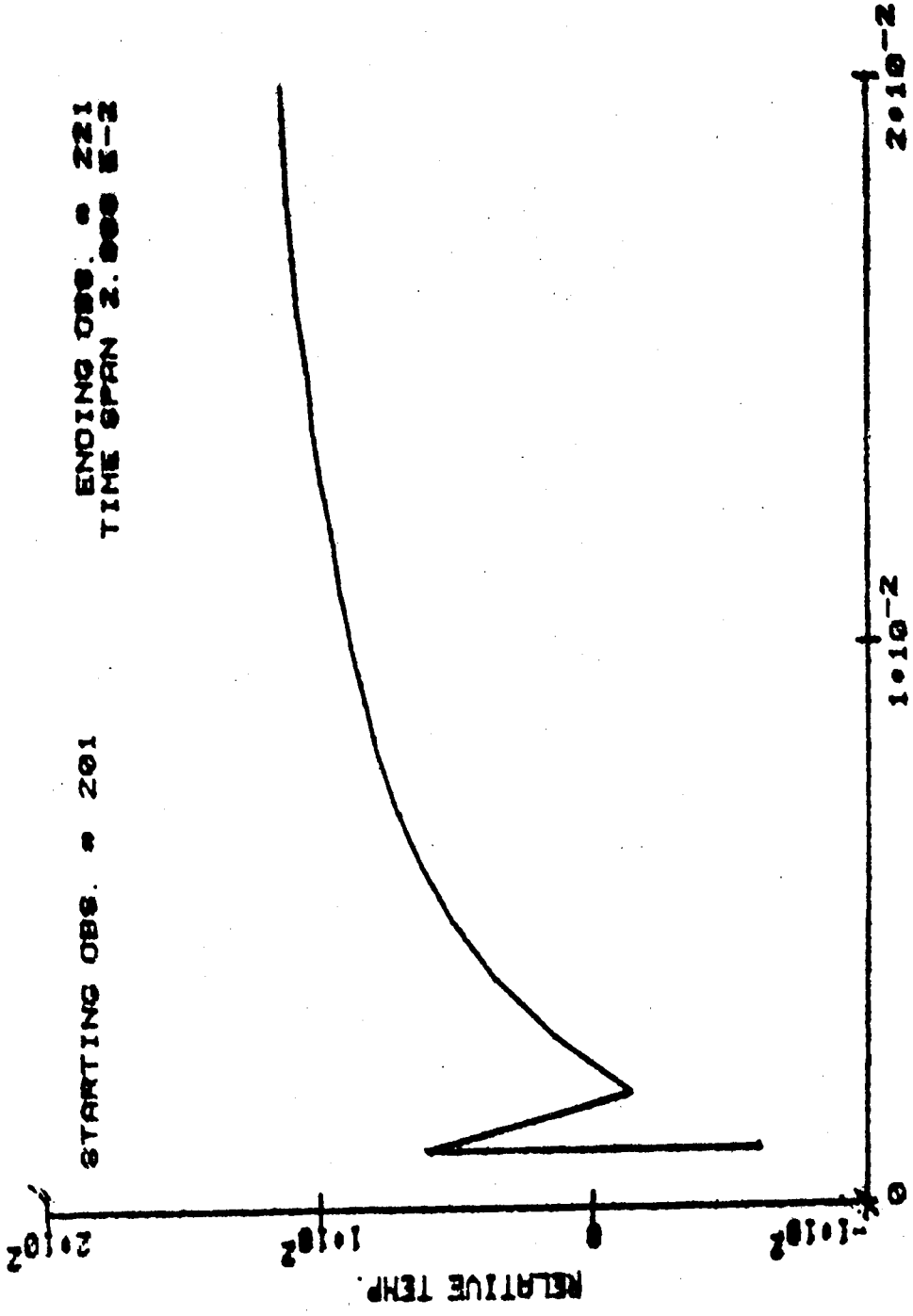


Figure 6.9 Voltmeter Transient Effect on LCSR Test in Laboratory.

voltmeter used to measure the RTD current, but never with the Vallhalla voltmeter used for this purpose. Because of this experience, we suspect that this was the cause of the spikes in the Turkey Point data through test records do not include an indication of the voltmeter used in each position.

6.3. DISCUSSION OF RESULTS

The data from the six tests were analyzed using the analytical transformation to see if reasonable results could be obtained. The data was "smoothed" by connecting the points directly before and after the spike to make them usable. A plot of the LCSR data overlayed with the converted equivalent plunge test result is shown in Figures 6.10 through 6.15. Plunge time constants were computed using the analytical transformation. They ranged from 0.0343 seconds to 0.0455 seconds, a full order of magnitude faster than any plunge test result obtained in the laboratory for the same type of sensor. Results of the transformation in the laboratory were sometimes much slower than the plunge test time constant. It is difficult to say explicitly why the transformation "failed slow" in the lab and "failed fast" in the plant, but it is possible that the difference in surface heat transfer or the effects of temperature between the in situ plant test and the lab test may be the cause. Regardless of the reason, the analytical results were discounted because the transformation was invalid for use with this sensor because the sensing element geometry violated the major assumption that the element be centrally located and because the test data were of poor quality.

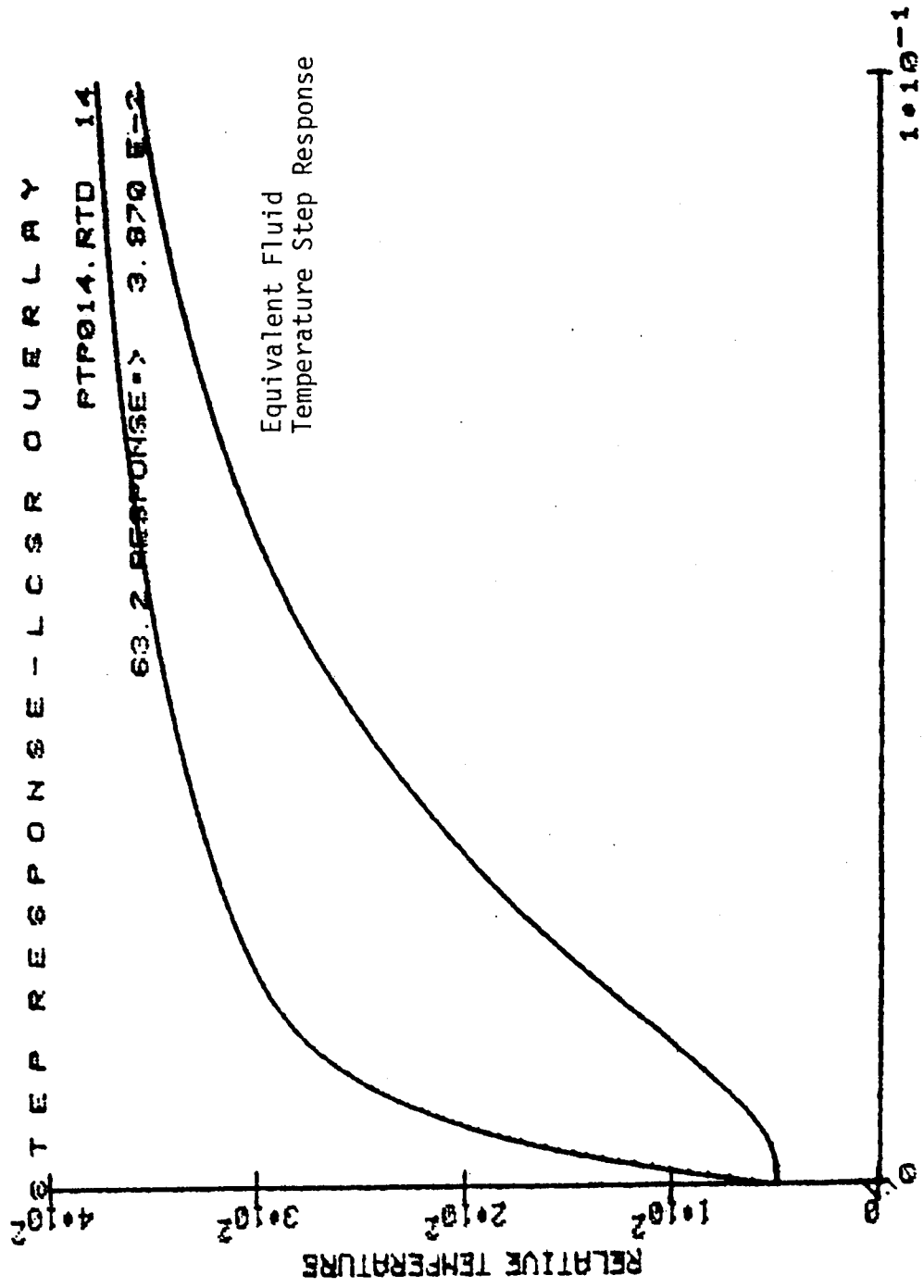


Figure 6.10 LCSR Test PTP014 RTD Transformed Results.

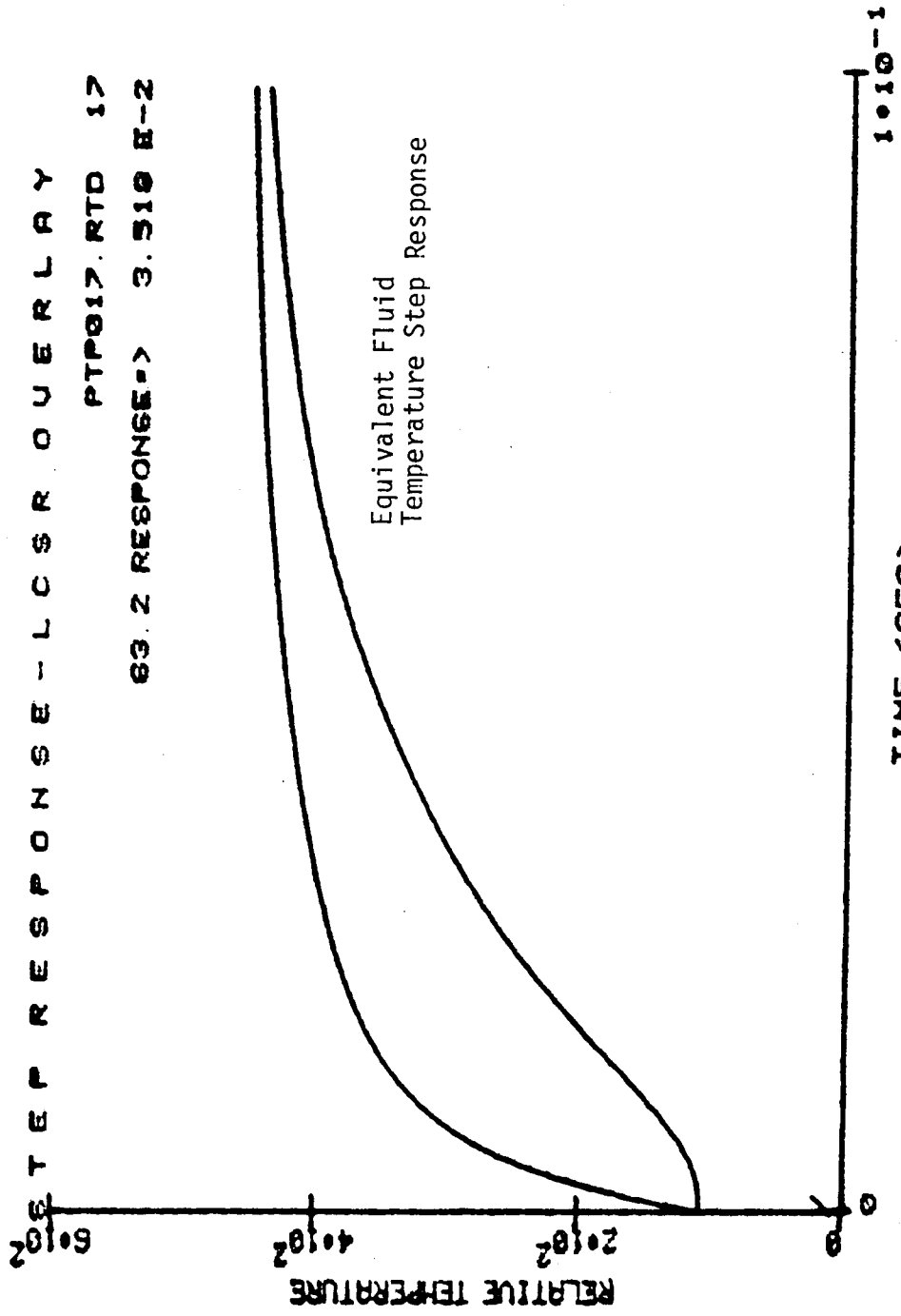


Figure 6.11 LCSR Test PTP017 RTD Transformed Results.

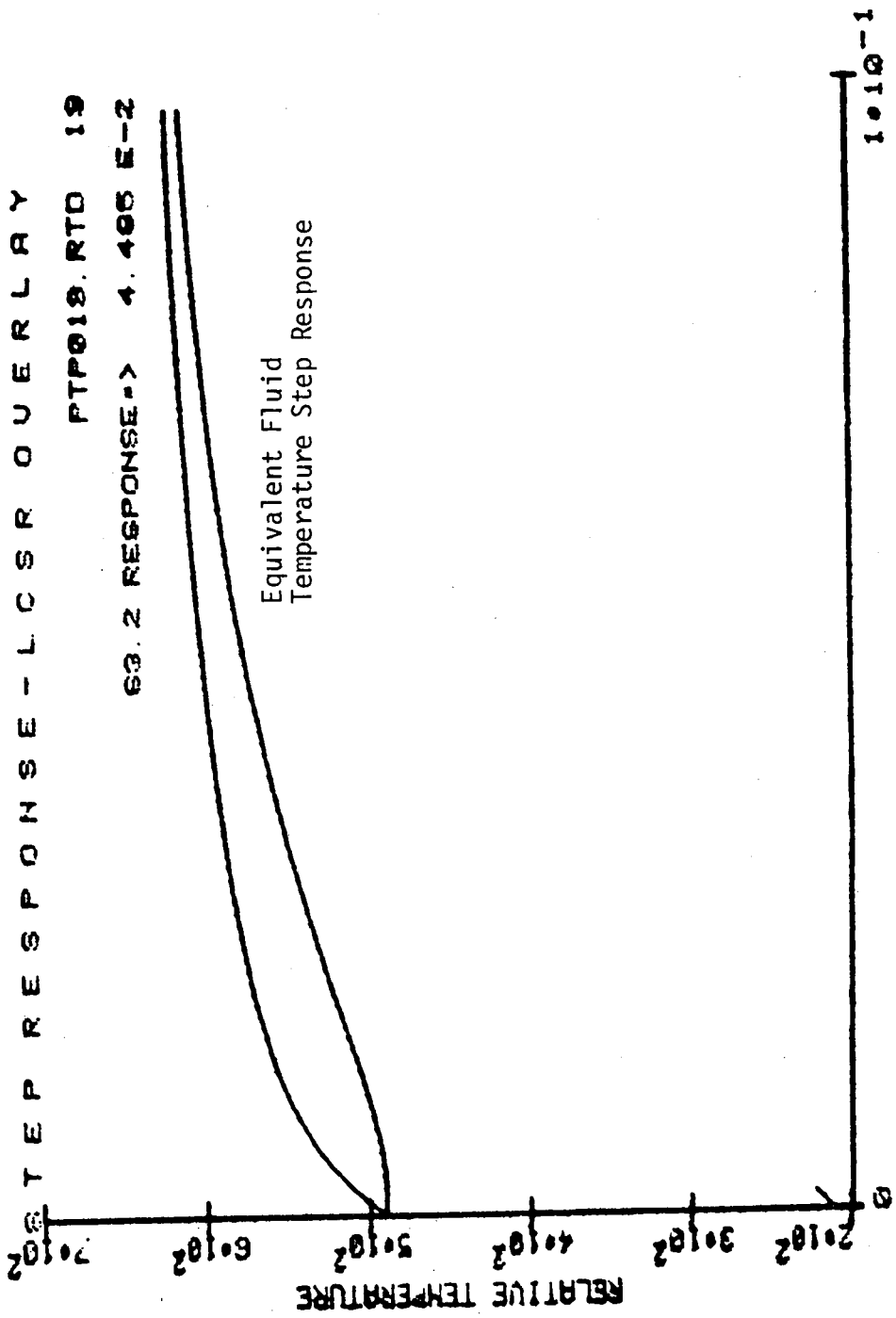


Figure 6.12 LCSR Test PTP019 RTD Transformed Results.

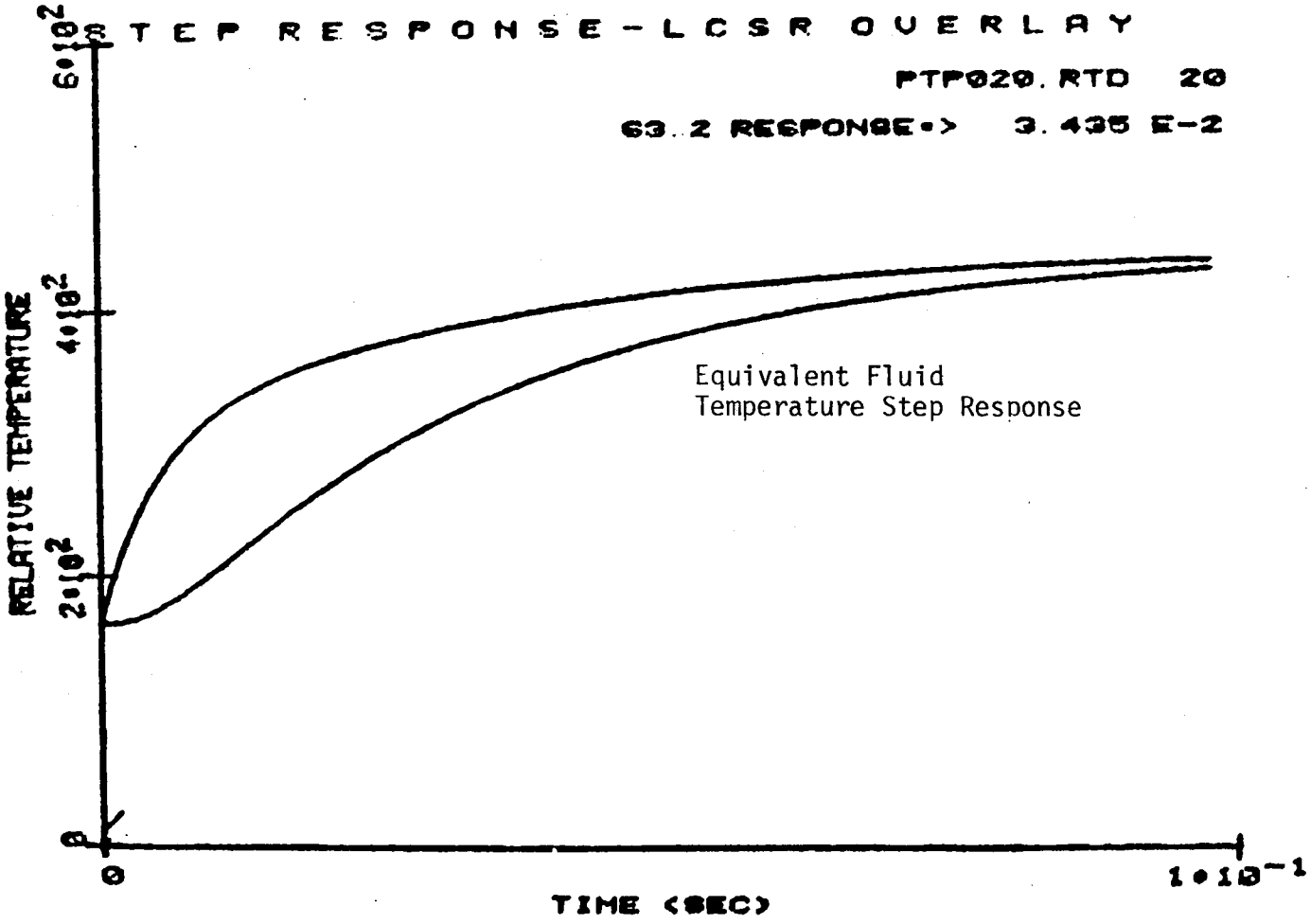


Figure 6.13 LCSR Test PTP020 RTD Transformed Results.

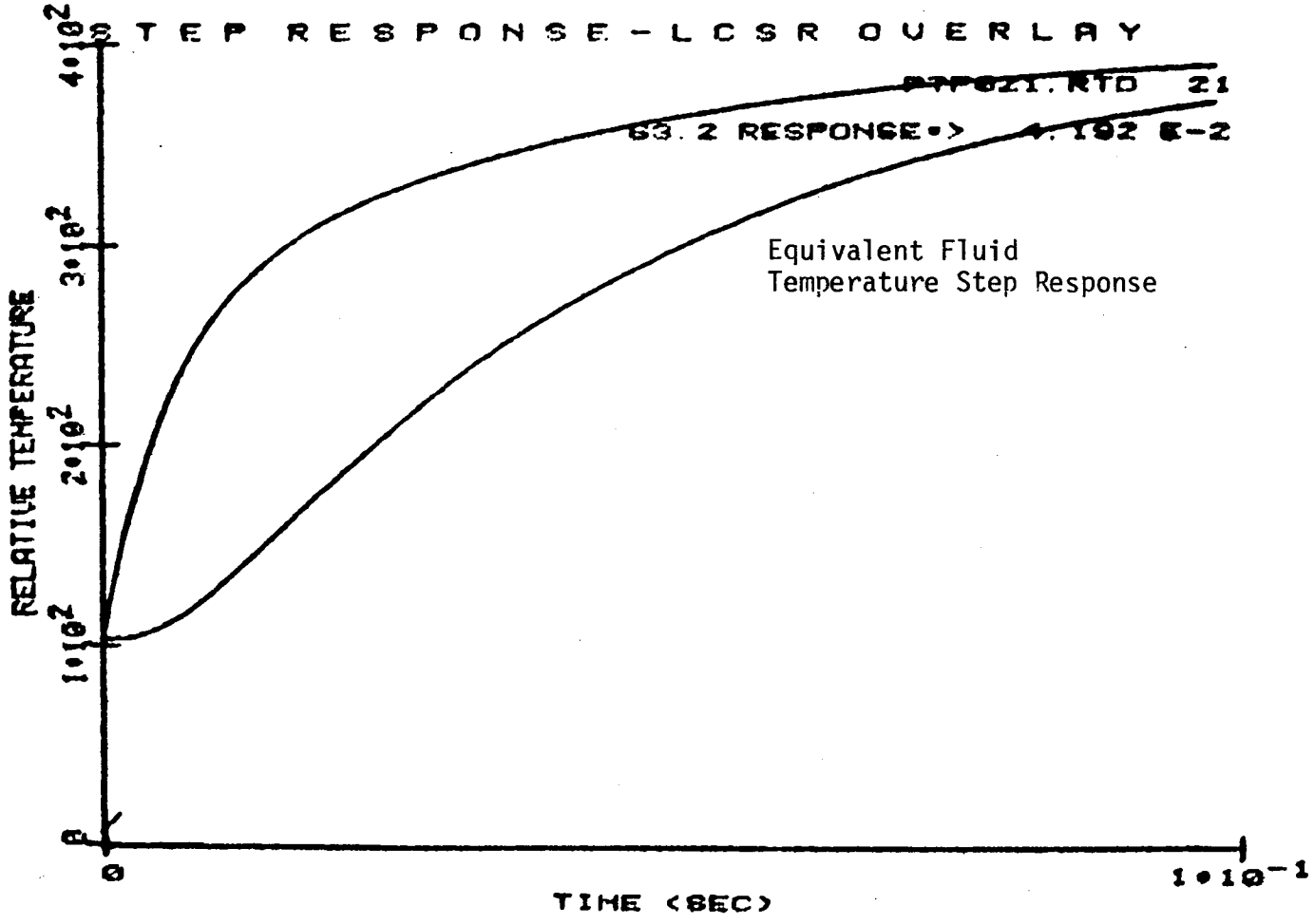


Figure 6.14 LCSR Test PTP021 RTD Transformed Results.

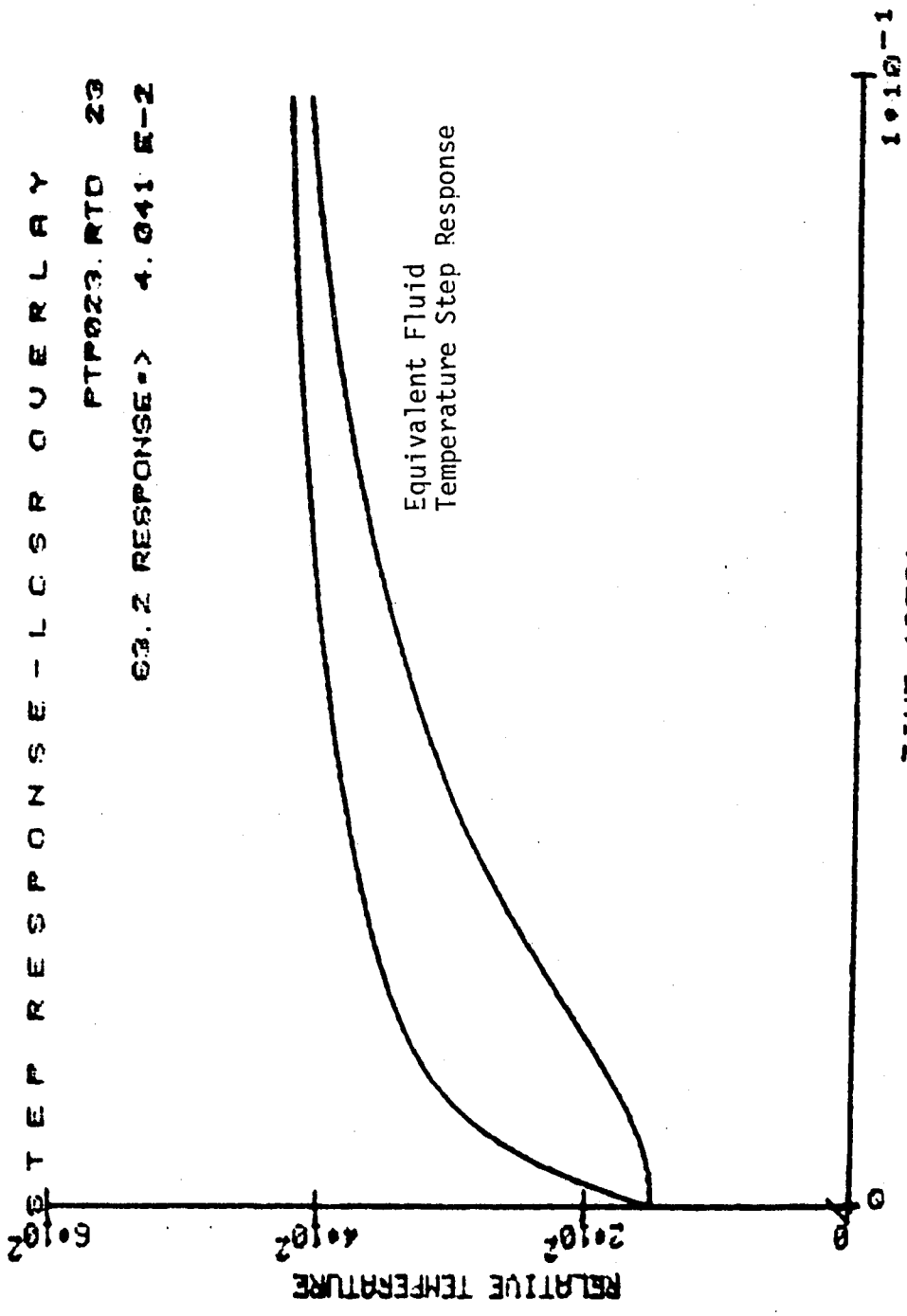


Figure 6.15 LCSR Test PTP023 RTD Transformed Results.

If one assumes that the results were not affected by the voltmeter feedback, it is possible to compare the LCSR results with the empirical results obtained in the laboratory. Figures 6.16 through 6.21 show the LCSR test results with their 63.2% time constants computed. These data indicate that the sensor response to an LCSR test in the plant is about twice as fast as the sensor in the lab. From Figure 5.22, page 101, an average value of 0.0117 seconds with a standard deviation of 0.0017 (mean value and standard deviation of the six test time constants) corresponds to a plunge test time constant of 0.25 seconds, or with a 99% confidence, a time constant equal to or less than 0.625 seconds. The plunge tests in the laboratory gave a time constant of 0.36 sec.

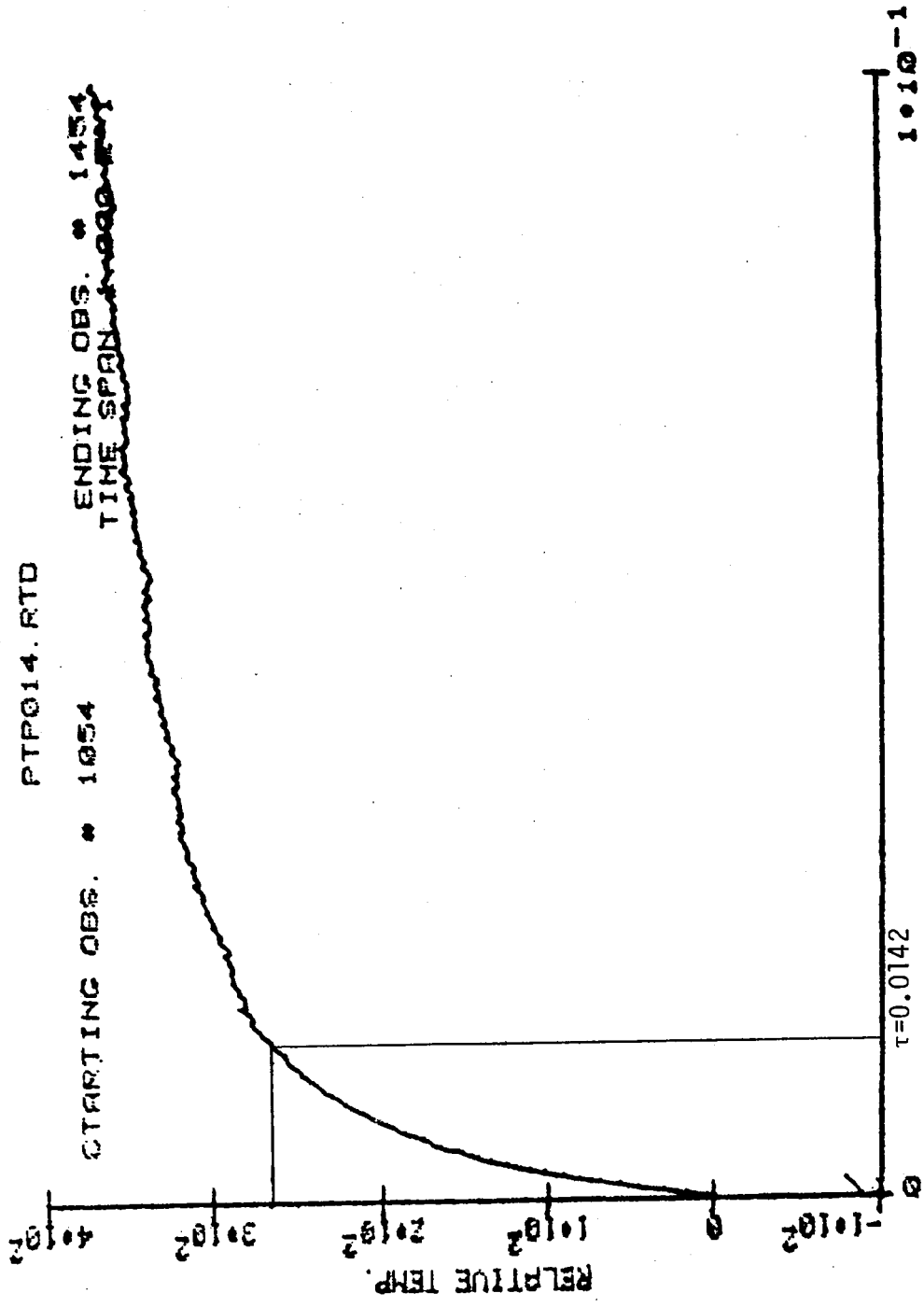


Figure 6.16 LCSR Test PTP014 RTD Time Constant.

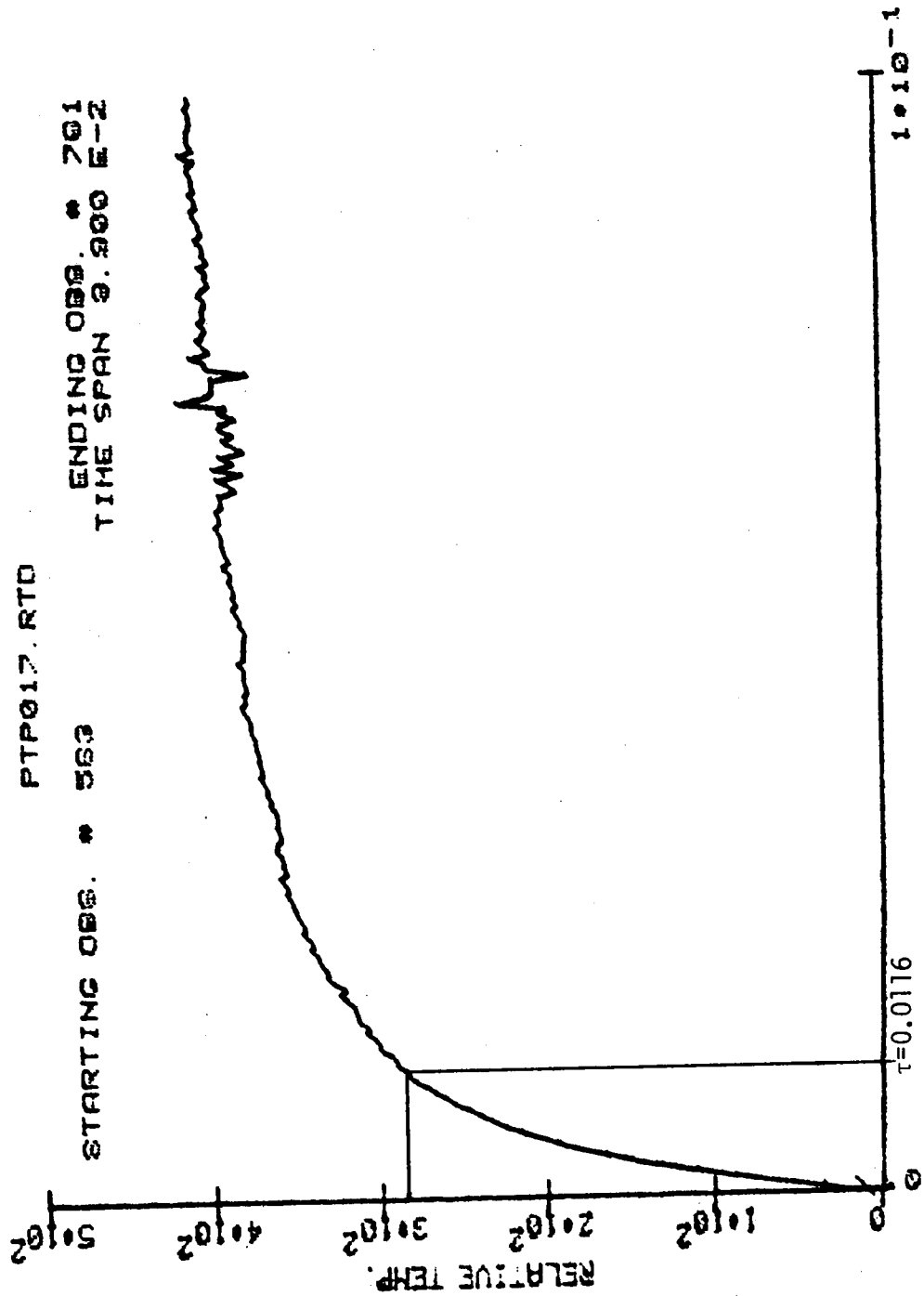


Figure 6.17 LCSR Test PTP017 RTD Time Constant.

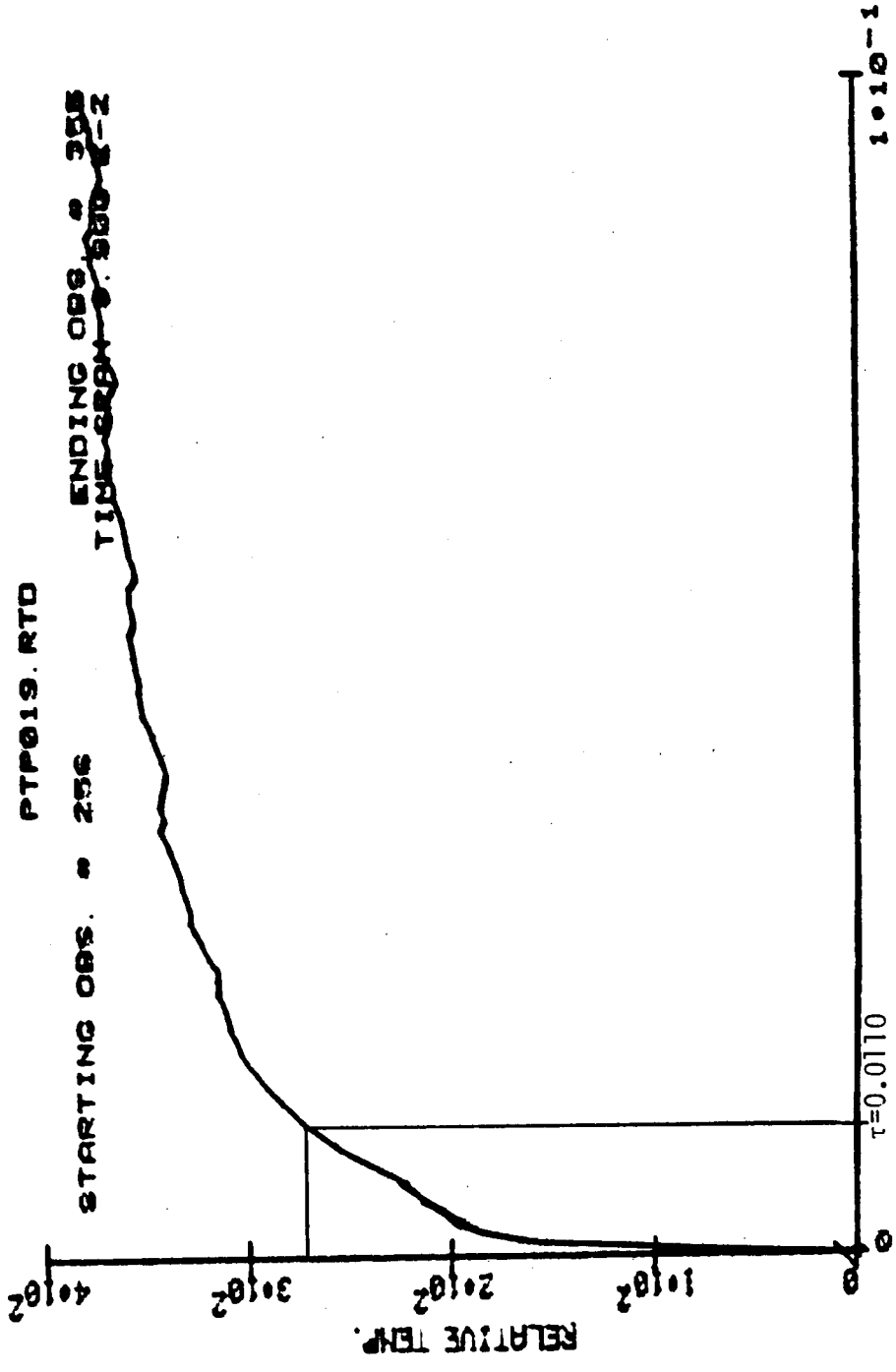


Figure 6.18 LCSR Test PTP019 RTD Time Constant.

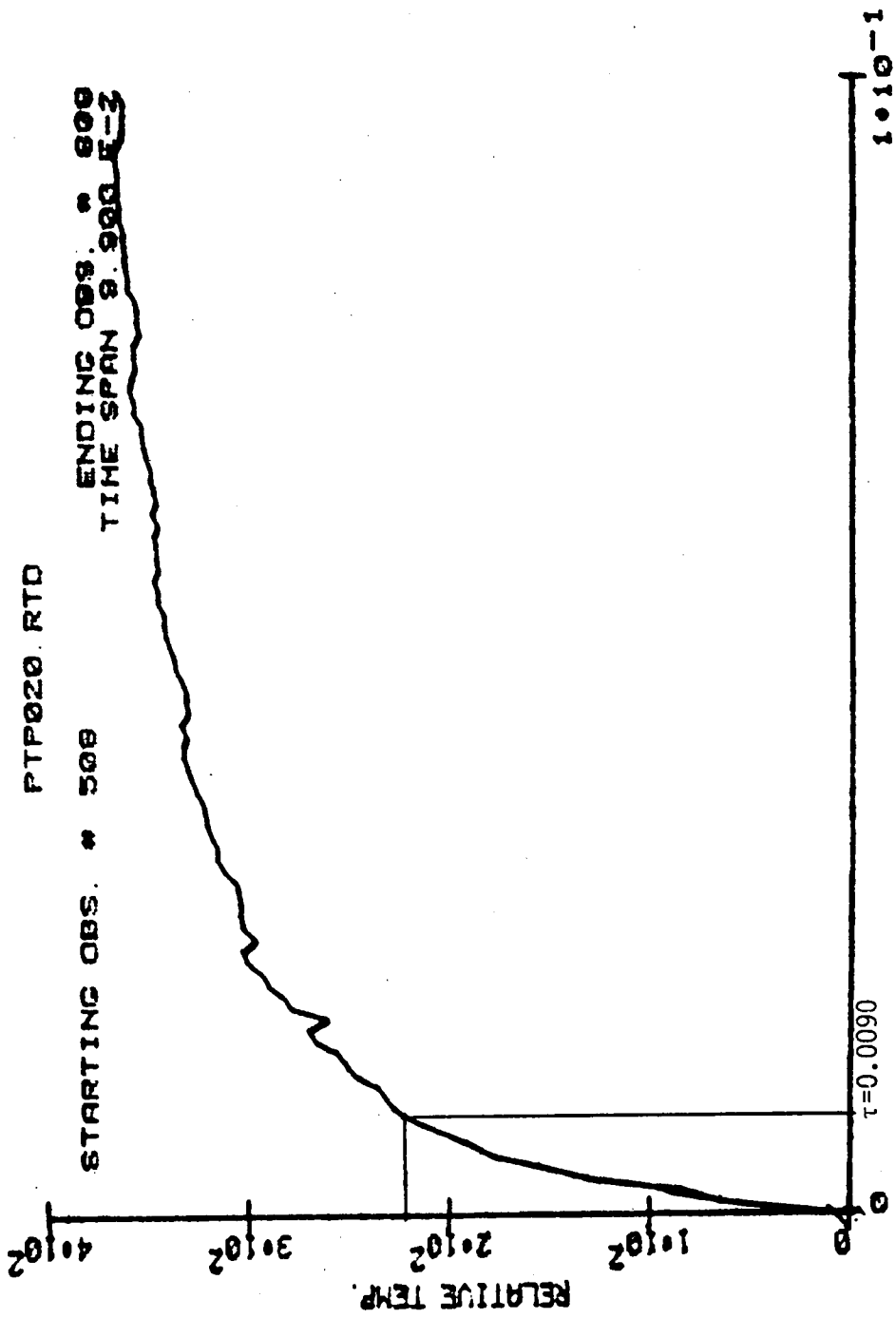


Figure 6.19 LCSR Test PTP020 RTD Time Constant.

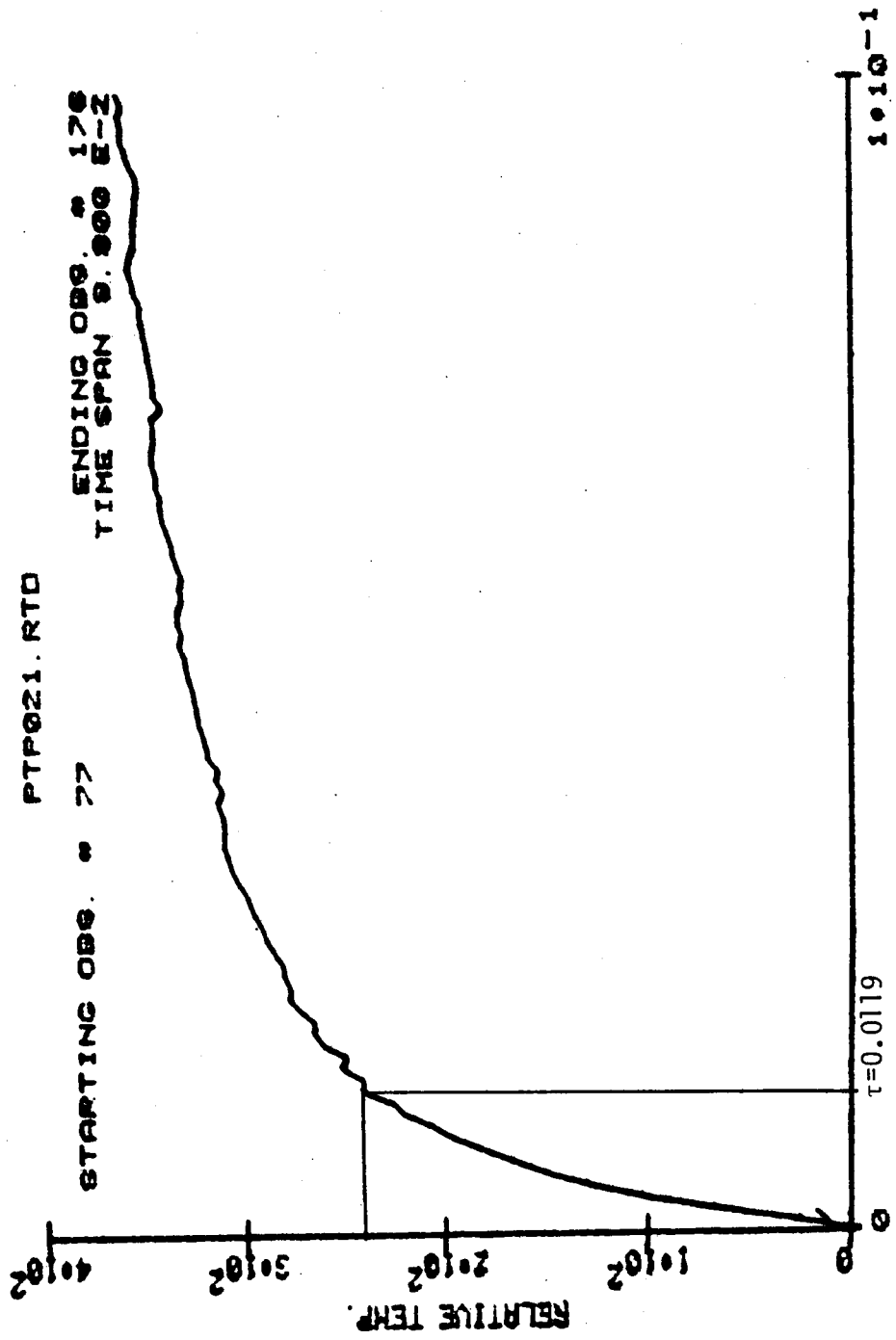


Figure 6.20 LCSR Test PTP021 RTD Time Constant.

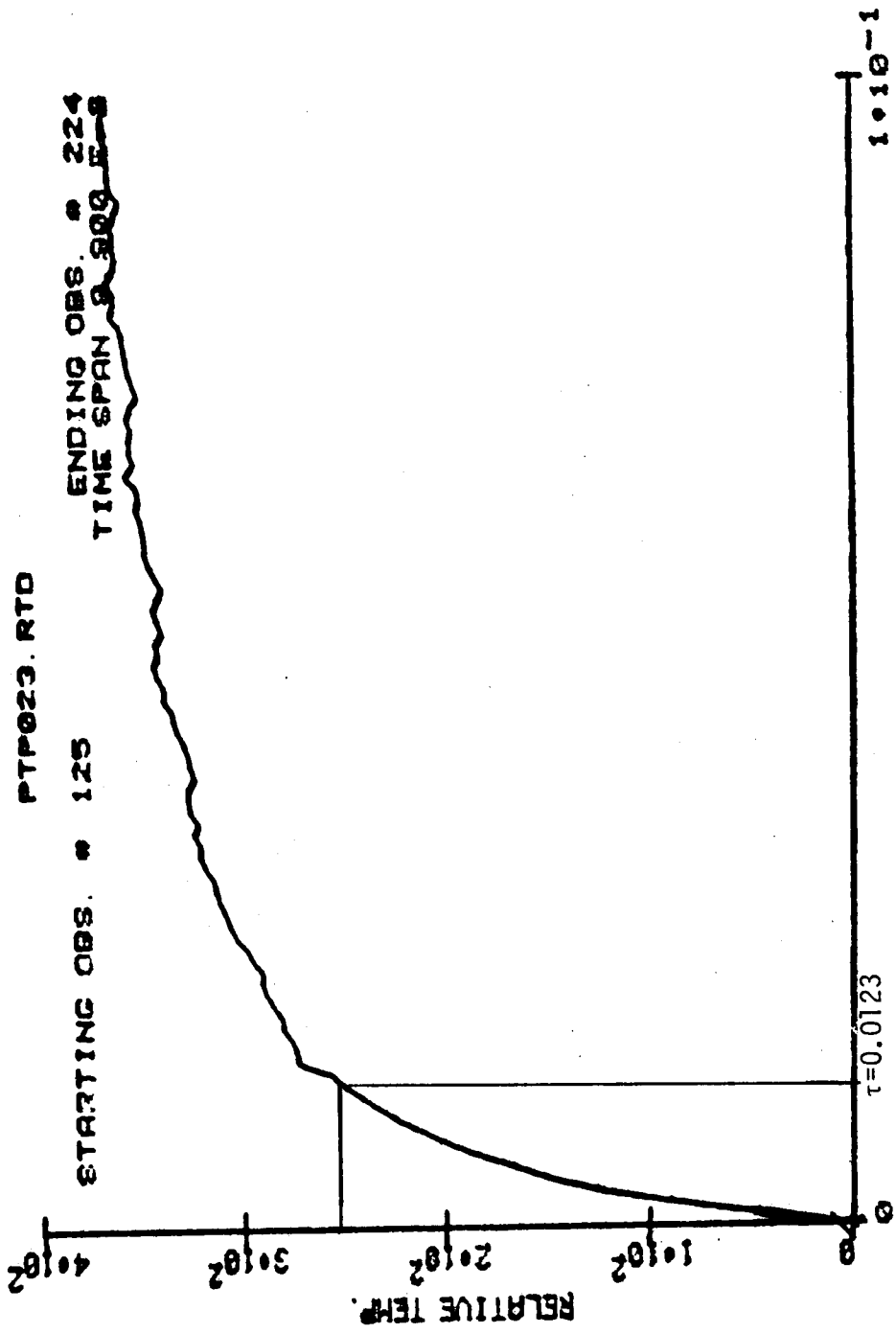


Figure 6.21 LCSR Test PTP023 RTD Time Constant.

CHAPTER 7

CONCLUSIONS AND RECOMMENDATIONS

7.1 CONCLUSIONS

It is important to consider the response time of resistance temperature detectors when analyzing the overall response characteristics of nuclear plant safety systems. Possible modes of sensor response time degradation have been proposed. The loop current step response test is an adequate method for in situ response time testing of platinum resistance temperature sensors.

Analytical transformation of LCSR data results in equivalent fluid temperature step perturbation responses. Use of the analytical transformation is restricted to sensors whose physical makeup adheres to assumptions inherent in the model used to describe sensor heat transfer. The assumptions are:

1. The actual sensor heat transfer must be primarily one-dimensional.
2. The sensing element must be located nearly in the center of the sensor.

In cases where the use of the analytical transformation is precluded because the assumptions are violated, empirical conversions of LCSR and self-heating test data may be made to obtain corresponding plunge test time constants. This work may be extrapoled to reactor applications if temperature and flow differences between laboratory tests and plant tests have negligible effects. Evidence from this research indicates that conservative estimates of plunge test time constants can be obtained in the laboratory through the use of a one-sided upper confidence bound.

In situ response time testing at nuclear plants can be conducted employing the methods described in this thesis. Quantitative measures of a sensor's response capability (sensor-system time constants) may be used to discover and identify sensor response time degradation problems.

7.2. RECOMMENDATIONS

During the course of this research, several areas were identified which require further research:

1. Other practical means of precise steady-state resistance measurement which are not susceptible to lead wire resistance errors need to be investigated. A possible method involves the use of multiple-wire bridges.
2. Further study involving failure modes and on resistance temperature sensors needs to be done. While current work has identified some sensor failure modes, it is also important to consider susceptibilities of sensor-systems to response time degradation.
3. An analytical transformation needs to be developed that will work on all types of existing sensors.
4. Possible effects of temperature experienced in operating nuclear reactors on the response time of resistance temperature sensors needs to be evaluated. If it can be shown that the effects on the response time are either minimal on conservative, then empirical correlation curves can be developed in the laboratory environment for direct application in in situ response time testing in commercial reactors.

5. If it is shown that the effects of temperature and flow are important, then response time testing using LCSR, self-heating and plunge tests must be conducted in the laboratory at actual reactor operating conditions in order to obtain valid empirical transformations.
6. The in-plant tests on a Rosemount 176-KF sensor should be repeated. The instrumentation problem that interferred with the Turkey Point tests is now understood and can be avoided. A second plant test program should include self-heating tests.

LIST OF REFERENCES

LIST OF REFERENCES

1. Curtis, D. J., "Platinum Resistance Interpolation Standards," Temperature: Its Measurement and Control in Science and Industry, Vol. 4, Part 2: 951-961 (1972).

2. Carr, K. R., "An Evaluation of Industrial Platinum Resistance Thermometers," Temperature: Its Measurement and Control in Science and Industry, Vol. 4, Part 2: 971-982 (1972).

3. Lucas, D. A., "Miniature Precision Platinum Resistance Thermometers," Temperature: Its Measurement and Control in Science and Industry, Vol. 4, Part 2: 963-965 (1972).

4. Adams, E. F., "Resistance Thermometry," Temperature: Its Measurement and Control in Science and Industry, Vol. 4, Part 2: 247-259 (1972).

5. Carroll, R. M. and Shepard, R. L., "Measurements of the Response Times of Thermocouples and Resistance Thermometers Using an in situ Method," Oak Ridge National Laboratory (to be published).

6. Warshawsky, I., "Multiple-Bridge Circuits for Measurement of Small Changes in Resistance," The Review of Scientific Instruments, Vol. 26: 711-715 (July, 1955).

7. Warshawsky, I., "Heat Conduction Errors and Time Lag in Cryogenic Thermometer Installation," ISA Transactions, Vol. 13, No. 4: 335-346 (1974).

8. "Periodic Testing of Electric Power and Protection Systems," U. S. Nuclear Regulatory Commission Regulatory Guide 1.118, Office of Standards Development (June, 1976).

9. Sanborn, V. A., Resistance Temperature Transducers, Metrology Press, Fort Collins, Colorado (1972).

10. United States Nuclear Regulatory Commission, "Operating Experience Bulletin Information Report," Office of Management Information and Program Control (1975).

11. Coville, P. and Dujols, P., "Thermal Conductivity of Insulants Used in Mineral Insulated Cable," Fifth Symposium on Temperature; SODERN (June, 1971).

12. Kottee, R. F., "Resistance Bridges," Journal of Research, National Bureau of Standards, Vol. 40 (1948).

13. "A Discussion on the Principles of Operation of Resistance Bridges," Rosemount Inc., Application Data Sheet 3013, Minneapolis (1976).

14. Kerlin, T. W., "Analytical Methods for Interpreting in situ Measurements of Response Times in Thermocouples and Resistance Thermometers," ORNL/TM-4912 (March, 1976).

15. John, F., "Advanced Numerical Analysis," New York University (1956).

16. Harrer, J. M. and Beckerley, J. G., "Nuclear Power Reactor Instrumentation Systems Handbook," U.S.A.E.C. Technical Information Center, Vol. 2, p. 97 (June 1975).

17. Myers, R. H. and Walpole, R. E., "Probability and Statistics for Engineers and Scientists," Macmillan Publishing Company, Inc., New York (1972).

18. Natrella, M. G., "Experimental Statistics," National Bureau of Standards Handbook, 91 (October 1966).

APPENDIXES

APPENDIX A

TWO-WIRE BRIDGE CIRCUIT ANALYSIS

The two-wire bridge was discussed in Section 2.4.2 and the circuit diagram was shown in Figure 2.7, page 24. A circuit analysis is done here to provide a basis for comparison of the bridges. Writing the equations for the voltage at points 2 and 4, we have

$$V_2 = V_1 - I_1 R_a \tag{A.1}$$

and

$$V_4 = V_1 - I_2 R_b \ . \tag{A.2}$$

The voltage difference between points 2 and 4 is:

$$\Delta V = V_2 - V_4 = I_2 R_b - I_1 R_a \tag{A.3}$$

where

V_i = voltage at node i

I_1 = current through upper path

I_2 = current through lower path

I = total current

R_i = resistance of resistor i.

Therefore, the equation for the current through each path can be obtained.

$$I_1 = \left(\frac{R_b + R_{RTD}}{R_a + R_b + R_d + R_{RTD}} \right) I \tag{A.4}$$

$$I_2 = \left(\frac{R_a+R_d}{R_a+R_b+R_d+R_{RTD}}\right)I \ . \tag{A.5}$$

Substituting Eqs. (A.4) and (A.5) into Eq. (A.3) results in,

$$\Delta V = \left(\frac{R_a+R_d}{R_a+R_b+R_d+R_{RTD}}\right)R_b I - \left(\frac{R_b+R_{RTD}}{R_a R_b+R_d+R_{RTD}}\right)R_a I \tag{A.6}$$

$$= \left(\frac{R_a R_b+R_b R_d-R_a R_b-R_a R_{RTD}}{R_a+R_b+R_d+R_{RTD}}\right)I \ . \tag{A.7}$$

Simplifying, we obtain

$$\Delta V = \left(\frac{R_b R_d-R_a R_{RTD}}{R_a+R_b+R_d+R_{RTD}}\right)I \ . \tag{A.8}$$

From Ohm's law we know that

$$V = IR \tag{A.9}$$

and the total resistance of the bridge circuit is obtained by

$$\frac{1}{R} = \frac{1}{R_a+R_d} + \frac{1}{R_b+R_{RTD}} \ . \tag{A.10}$$

Solving for the total current, I, results in,

$$I = V \cdot \frac{1}{R} = V\left(\frac{1}{R_a+R_d} + \frac{1}{R_b+R_{RTD}}\right) \tag{A.11}$$

$$I = V\left(\frac{R_a+R_b+R_d+R_{RTD}}{(R_a+R_d)(R_b+R_{RTD})}\right) \ . \tag{A.12}$$

Substituting this result for the total current in the circuit into Eq. (A.8) gives us an expression for the normalized change in voltage, $\frac{\Delta V}{V}$, in terms of the bridge resistances,

$$\frac{\Delta V}{V} = \left(\frac{R_b R_d - R_a R_{RTD}}{R_a+R_b+R_d+R_{RTD}}\right)\left(\frac{R_a+R_b+R_d+R_{RTD}}{(R_a+R_d)(R_b+R_{RTD})}\right) . \tag{A.13}$$

Simplifying, we obtain

$$\frac{\Delta V}{V} = \frac{R_b R_d - R_a R_{RTD}}{(R_a+R_d)(R_b+R_{RTD})} . \tag{A.14}$$

When there is a significant resistance contribution in the lead wires, the output of the bridge is affected. If we let

$$R_{RTD} = R_{RTD} + R_{Leads}, \tag{A.15}$$

then substitute into Eq. (A.14) we obtain,

$$\frac{\Delta V}{V} = \frac{R_b R_d - R_a(R_{RTD}+R_L)}{(R_a+R_d)(R_b+R_{RTD}+R_L)} \tag{A.16}$$

$$\frac{\Delta V}{V} = \frac{R_b R_d - R_a R_{RTD}}{(R_a+R_d)(R_b+R_{RTD}+R_L)} - \frac{R_a R_L}{(R_a+R_d)(R_b+R_{RTD}+R_L)} . \tag{A.17}$$

We recognize that

$$\frac{R_b R_d - R_a R_{RTD}}{(R_a+R_d)(R_b+R_{RTD}+R_L)} = \frac{R_b R_d - R_a R_{RTD}}{(R_a+R_d)(R_b+R_{RTD})} \cdot \frac{R_b+R_{RTD}}{R_b+R_{RTD}+R_L}$$

$$= \left(\frac{\Delta V}{V}\right)_{RTD} \cdot \left(\frac{R_b+R_{RTD}}{R_b+R_{RTD}+R_L}\right) \tag{A.19}$$

where $(\frac{\Delta V}{V})_{RTD}$ is the true output of the bridge that would be observed if the RTD's response were not influenced by lead wire resistance error. Combining with Eq. (A.17) we obtain,

$$\frac{\Delta V}{V} = (\frac{\Delta V}{V})_{RTD} \cdot \left[\frac{R_b+R_{RTD}}{R_b+R_{RTD}+R_L}\right] - \frac{R_a}{R_a+R_d} \cdot \left[\frac{R_L}{R_b+R_{RTD}+R_L}\right]. \qquad (A.20)$$

APPENDIX B

USE OF COMPUTER-AIDED TRANSFORMATION ON LCSR LABORATORY TEST DATA

The FORTRAN program LCSR was written by D. C. Warner for use in automatically compiling, rearranging, and analyzing LCSR test data. The result from the computer aided analysis is the transformed LCSR time constant. This is the time constant that would have resulted had a step change in fluid temperature occurred rather than a step change in internal heating. The theory behind the LCSR transformation was described in Section 3.2, page 41. This section lists results of analysis of LCSR tests taken on different sensors in the laboratory.

Typical results from transformed LCSR results are compared to plunge test results in Table B.1. As listed in the table, the LCSR transformation predicts the plunge test time constant to a good degree of accuracy on all sensors except the Rosemount 176-KF sensor. This is attributed to the construction details of the RTD (sensing wire near surface) which violate one of the necessary assumptions in the transformation.

Figure B.1 shows a typical result of the computer-aided transformation of an LCSR test performed in the laboratory on the bare 176-KF sensor. The top curve is a plot of the LCSR data fitted by the exponential stripping technique. The analytical transformation of these data predicted an equivalent plunge test time constant of 0.22 seconds. The actual plunge test time constant for this sensor is about 0.4 seconds. The lower curve is a trace of the equivalent fluid temperature step response

TABLE B.1

TRANSFORMED LCSR TEST DATA*

Sensor Type and Configuration	Predicted Plunge Test Time Constant (sec)	Plunge Test Time Constant (sec)	Error (%)
Rosemount No. 177GY with thermowell	6.15	6.00	2.6
Rosemount No. 104AFC with thermowell	5.80	6.08	4.6
Rosemount No. 104AFC without thermowell	3.13	3.00	4.4
Laboratory Type 1 no thermowell	8.11	8.29	2.2
Rosemount No. 176-KF	..**	0.36	---

*Data was obtained from H. M. Hashemian.

**Transformation failed as described in Section 5.4, page 85.

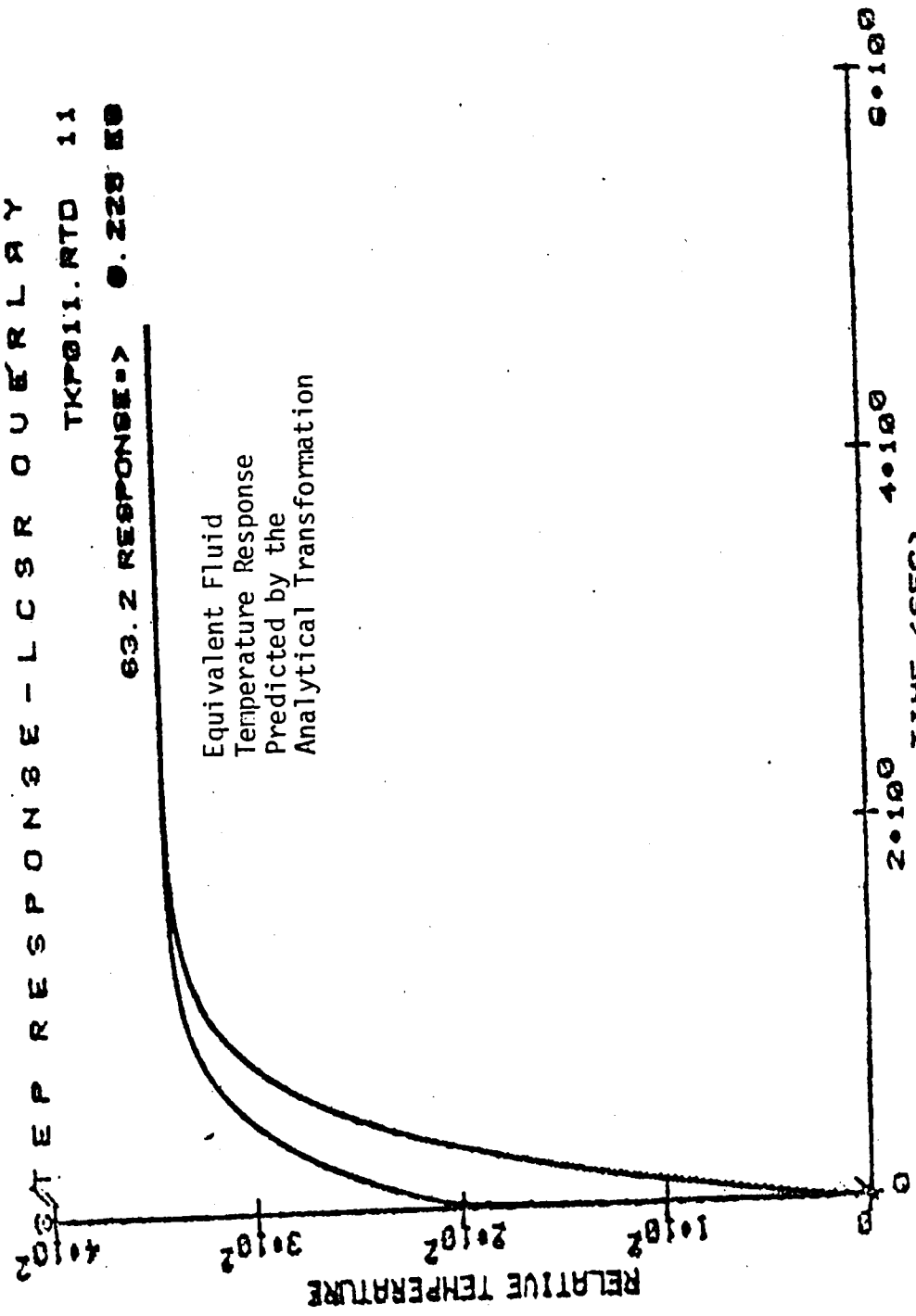


Figure B.1 Computer-Aided LCSR Transformed Result of the Bare 176-KF Sensor.

synthesized from the poles of the LCSR curve equation. Because the sensing coil is not centrally located, the central node step response shown here is not the true step response of the sensor.

APPENDIX C

STATISTICAL ANALYSIS AND INTERPRETATION OF LABORATORY TEST RESULTS

A statistical analysis[17,18] was performed on the laboratory test data. An error analysis was done to give an indication of the repeatibility of the tests and a means of interpreting the results in order to draw conservative conclusions from the data.

The LCSR and plunge tests were replicated at each heat transfer configuration. (See Section 5.3, page 71, for a description of these tests.) The sample mean, $\bar{X}$, and the sample standard deviation, s, were computed for each set of tests. The sample mean, $\bar{X}$, is a point estimator of the true population mean μ. Likewise, the sample standard deviation, s, is an estimator of the actual population standard deviation, σ.

If the number of trials, n, taken of each test were large ($n > 30$), the true population distribution could be assumed to be normal. Since the tests were very time-consuming, only four tests were done for each configuration. Therefore, small sampling theory must be used.[17,18] The t-distribution is used in statistics for small samples and was implemented in this analysis. It is given by the defining equation[17]

$$t = \frac{\bar{X} - \mu}{S/\sqrt{n}} \qquad (C.1)$$

where

t = value of the t-distribution

$\bar{x}$ = sample mean

μ = true mean

S = sample standard deviation

n = sample size.

When a sample is taken from a population, it is assumed that the mean of this sample will closely approximate the true population mean. If after taking many samples, it is found that the true mean is contained in an interval enclosing the sample mean 99% of the time, then one can say that one is operating at a 99% confidence level. This concept is given in equation form[17] by

$$X_U = \bar{X} + t_{\alpha/2} \frac{S}{\sqrt{n}} \tag{C.2}$$

$$X_L = \bar{X} - t_{\alpha/2} \frac{S}{\sqrt{n}} \tag{C.3}$$

where

$\bar{X}$ = sample mean

X_U = upper bound of a $100(1-\alpha)\%$ confidence interval %

X_L = lower bound of a $100(1-\alpha)\%$ confidence interval

S = sample standard deviation

n = number of trials in sample

$t_{\alpha/2}$ = the value of the t-distribution with n-1 degrees of freedom above which we can find an area of $\alpha/2$.

The main purpose of time response testing is to assure the capability of the sensor to respond quickly to fluid temperature perturbations. This involves checking to determine whether the plunge test time constant is less than a maximum value that insures adequate performance.

If a sample of LCSR tests is taken and a corresponding plunge test time constant is predicted from empirical data, one is not concerned whether the true mean is bracketed by a specific interval around the sample mean. Rather, the concern is whether the value of τ_{PLUNGE} obtained is assuredly less than a maximum value or upper bound.

In order to draw conservative conclusions as to the acceptability of a sensor's time response performance, a one-sided 99% confidence interval was chosen to bound the predicted values of τ_{PLUNGE}. This upper bound is given by,

$$X_U = \bar{X} + t_{99} \frac{S}{\sqrt{n}} \qquad (C.4)$$

where

t_α = the value of the t-distribution n with $\nu = n - 1$ degrees of freedon above which there is an area of 1%

= 4.517 for n (sample size) = 4.

This upper bound was computed for each point on the empirical curves (see Table C.1). A template was used to draw a curve enclosing the outermost (greatest error) points. From these curves, Figures C.1 and C.2 the following observations can be made:

1. Given a value of the mean of a sample of LCSR time constants and the sample standard deviation, it can be stated that one is 99% confident that the predicted value of the plunge test time

TABLE C.1

UPPER BOUNDS FOR 99% CONFIDENCE INTERVAL

Sample No.	τ_{PLUNGE} (sec) Mean ($\bar{x}$)	Upper Bound (x_0)	Lower Bound (x_1)	τ_{LCSR} (sec) Mean ($\bar{x}$)	Upper Bound (x_U)	Lower Bound (x_L)
1	0.362	0.427	0.297	0.0284	0.0343	0.0225
2	3.90	4.18	3.62	0.802	0.827	0.777
3	17.7	21.7	13.7	4.69	4.92	4.46
4	9.30	9.64	8.96	1.69	1.78	1.60
5	11.76	12.27	11.25	2.46	2.65	2.27
6	12.83	13.73	11.93	3.87	4.06	3.68
7	24.2	24.56	23.84	6.48	6.77	6.19
8	9.63	9.77	9.49	2.22	2.32	2.12
9	5.62	5.70	5.54	1.07	1.10	1.04
10	20.97	21.62	20.32	5.10	5.15	5.05
11	3.17	3.33	3.01	0.62	0.65	0.59
12	2.19	2.39	1.99	0.41	0.42	0.40
13	1.63	1.74	1.52	0.33	0.37	0.29
14	13.49	13.67	13.31	2.73	2.90	2.56
15	16.09	16.29	15.89	4.02	4.18	3.86
16	15.22	15.34	15.10	3.61	3.89	3.33
17	17.05	17.44	16.66	3.57	3.65	3.49
18	25.6	26.4	24.8	7.06	7.32	6.80
19	15.73	16.16	15.30	4.44	4.54	4.34
20	19.84	20.40	19.28	4.57	4.73	4.41
21	21.33	21.55	21.11	5.17	5.30	5.04
22	22.4	23.1	21.7	5.53	5.59	5.47

TABLE C.1 (Continued)

Sample No.	τ_{PLUNGE} (sec) Mean ($\bar{x}$)	Upper Bound (x_0)	Lower Bound (x_1)	τ_{LCSR} (sec) Mean ($\bar{x}$)	Upper Bound (x_U)	Lower Bound (x_L)
23	0.486	0.059	0.382	0.038	0.043	0.033
24	2.42	2.46	2.38	0.446	0.505	0.383
25	1.5	1.8	1.20	0.238	0.254	0.222
26	1.83	2.09	1.57	0.311	0.322	0.300
27	2.11	2.21	2.01	0.373	0.391	0.355
28	0.92	1.01	0.83	0.146	0.157	0.135
29	1.18	1.36	1.00	0.188	0.302	0.074
30	0.665	0.672	0.658	0.074	0.090	0.058
31	2.97	3.07	2.87	0.563	0.577	0.549

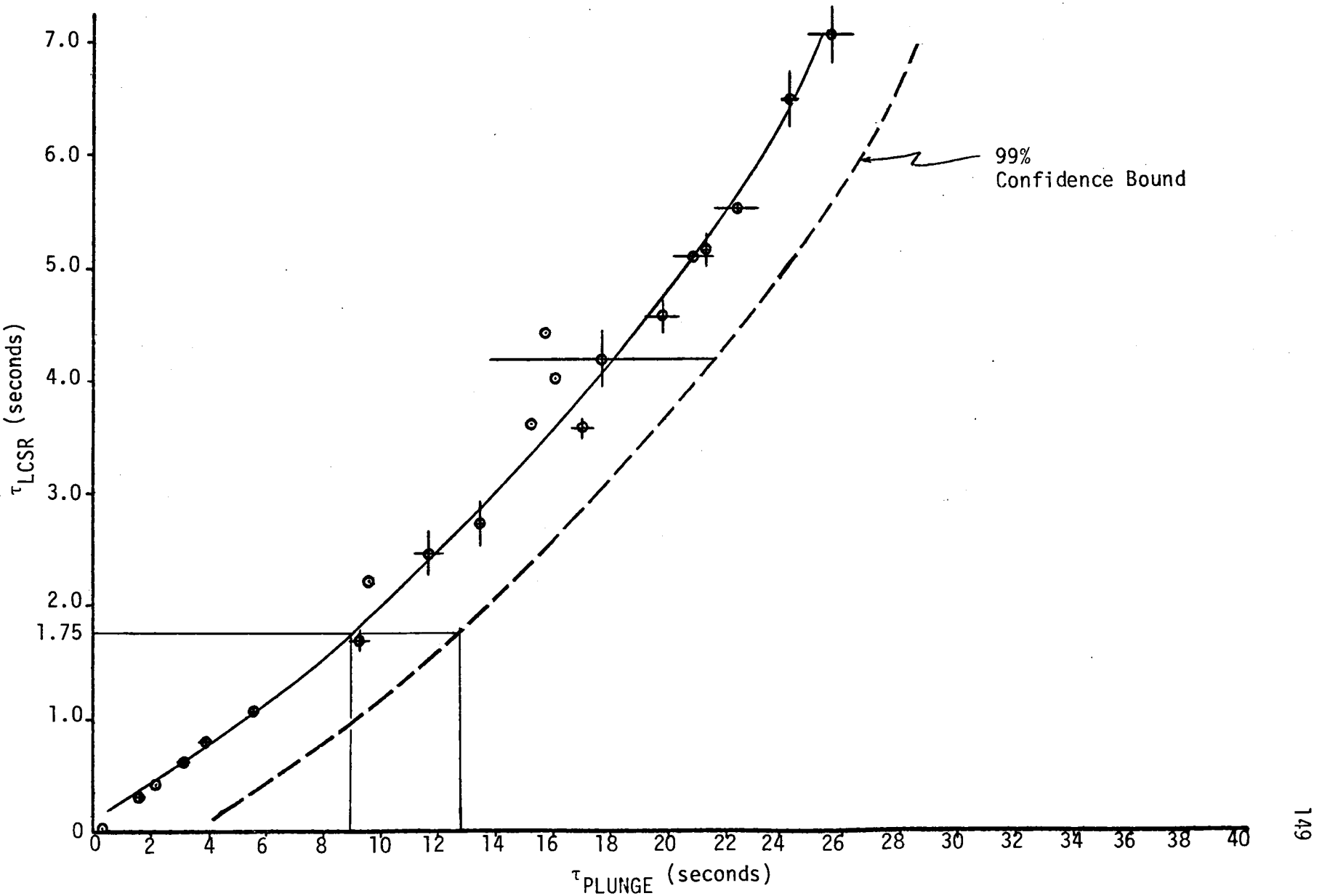


Figure C.1 τ_{LCSR} versus τ_{PLUNGE} Interpretive Example.

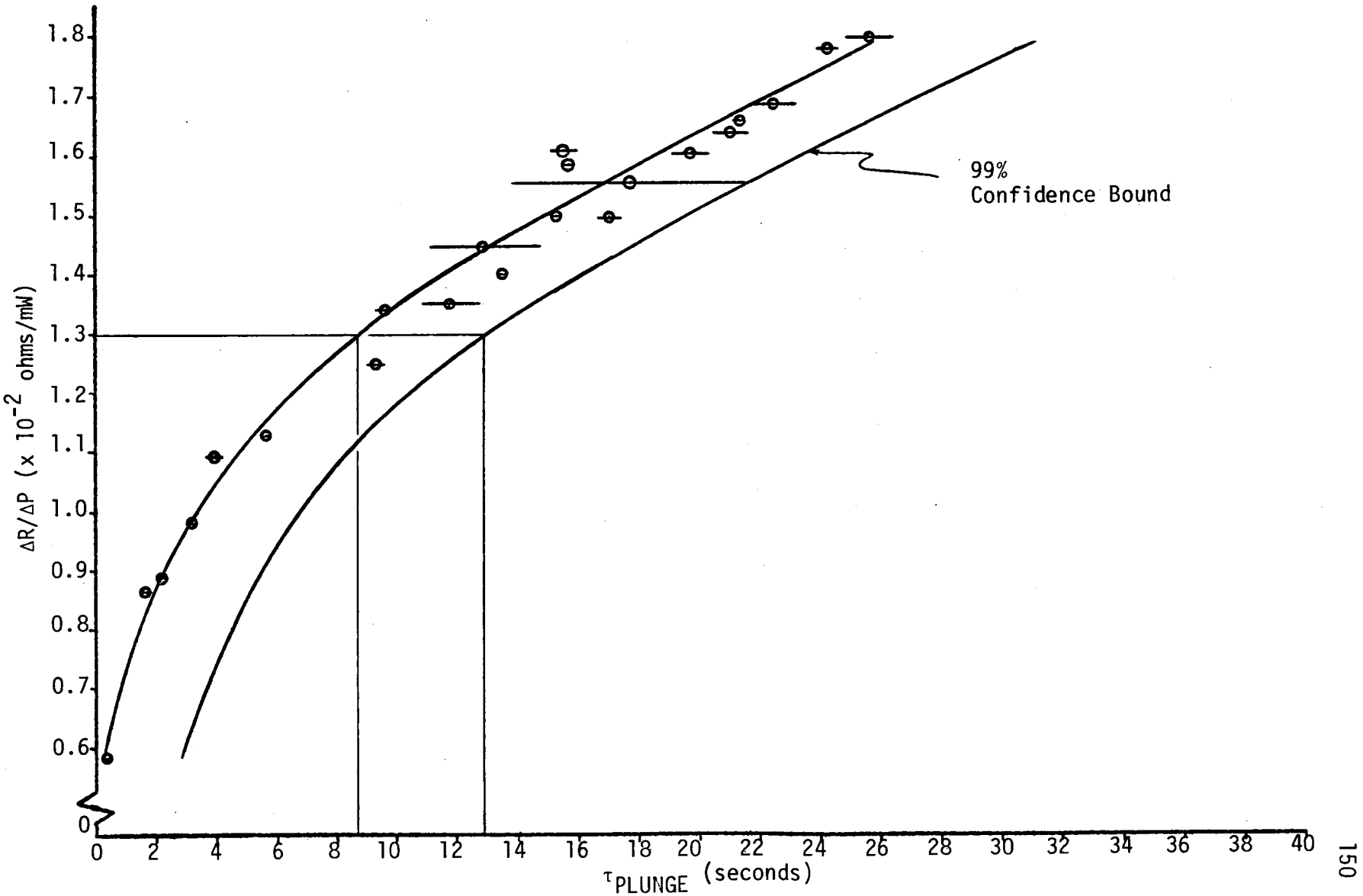


Figure C.2 Self-Heating Slope versus τ_{PLUNGE} Interpretive Example.

constant is equal to or less than the true value corresponding to the value on bounding curve.

2. Likewise, given a value of the mean of a sample of self-heating test results and the sample standard deviation, it can be said that the predicted value of τ_{PLUNGE} will be bounded by the corresponding point, read off the bounding curve, 99% of the time.

For example, given a mean of a set of LCSR results of 1.75 seconds, corrected by the appropriate standard deviation, than from Figure C.1, one can be 99% confident that the true mean of τ_{PLUNGE} is less than or equal to 12.9 seconds. Likewise, from Figure C.2, if the mean of the self-heating test results is given as 0.013 ohm/mW, then one can predict the corresponding value of τ_{PLUNGE} to be 13.0 seconds or less with a 99% confidence.

VITA

John Steven Arendt was born in Oak Ridge, Tennessee on December 17, 1952. He is the son of Mr. and Mrs. John W. Arendt. After graduating from Oak Ridge High School in June 1970, Steve entered the undergraduate program in Nuclear Engineering at The University of Tennessee. During his undergraduate work, he participated in the Cooperative Engineering Program and was employed by Florida Power and Light Company in Miami, Florida.

After being awarded a Bachelor of Science degree in June 1975, Steve entered the graduate nuclear engineering program the following September. After receiving the Master of Engineering degree in March 1977, he will begin work pursuing a Doctor of Philosophy degree in the field of reliability and safety engineering.

Steve is presently engaged to be married to Miss Susan Kay Scott of Knoxville.